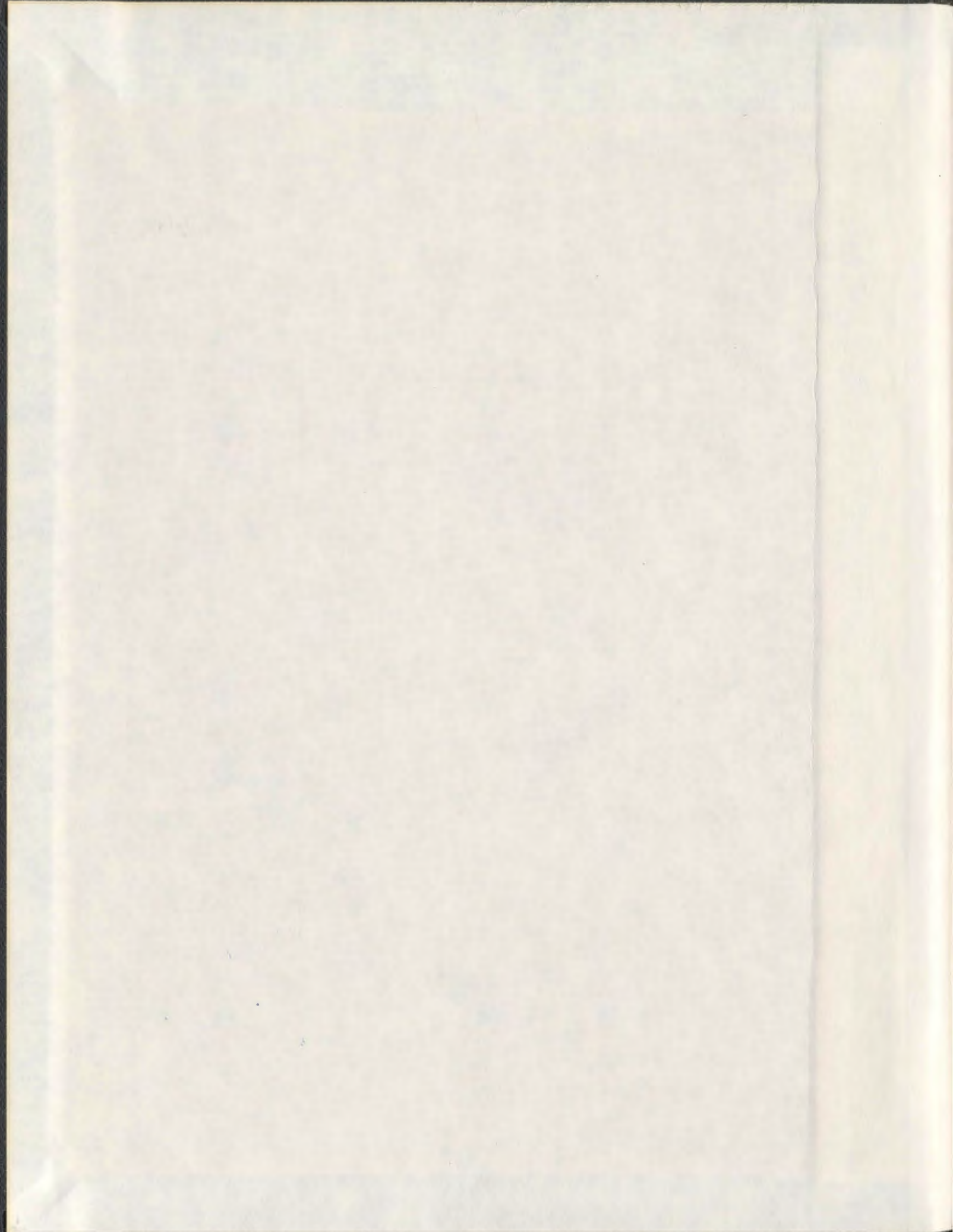


**MAPPING CAPELIN DEMERSAL SPAWNING
HABITAT OFF NORTHEAST NEWFOUNDLAND**

ANDRÉ ROY



**Mapping Capelin Demersal Spawning Habitat
off Northeast Newfoundland**

by

© André Roy

**A thesis submitted to the
School of Graduate Studies
in partial fulfilment of the
requirements for the degree of
Masters of Science**

Geography

Memorial University of Newfoundland

April, 2013

St. John's, Newfoundland and Labrador

Abstract

Habitat mapping is an essential tool for the management and conservation of our marine resources. In this study, multibeam echosounders, which have become important instruments for the mapping of benthic habitat, were used to map capelin demersal spawning sites along the northeast coast of Newfoundland. The EM3000 multibeam echosounder was used in this study to survey an area near Cape Freels containing five known capelin spawning sites. Two types of information were extracted from the acoustic multibeam data: bathymetry, providing a high resolution grid from which the morphologic characteristics of the spawning site could be extracted; and backscatter information, providing a proxy for the substrate grain size.

Studying the morphology of the spawning sites revealed that spawning is taking place on flat areas of the seafloor with a slope value of generally less than 2° and a rugosity ratio of less than 1.19. The spawning sites are situated inside depressions, confirming the findings of a previous study using single-beam sonar data. The backscatter information was used to identify the grain size of the spawning substrate, which varies from medium sand to pebble, to delineate the areas of suitable substrate in the study area. Maps identifying areas suitable for capelin spawning were compiled from the morphologic characteristics. It is estimated that 32% of the seafloor in the study area is suitable for capelin spawning. In 53% of the area, the grain size of the substrate is too large to be suitable for spawning; 5% has finer than suitable substrate; and 10% of the seafloor could not be classified. The multibeam data provided all the information necessary to build habitat maps showing the areas of the seafloor which could potentially support demersal spawning.

Acknowledgments

My interest in capelin behaviour began during my work as a hydrographer. I was asked to organize a bathymetric multibeam survey of known spawning sites and their surrounding areas. A group of scientists led by Dr. John T. Anderson joined the survey to help with data collection; while they were on board the survey vessel, they ran a series of preliminary analysis on the new data. Through many conversations exchanging information and knowledge, my interest in data analysis grew. The dataset collected for the study of capelin behaviour presented a perfect opportunity for me to explore the potential of data analysis and, further, to enrol in a formal study program.

First, I would like to thank my supervisory committee, Dr. John T. Anderson, Dr. Trevor Bell, and Dr. Rodolphe Devillers for their assistance, support, patience, and constant encouragement throughout this project. I would also like to thank Dr. Len Zedel for his guidance and advice concerning hydroacoustic matters, and for his enthusiasm and encouragement. I acknowledge, as well, the Department of Fisheries and Oceans and the Canadian Hydrographic Service for providing me with educational leave and the necessary data to complete this study. Last but not least, I would like to thank my wife, Shirley Ryan, for sharing her writing skills, for her unconditional support, and for her patience towards this accomplishment.

Table of Contents

Abstract	ii
Acknowledgments.....	iii
Table of Contents.....	iv
List of Tables	viii
List of Figures	ix
List of Appendices	xiii
1 INTRODUCTION.....	1
1.1 Foreword	1
1.2 Capelin	1
1.3 Study context.....	3
1.4 Dataset.....	5
1.5 Methodology overview	5
1.6 Thesis structure	7
2 LITERATURE REVIEW AND RESEARCH QUESTIONS	9
2.1 Capelin demersal spawning conceptual model	9
2.2 Habitat mapping	13
2.3 Sonar principles.....	14
2.4 Multibeam echosounder	15
2.5 Multibeam dataset	17
3 STUDY AREA DESCRIPTION	19
3.1 Geographic description	19
3.2 Known spawning sites.....	20
3.3 Substrate characteristics of known spawning sites	21

3.4	Geologic setting.....	23
3.5	Oceanography.....	25
3.6	Marine ecosystem.....	26
4	DATA SOURCES AND METHODS.....	27
4.1	Data acquisition and processing.....	29
4.1.1	Multibeam dataset.....	29
4.1.2	Bathymetric data and its processing	31
4.1.3	Compensation of backscatter data.....	33
4.1.4	Processing of backscatter data	36
4.1.5	Bottom samples.....	38
4.2	Data analysis	39
4.2.1	Spatial scale and resolution.....	40
4.2.1.1	Data resolution for the known spawning sites and spawning areas	40
4.2.1.2	Definition of spawning site spatial scale.....	40
4.2.1.3	Data resolution for study area	41
4.2.2	Backscatter.....	42
4.2.3	Bathymetry.....	44
4.3	Data classification	48
4.3.1	Supervised classification.....	48
4.3.1.1	Validation of the classification.....	50
4.3.1.2	Spawning areas classification (1 m resolution).....	50
4.3.1.3	Study area classification (5 m resolution).....	51
5	RESULTS.....	53
5.1	Similarity of backscatter datasets.....	53
5.2	Definition of fine-grained substrate characteristics	56
5.3	Dimension of demersal spawning sites	57
5.3.1	Backscatter results	58
5.3.2	Bathymetry results	59

5.4	Morphologic characteristics	61
5.4.1	Backscatter	61
5.4.2	Bathymetry of the study area and the spawning areas	63
5.4.3	Morphology derived from depth	70
5.4.3.1	Slope, curvature, and rugosity	71
5.4.3.2	Bathymetric Position Index (BPI)	74
5.4.4	Unclassified area	77
5.5	Relief of spawning sites in relation to depth	79
5.6	Supervised classification	80
5.6.1	Crackers Rocks classification	81
5.6.2	Gull Island 1 classification	83
5.6.3	Gull Island 2 classification	85
5.6.4	Turr Island classification	87
5.6.5	Hincks Rock classification	89
5.6.6	Classification of the study area and resolution	91
5.6.7	Study area classification	93
5.6.8	Substrate distribution	94
5.7	Classification validation	97
5.7.1	Classification of spawning areas	97
5.7.2	Classification of the study area	98
6	DISCUSSION AND CONCLUSION	100
6.1	Study results	100
6.1.1	Spawning sites	101
6.1.1.1	What is the minimum footprint of a spawning site?	101
6.1.1.2	What backscatter characteristics define a demersal capelin spawning substrate?	101
6.1.1.3	What morphological characteristics define a demersal capelin spawning site?	103
6.1.1.4	Were spawning sites located in topographic depressions?	104

6.1.1.5	Do spawning sites occur in gravel ripple troughs on the seafloor?.....	105
6.1.2	Demersal capelin spawning site conceptual model.....	105
6.1.3	Identification of potential spawning habitat.....	105
6.2	Study limitations and data constraints.....	108
6.2.1	Supervised classification validation.....	108
6.2.2	Backscatter.....	108
6.3	Further research.....	110
6.3.1	Study of other known spawning sites.....	110
6.3.2	Demersal spawning vs. beach spawning.....	111
6.3.3	Water temperature change model.....	111
6.3.4	Low backscatter value over bedrock.....	112
6.4	Conclusions.....	112
References	114
Appendices	119

List of Tables

Table 3-1: List of the known capelin demersal spawning sites, including location and depth.	22
Table 3-2: Result of a supervised classification of the substrate for the known spawning sites from Rose-Taylor (2006).....	23
Table 4-1: List of the layers and their resolutions created into GIS for analysis.	47
Table 4-2: Classifications decision chart for areas that correlate to more than one class. An x is marked when all the characteristics of a specific category were met.	50
Table 4-3: Spawning substrates defining the corresponding classes.	52
Table 5-1: Statistics of the differences between the two backscatter datasets. Backscatter is expressed in dimensionless units on a scale of 0-255.....	56
Table 5-2: Number of samples (n) included in the circular areas of a given radius.	58
Table 5-3: Compilation of the minimum and maximum values for the mean and the standard deviation observed from the 1m backscatter data. The values were compiled for the three categories of substrate. Backscatter is expressed in dimensionless units on a scale of 0-255.....	61
Table 5-4: Compilation of the minimum and maximum values for the broad and fine-scale BPI, slope, curvature, and rugosity for each of the three substrate types. They were extracted from the sampling of the bathymetric data produced at 1 m resolution.	71
Table 5-5: Variation of the range of the BPI index resulting from different values used for a broad-scale BPI calculation. Sets of BPI values correspond to the inner and outer annulus values.	75
Table 5-6: Numerical results and differences between the classifications at 1 m and 5 m.	96
Table 5-7: Variability of the percentage of correlation between the seafloor classification and the bottom samples, based on the presence of sample corresponding substrate, within a radius of 10 m, 20 m, 30 m, and 40 m.	99
Table 6-1: Locations and names of other known demersal spawning sites on the Straight Shore (Davoren et al., 2007).....	111

List of Figures

Figure 1-1: Map depicting the northeast coast of Newfoundland. The location of the study area is positioned at the centre of the map and indicated in orange.....	4
Figure 2-1: Graphic obtained with permission from Rose-Taylor (2006) showing the bathymetric value of the spawning site vs. the mean depth and standard deviation of the 1 km ² area surrounding the spawning sites. Black diamonds denote point depths. The dashed blue line is the regression line of the equation $Y=0.87X-2.47$ ($R^2=0.60$). The solid line is the one-to-one correspondence line.....	12
Figure 2-2: Depiction of an acoustic swath transmitted from a hull-mounted multibeam echosounder system (Source: http://www.marinearchaeologists.com/what_we_do.htm).	16
Figure 3-1: Map showing the multibeam survey area. Dark blue indicates water depth of less than 50 m; green indicates water depth greater than 50 m. Each spawning site is identified by a red square with its abbreviated name. This information is superimposed on Canadian Nautical Chart no. 4857.	21
Figure 3-2: Map of the Northwest Atlantic region showing the Labrador Current and its branches. Adapted with permission from E. Colbourne (Colbourne et al., 1997)	26
Figure 4-1: Flow chart of the operations to describe and classify demersal capelin spawning sites from multibeam sonar data.	28
Figure 4-2: Map showing the spatial and temporal multibeam coverage by the launches <i>Plover</i> and <i>Pipit</i> across the study area.	30
Figure 4-3: Map showing the survey lines (in green) over a portion of the study area. The survey lines are superimposed on the Canadian nautical chart 4857 which depicts depth in metres.....	30
Figure 4-4: Map showing the uncertainty associated with bathymetric multibeam data. Most of the study area has a predicted bathymetric uncertainty below 0.4 m. The black squares show the location of the 1 km ² grid cells surrounding the known spawning sites.	33
Figure 4-5: Image depicting the correction for angle of incidence. Angle a is the angle of incidence given by the beam angle θ . The red line is the tangent at the backscatter point giving the slope of the seafloor, angle b. The equation $a-b=c$ gives the corrected angle of incidence between the beam and the seafloor. Hz identifies the horizon and Vz the vertical to the horizon.	35
Figure 4-6: Location and nature of the bottom samples used to validate the classification of substrate suitable for demersal capelin spawning. A brown shadow outlines the study area. An inset depicts an area having a high density of samples. It is located at the Gull Island 1 and 2 spawning areas.....	39
Figure 4-7: Example showing the circles used for the variance study at the Hincks Rocks spawning site, superimposed on a greyscale backscatter image. The black circles are centred on the known spawning site and the yellow numbers are the associated radius values in metres.....	41

Figure 4-8: Distribution of the mean backscatter values for each cell in the 20 m circle centred on the Hincks Rock spawning site. The vertical blue line indicates the mean value. The dashed lines show the standard deviation intervals. The shadowed green area delimited with red lines indicates the range of values chosen to represent the mean backscatter value for this spawning site. Backscatter is expressed in dimensionless units on a scale of 0-255.....44

Figure 4-9: Graphic depicting the BPI and how it determines if a point is located on a peak, trough, slope, or flat (Partial Weiss, 2001). In the figure, irad is the inner radius of annulus in cells and orad is the outer radius of annulus in cells.47

Figure 4-10: Display of error circles around a coarse substrate bottom sample, superimposed on a portion of the study area classification, depicting the different classes it can be associated with, depending on its position error.....51

Figure 5-1: Map of the mean compensated backscatter at a spatial resolution of 5 m. Backscatter is expressed in dimensionless units on a scale of 0-255. The dataset is superimposed onto Canadian nautical chart 4857. The areas in which the two datasets overlap are also shown on the map. The enlargement shows the homogeneity of the data.55

Figure 5-2: Distribution of the difference between the backscatter data from the *Pipit* and from the *Plover*, where both datasets overlap spatially, showing a) the difference in mean backscatter, and b) the difference in the backscatter standard deviation. Backscatter is expressed in dimensionless units on a scale of 0-255.56

Figure 5-3: Map showing the location of the supplementary bottom samples used to establish the characteristics of the fine substrate. The samples are overlaid on the 1 m resolution image of the mean backscatter. Backscatter is expressed in dimensionless units on a scale of 0-255. Nautical chart 4857 is displayed as a background with depth depicted in metres.57

Figure 5-4: Results of the variance study for backscatter values from the five known demersal spawning sites. Backscatter is expressed in dimensionless units on a scale of 0-255. The sites are labelled by their abbreviations. The graphics show: a) standard deviation, and b) maximum variance of backscatter values for a circular area of a given radius.59

Figure 5-5: Results of the variance study for depth values from the five test demersal spawning sites. The sites are labelled by their abbreviations. The graphs depict the a) standard deviation, b) mean, c) minimum, and d) maximum variance of bathymetry values for a circular area of given radius.....60

Figure 5-6: Normalized frequency distribution of the mean backscatter values. Backscatter is expressed in dimensionless units on a scale of 0-255.....62

Figure 5-7: Normalized frequency distribution of the standard deviation backscatter values. Backscatter is expressed in dimensionless units on a scale of 0-255.....63

Figure 5-8: Map showing the multibeam survey areas with the corresponding known capelin demersal spawning sites.64

Figure 5-9: One km ² subset of the multibeam bathymetric data centred on the known capelin demersal spawning site at Cracker Rock. The images present a 4x vertical exaggeration; the colour represents the depth. The shallowest parts are coloured in red and gradually move toward dark blue as the depths increase. An artificial sun illumination from the northeast at an elevation of 45° enhances the texture of the image. Two cross sections of the spawning site are also presented. The arrows in the top image identify the cross sections by colour and orientation. The dot at the centre of the profile marks the known spawning site.....	65
Figure 5-10: One km ² subset of the multibeam bathymetric data centred on the known capelin demersal spawning site at Gull Island 1. See Figure 5-9 for explanation of figure details.....	66
Figure 5-11: One km ² subset of the multibeam bathymetric data centred on the known capelin demersal spawning site at Gull Island 2. See Figure 5-9 for explanation of figure details.....	67
Figure 5-12: One km ² subset of the multibeam bathymetric data centred on the known capelin demersal spawning site at Turr Island. See Figure 5-9 for explanation of figure details.....	68
Figure 5-13: One km ² subset of the multibeam bathymetric data centred on the known capelin demersal spawning site at Hincks Rock. See Figure 5-9 for explanation of figure details.....	69
Figure 5-14: Superimposed depth profiles of the five known spawning sites, shown at a 10X vertical exaggeration.....	70
Figure 5-15: Normalized frequency distribution of the slope values. The x axis is displayed as a logarithmic scale of base 2 to show the differences for the small values.....	72
Figure 5-16: Normalized frequency distribution of the curvature values. The x axis is displayed as a logarithmic scale of 2 to show the differences for the small values.....	73
Figure 5-17: Normalized frequency distribution of the rugosity values.....	73
Figure 5-18: Results of broad-scale BPI computation at Gull Island 2 for a) 25, 125 m b) 40, 200 m c) 50, 250 m and d) 60, 300 m. Each pair of values presents the inner and outer distances of the annulus used for the calculation of BPI. The black areas represent peaks and the grey areas are the transition from peak to trough. The trough areas have been made transparent to display the colour-coded bathymetry in the background. The blank area represents Gull Island.....	75
Figure 5-19: Normalized frequency distribution of the broad-scale BPI values.....	77
Figure 5-20: Normalized frequency distribution of the fine-scale BPI values.....	77
Figure 5-21: Distribution of values for seafloor characteristics. The first three boxplots on each graphic show the data distribution for the three substrate classes from all the spawning areas, whereas the last two boxplots show the distribution of all the data compiled at 1 m and 5 m resolutions. Backscatter is expressed in dimensionless units on a scale of 0-255.....	78

Figure 5-22: Pearson correlation between depth and broad-scale BPI. Spawning sites are indicated by green squares and a linear trendline shows the best-fit linear relationship. The R ² value indicates the strength of the correlation.	79
Figure 5-23: Legend for the classification maps of the five known spawning sites.	80
Figure 5-24: Maps of the suitable substrate for demersal capelin spawning at the Crackers Rocks site displayed with the bathymetry. See Figure 5-23 for legend details.	82
Figure 5-25 : Maps of the suitable substrate for demersal capelin spawning at the Gull Island 1 site displayed with the bathymetry. See Figure 5-23 for legend details.	84
Figure 5-26: Maps of the suitable substrate for demersal capelin spawning at the Gull Island 2 site displayed with the bathymetry. See Figure 5-23 for legend details.	86
Figure 5-27: Map of the suitable substrate for demersal capelin spawning at the Turr Island site displayed with the bathymetry. See Figure 5-23 for legend details.	88
Figure 5-28: Map of the suitable substrate for demersal capelin spawning at the Hincks Rock site displayed with the bathymetry. See Figure 5-23 for legend details.	90
Figure 5-29: Pie charts depicting the percentage of seafloor occupied by each class of substrate within the 1 km ² spawning area for each of the five known spawning sites.	91
Figure 5-30: Pie charts depicting the percentages of each class for the five known spawning areas. The values are compiled separately for the two spatial resolutions used: a) 1 m and b) 5 m using the 1 m resolution characteristics values.	92
Figure 5-31: Pearson correlation between the percent coverage of the substrate classes for the five known spawning areas at a resolution of 1 m (Figure 32 a), compared to those at a resolution of 5 m (Figure 32 b). The values for the characteristics determined at 1 m resolution were used for both classifications.	93
Figure 5-32: Map depicting the seafloor suitability for demersal capelin spawning for the whole study area. The bottom samples are overlaid over the classification.	94
Figure 5-33: Percentage of seafloor occupied by each substrate class within the study area.	94
Figure 5-34 : Distribution of the bottom samples from each the study area.	97
Figure 5-35: Display of the correlation evaluating the validity of the substrate classification of the five known spawning areas as compared to the distribution of bottom samples throughout the study area. The three classes are represented by squares and a linear trendline showed the strength of the correlation.	98
Figure 5-36: Display of a correlation evaluating the validity of the substrate classification of the study area (5 m resolution) in comparison with the distribution of bottom samples throughout the entire study area.	99

Figure 6-1: Images of a rock outcrop close to the GI2 spawning site at 1 m resolution. The backscatter image (left) depicts low values for rock outcrops. Backscatter is expressed in dimensionless units on a scale of 0-255. The rugosity layer (right) shows low values on the peaks and edges of the rock outcrops.103

Figure 6-2: Images of bedrock in the vicinity of Newtown a) on land from a 2008 SPOT (www.geobase.ca) image at 10 m resolution and b) on the seafloor from a 5 m resolution multibeam image.107

Figure 6-3: Rose diagram of the orientation and frequency of observed faults a) on land and b) on the seafloor. Every three concentric rings represent one observation.107

Figure 6-4: Backscatter image at 1 m resolution of the GI2 spawning area. The brown background highlights the area that has no data. This image displays the linear artefact at nadir as well as the higher backscatter value (brighter areas) surrounding the lower backscatter values for bedrock (darker areas).109

List of Appendices

Appendix A. QTC MultiView unsupervised classification 119

Appendix B. Processed bottom samples within the study areas 128

Appendix C. Values for the 20 m Radius samples for the suitable, coarse and fine substrates 132

Appendix D. Maps of characteristics from spawning areas 136

1 INTRODUCTION

1.1 Foreword

The subject of this thesis is the mapping of capelin (*Mallotus villosus*) demersal spawning sites on the northeast coast of Newfoundland. This project is intended to determine the morphologic and acoustic characteristics of known spawning sites, identified previously through the observation of seabird behaviour and through the acoustic tracking of mature capelin schools by Davoren et al. (2006). By studying these known sites and analyzing information gathered from them, other potential sites for demersal spawning throughout the study area were identified and mapped. This study follows from acoustic classification work completed by Davoren et al. (2006).

1.2 Capelin

Capelin are a forage pelagic fish species crucial to the ecosystem of the northeast coast of Newfoundland. Many species, including whales, seals, cod, and seabirds, feed on them (Dodson et al., 1991; Davoren et al., 2007; Penton and Davoren, 2008). The capelin fishery is also important for the people of the northeast coast of Newfoundland. Capelin is fished both as a commercial species and for bait in support of other fisheries. Competing pressures on the substrate, including bottom trawling and gold placer mining, impact the spawning environment (Ellis, 2001). Understanding the location and characteristics of capelin spawning sites will help managers discern the impact of human activities on the ecosystem and help guide conservation management policies. This study of the nature and

patterns of the spawning substrate will provide important information for any remediation work on demersal spawning grounds. The protection of the spawning grounds must be part of fisheries management to ensure the sustainability of the fisheries industry in Newfoundland.

Significant alterations may occur in ecosystems due to changing climate. Water temperature is a vital component of capelin spawning grounds, and any climatic change affecting the water temperature is likely to have a notable impact on the species (Nakashima and Wheeler, 2002). On the northeast coast of Newfoundland, capelin most often spawn on beaches rather than demersal sites, although our knowledge of the latter is poorly documented (Nakashima and Wheeler, 2002). In fact, the study of capelin demersal spawning is fairly recent in Newfoundland; Nakashima and Wheeler (2002) and Davoren et al. (2006) identified some of the first demersal sites on the northeast coast of Newfoundland. In the event of an increase in water temperature on and near beaches due to climate warming, Nakashima and Wheeler (2002) suggested capelin may move their spawning sites from beaches to demersal sites. An event of this magnitude will require an in-depth and accurate knowledge base from which to evaluate the consequence of water temperature change on capelin population and recruitment (Davoren et al., 2007). Habitat mapping contributes to this knowledge (Kenny et al., 2003) by offering a precise description of those sites.

1.3 Study context

Previous studies focusing on demersal spawning (Rose-Taylor, 2006; Davoren et al., 2007) used single-beam acoustic sonar technology and, because of the limited seafloor coverage inherent to the single-beam system, focused on bottom classification in the immediate vicinity of known capelin spawning sites. This limitation prompted Rose-Taylor (2006) to suggest that the use of multibeam technology would achieve wider and more complete coverage of the seafloor. In 2006, scientists from the Geography Department of Memorial University of Newfoundland and the Department of Fisheries and Oceans organized a project for the execution of a multibeam survey on the northeast coast of Newfoundland (Figure 1-1). The survey took place during the months of July 2006 and July 2007.

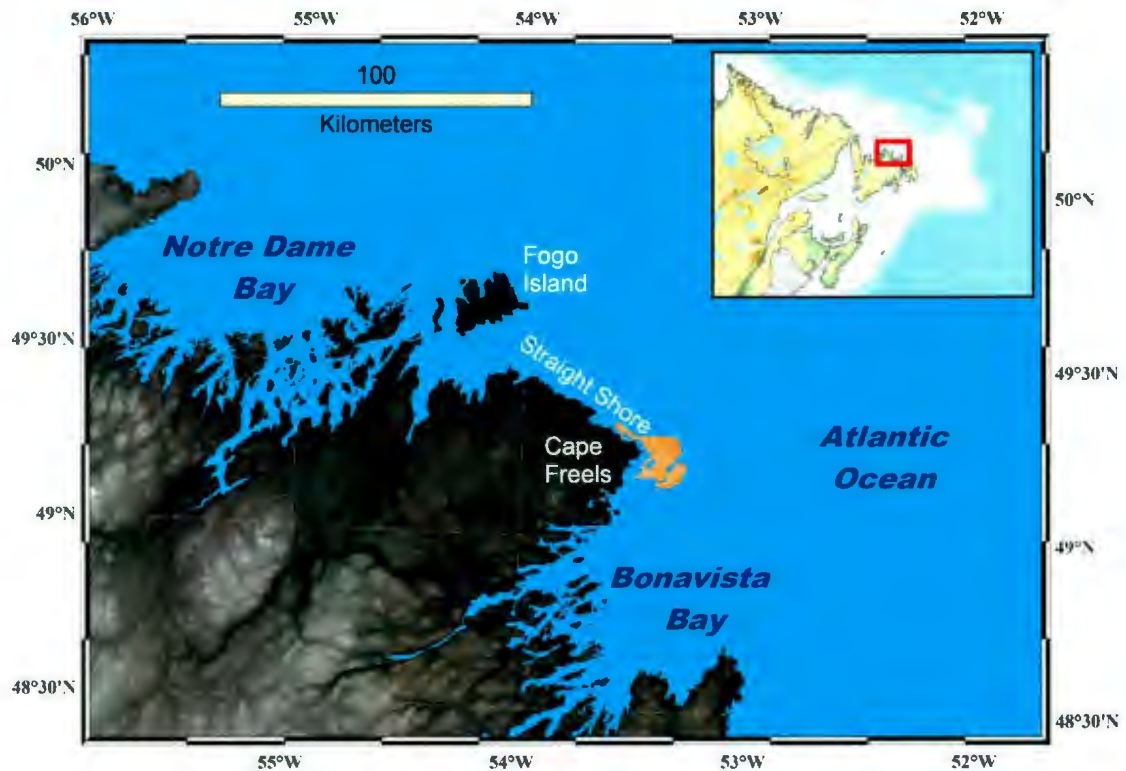


Figure 1-1: Map depicting the northeast coast of Newfoundland. The location of the study area is positioned at the centre of the map and indicated in orange.

The multibeam echosounder can provide 100% coverage of the seafloor over an area of many square kilometres, opening up the possibility of collecting data over a significantly larger study area. This permits a thorough study of capelin spawning sites and their relation to the characteristics of the surrounding seafloor. With the advantages offered by multibeam technology, the research acoustically classified known capelin spawning sites in the study area and assessed the feasibility of mapping potential spawning sites using multibeam-derived seabed characteristics.

1.4 Dataset

The dataset acquired for this research is acoustic in nature and was collected from a multibeam echosounder system. The Department of Fisheries and Oceans (DFO) acquired the dataset in a collaborative effort between the Canadian Hydrographic Service (CHS) and the Ecological Science Section. Both partners are divisions of the Science Branch of the Department of Fisheries and Oceans. The goal of the data collection was to pursue the study of capelin spawning sites started by Rose-Taylor (2006) and Davoren et al. (2007). The acoustic survey was conducted from the CCGS *Matthew* and two survey launches, the *Plover* and the *Pipit*. The data were collected with the intention of studying the bathymetric, backscatter, and water column data. This thesis focuses on the analysis of the bathymetric and backscatter data.

1.5 Methodology overview

This habitat mapping project was developed, based on the knowledge of known demersal spawning sites. The known spawning sites were identified from bottom grabs that contained fertilized capelin eggs within “spawning-suitable” substrate (Davoren et al., 2006). Each bottom grab represented only one point on the seafloor, however, and could not indicate the extent of an actual spawning site. The size of the spawning sites needed to be established before its characteristics were identified. To determine the footprint of each spawning site, the variance of the seafloor characteristics surrounding that site was analyzed. The size of a spawning site was identified as the area in which the seafloor characteristics remain similar around a known site.

After determining the general size of spawning sites, the seafloor morphologic and backscatter characteristics of the known spawning sites were compiled. Those characteristics defined the criteria that can be used to identify additional suitable spawning ground throughout the study area. The same analysis was performed for areas that are known, from bottom samples, to have an unsuitable substrate for capelin spawning (historic absence of capelin eggs). For each morphologic and backscatter characteristic, a range of values corresponding to suitable and unsuitable spawning substrate was established. Seafloor characteristics of the study area were tested against those ranges to determine its suitability for capelin spawning.

An area of 1 km² was estimated by Rose-Taylor (2007) to be the minimum seafloor area to contain all substrate types present within the study area (Rose-Taylor, 2007). Consequently, a seafloor classification map of 1 km² was made around each of the five known demersal spawning sites. The classification was based on the seafloor characteristics found in the known spawning sites, as well as those in the unsuitable sites. The classification was conducted initially with the dataset compiled at a resolution of 1 m, and then repeated at a resolution of 5 m; the two results were compared. Using the 5 m resolution dataset and the same seafloor classification procedure, a classification map of the entire study area was created. The map displays the distribution of the acoustically suitable substrate for capelin spawning throughout the region. It provides a general estimate only of the proportion of suitable spawning substrate for the seafloor located off

Cape Freels on the northeast coast of Newfoundland. Comparing all the available bottom samples with their corresponding substrate classes validated the acoustic classification.

1.6 Thesis structure

This thesis contains a total of six chapters, references, and appendices. Chapter Two provides a review of the knowledge available on capelin demersal spawning and principles of marine habitat mapping. It also identifies the knowledge gaps that are addressed by this study. Information is also presented to support the methodology of the study, explaining the multibeam echosounder principles and the necessary technical information on the dataset used for this study. Throughout, pertinent research questions are formulated.

Chapter Three describes the geography of the study area. It provides a description of the known demersal spawning sites and the geological settings, oceanography, and ecosystem environment in which they are located.

Chapter Four presents a step-by-step description of the methodology for data analysis. It presents the steps used to acquire, process, and analyze the acoustic data and determine seafloor characteristics. The methods used to establish parameters, such as the data resolution and spatial scale of the study, are also outlined. The seafloor characteristics that will be used for the classification are listed and explained. This chapter concludes with the method used to validate the classification.

Chapter Five details the results of the study. First, the study parameters are described, including a variance study establishing the spatial scale of a spawning site and its seafloor characteristics. The next section presents the results of the substrate study, which establishes value ranges for the seafloor characteristics of spawning sites. The results of the supervised classification are described next, illustrated by maps depicting the seafloor classes and their distribution. Comments and explanations are provided with each map. The results of the validation of the classification, based on the comparison of bottom samples, observations, and the mapped classification, are presented.

Chapter Six discusses the results of the study, outlining its strengths and limitations. This final chapter reviews the original research questions and evaluates how well they were addressed. The chapter ends by outlining a direction for further studies of capelin demersal spawning.

The final section of this thesis includes a list of references and appendices. Within the appendices, an unsupervised classification performed with commercial software is presented, followed by the parameters used during the study that were too lengthy to be incorporated within the text. Maps of seafloor characteristics are also included.

2 LITERATURE REVIEW AND RESEARCH QUESTIONS

This section presents a review of existing literature about capelin demersal spawning and the principles of marine habitat mapping. A conceptual model for demersal spawning is outlined and, from that model, knowledge gaps are identified. Opportunities to add components to the conceptual model and validate previous demersal spawning research are presented. This chapter also presents information supporting the study methodology by explaining the multibeam echosounder principles, the technical attributes of the dataset, and the potential of multibeam data for habitat mapping. The research questions for this project are introduced throughout this chapter.

2.1 Capelin demersal spawning conceptual model

Capelin is an important pelagic fish of the North Atlantic. Capelin spawning takes place offshore in Icelandic waters, the Barents Sea (Dodson et al., 1991), and on the Southeast Shoal of the Grand Banks of Newfoundland (Carscadden et al., 1989). Along the east coast of Canada, capelin migrate from deep water along the continental shelf toward the beach (Carscadden et al., 1989). Although it is believed that the majority of capelin that spawn on the coast of Newfoundland do so on beaches, demersal spawning sites were also identified along the Straight Shore of Newfoundland (Davoren et al., 2006).

Many studies have identified substrate composition and water temperature as the two key factors in the selection of a spawning location by capelin (Carscadden et al., 1989; Davoren et al., 2006; Rose-Taylor, 2006). A conceptual model of the most suitable

environment for capelin demersal spawning was developed in Rose-Taylor (2006). According to the model, capelin are most likely to spawn on glacially derived sediments that vary in size from sand to pebbles, in water temperatures between 2°C and 12°C (Rose-Taylor, 2006). Glacial deposits of sand and gravel, reworked by waves and currents, have accumulated between the rocky outcrops on the seafloor off the northeast coast of Newfoundland (Shaw et al., 1999). These deposits provide the necessary substrate at the desired depth range for capelin demersal spawning (Carscadden et al., 1989; Rose-Taylor, 2006).

Rose-Taylor's conceptual model provides the basis for this study; however, while gathering information in preparation for the research, knowledge gaps were identified. The literature review did not reveal any estimates of the minimum size of a spawning site. Establishing the minimum size of a spawning site permits the designation of its spatial scale. The spatial scale — the size of the area in which spawning occurs — has to be known prior to measuring the morphological characteristics. Once a morphological analysis of the spawning sites has been completed, it will be possible to evaluate which characteristics are relevant to demersal capelin spawning grounds. Given this knowledge gap, two research questions were formulated:

- What is the minimum footprint of a spawning site?
- What morphologic characteristics define a capelin spawning site?

Adding a morphologic description of demersal spawning sites opens the possibility of expanding the conceptual model for demersal capelin spawning on the northeast coast of Newfoundland. If it can be demonstrated that one or more of the morphologic characteristics are consistent across all sites, those characteristics could be added to the conceptual model. A third research question was formulated:

- Does the morphologic description of capelin demersal spawning sites contribute additional definition to the conceptual model?

Rose-Taylor's (2006) thesis raised questions about the characteristics of spawning sites, which can be answered with the information provided by the multibeam dataset. The questions originated from the analysis of the depth of the spawning site and the average depth of its surroundings. The correlation between the mean depth of a spawning area and the depth of the spawning site yielded an R^2 value of 0.6 (Figure 2-1). As Figure 2-1 from Rose-Taylor (2006) shows, all spawning sites are deeper than the average depth of the surrounding waters, suggesting that the sites are located in topographic depressions. The graphic also suggests that the magnitude of the depressions increases with depth. However, the low density of the single-beam bathymetric data did not permit further investigation of this hypothesis.

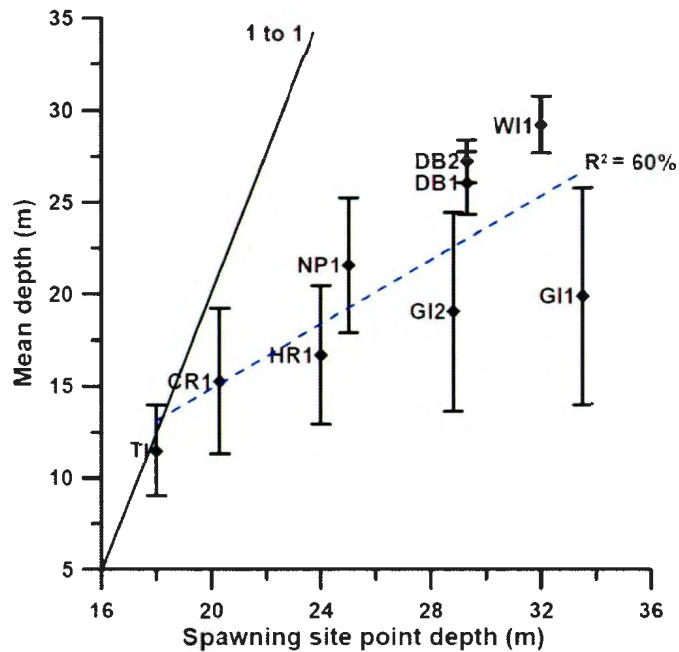


Figure 2-1: Graphic obtained with permission from Rose-Taylor (2006) showing the bathymetric value of the spawning site vs. the mean depth and standard deviation of the 1 km² area surrounding the spawning sites. Black diamonds denote point depths. The dashed blue line is the regression line of the equation $Y=0.87X-2.47$ ($R^2=0.60$). The solid line is the one-to-one correspondence line.

The capability of multibeam echosounders to provide high-resolution, three-dimensional data of the seafloor allows the following research questions to be addressed:

- Are spawning sites located in topographic depressions?
- Do spawning sites have greater relief at greater depths?

Rose-Taylor (2006) suggested an association between the depth of spawning sites and the depth of gravel ripple troughs described in Shaw et al. (1999). She argued that the ripple troughs may be the seabed landform associated with demersal spawning grounds.

Assuming the multibeam bathymetric dataset is able to demonstrate that capelin spawning

sites are located in topographic depressions, then it should also be able to address the following question:

- Do spawning sites occur in gravel ripple troughs on the seafloor?

2.2 Habitat mapping

Habitat mapping provides a picture of the state of a habitat within the ecosystem, and is an essential tool for the management and conservation of our marine resources (Kostylev et al., 2001; Wilson et al., 2007; Valavanis et al., 2008). Spawning grounds are critical to capelin and their habitat and should be considered in the operation of responsible fisheries management plans (Valavanis et al., 2008). Acoustic backscatter data have previously been used to map trout spawning habitats in northern Lake Michigan (Edsall et al., 1989). Large mosaics of backscatter data were built to identify the precise location of the correct spawning substrate within large historic spawning grounds. In another study, the interpretation of multibeam data led to the substrate identification and the benthic habitat classification for megabenthos on Brown Bank, Nova Scotia (Kostylev et al., 2001). Benthic habitat classification projects, such as Brown and Collier (2007), associated backscatter values with different substrates, and created habitat maps for the Loch Linnhe artificial reef site on the west coast of Scotland. These are just a few examples of the use of acoustic data for habitat mapping.

For this study, acoustic remote sensing of the seafloor and data processing using Geographic Information System (GIS) were used to build habitat maps showing the

morphology and substrate arrangement of the spawning grounds. This was made possible by the application of multibeam sonar technology, which can provide 100% acoustical coverage with overlapping sonification of the seafloor (Mayer, 2006). The multibeam echosounder generates two useful datasets: bathymetry, which provides high-density three-dimensional models of the seafloor; and backscatter data, which gives the arrangement, delineation, and proxy grain size of the substrate (Bachman, 1985). The high-density data permits the extraction of the morphologic characteristics of the seafloor (Lanier et al., 2007, Wilson et al., 2007). The complete coverage of the seafloor by multibeam systems provides a remarkable advantage over sampling by a single-beam system (single-beam offers only approximately 5% coverage of the seafloor for similar line spacing). The advantage gained from complete coverage is, however, accompanied by a greater difficulty in manipulating and analyzing larger datasets. This challenge is addressed with the use of GIS. Algorithms to calculate specific characteristics such as slope, roughness, and bathymetric position index, to name just a few, have been developed to efficiently analyze bathymetric raster and vector data (Wilson et al., 2007). In general, multibeam echo sounding requires good sea conditions to perform well and ambient noise in the water column may degrade the data. Large quantities of algae may also prevent the detection of the seafloor and the associated substrate characteristics.

2.3 Sonar principles

A hydro-acoustic instrument was used for the remote sensing of the seafloor. The speed at which sound travels in a medium (water in this case) is a function of the density of the

medium. The denser the medium, the faster sound will travel through it. Sound propagates in a specific direction until it encounters a change in density, at which point it scatters in different directions with different intensities. The difference in density, in combination with the angle of incidence of the sound wave with the interface, dictates how the sound wave will be scattered (Medwin and Clay, 1997). When a sound wave propagates through water, much of the energy is lost through geometric spherical spreading and attenuation due to the viscosity of water (Medwin and Clay, 1997). The higher the frequency of a sound wave, the greater the absorption of energy by the ambient water. For that reason, given an equivalent amount of energy, an acoustic wave of a lower frequency will travel further than one of a higher frequency (Medwin and Clay, 1997). The frequency of a sound wave is equal to its speed divided by its wavelength. Because the speed of sound is almost constant in water, the size of the wavelength will directly affect its frequency (for example, a smaller wavelength will give a higher frequency). To detect an object using hydro-acoustic technology, the wavelength needs to be approximately less than twice the size of the object in question (Medwin and Clay, 1997). Therefore, a higher frequency will permit the detection of smaller objects.

2.4 Multibeam echosounder

Development of multibeam echosounder technology began during the early 1970s (Hughes Clarke et al., 1996) and was available for commercial application by the 1980s. Its potential for scientific investigation was quickly demonstrated (Hughes Clarke et al., 1996). The parallel development of dynamic positioning, motion sensors, sound velocity

measurements, and computing science made it possible to construct precise multibeam echosounders for water less than 100 m depth (Mayer, 2006). A multibeam echosounder transmits a swath-shaped sound pulse (Figure 2-2). Depending on the system, the across-track angle may vary from 90 to 150 degrees, and the along-track angle may vary from a fraction of a degree to a few degrees. After being reflected from the seafloor, the signal is returned to the transducer, which gathers a time series of amplitude values. A fan-shaped collection of beams is formed from the analysis of the time series, and a depth value is calculated from the geometry of each beam. The result is a series of return signals from which sounding values were calculated, creating a profile of the seafloor. As the ship moves forward, the succession of these profiles, or swaths, form a high-density model of depth points, resulting in a three-dimensional image of the seafloor (Hughes Clarke et al., 1996). Using the same time series, the analysis of amplitude values will produce a backscatter dataset that can be used as a proxy for substrate grain size and seafloor roughness (Fonseca and Mayer, 2007).

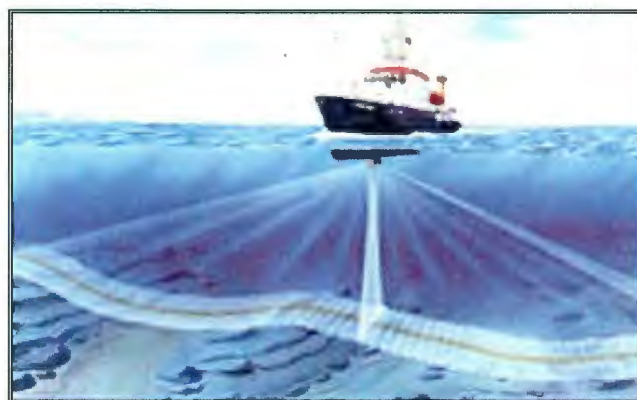


Figure 2-2: Depiction of an acoustic swath transmitted from a hull-mounted multibeam echosounder system (Source: http://www.marinearchaeologists.com/what_we_do.htm).

The three-dimensional images of the seafloor provided by the multibeam data contributes to our knowledge of capelin spawning grounds. While this study focuses on accessing detailed morphology of spawning sites, the multibeam dataset could facilitate testing previous assumptions about capelin behaviour. For example, the study of spawning sites and their surroundings may indicate whether demersal spawning occurs on ancient submerged beaches preserved on the seafloor. It has been suggested that demersal spawning capelin return to beaches that were once the active shoreline when relative sea levels were below present (Davoren et al., 2007). It has also been hypothesized that capelin approach demersal spawning sites by following trenches on the seafloor (Davoren et al., 2006). The bathymetry generated by the multibeam survey may provide useful supporting information for a test of this hypothesis.

2.5 Multibeam dataset

The dataset produced from the multibeam technology offers the high resolution necessary to identify morphologic characteristics from the bathymetric data (Lanier et al., 2007; Wilson et al., 2007). The full coverage of the seafloor provided a three-dimensional visualization, allowing the morphology of spawning sites to be compared with that of the surrounding area. The backscatter dataset, which also covered 100% of the seafloor, was used as a proxy for grain size and an indication of seafloor roughness (Fonseca and Mayer, 2007) for the entire study area. The dataset is digital and was processed within a GIS to facilitate analysis and the production of easy-to-interpret graphic material and

maps. By taking into account the inherent advantages of multibeam technology, these research questions were formulated:

- Can potential capelin spawning grounds be identified from the classification of multibeam data?
- If so, can multibeam echosounder data provide a prospecting tool for identifying potential spawning habitat?

3 STUDY AREA DESCRIPTION

This chapter presents short geographic descriptions of the area of this study and the known spawning sites. The chapter also provides descriptions of the geologic setting, the oceanography, and ecosystems of the study area.

3.1 Geographic description

The study area is located on the northeast coast of Newfoundland, along an area called the Straight Shore (Figure 1-1). This area is recognized throughout Newfoundland for its abundant beaches (Shaw et al., 1999) on which capelin spawn (Davoren et al., 2007). The northeast orientation of this coast, perpendicular to the dominant onshore winds during spawning season, aids the early larval survival of capelin (Leggett et al., 1984). The study area, located specifically on the eastern extremity of the Straight Shore (Figure 1-1), is delimited by the extent of the multibeam acoustic dataset, which covers 188 km² (Figure 1-1) east of Cape Freels. The survey area encloses five demersal spawning sites identified by Davoren et al. (2006), as well as areas closer to the shore and into deeper water. The main body of the survey reaches up to 14 km from the shore, starting in the south at Pound Cove, and ending at 49°18'N latitude. In addition to the main survey area, a smaller area partly covers a bay between North Bill and Northern Cat Island. The depth of the study area ranges from 5 to 110 m (Figure 3-1).

3.2 Known spawning sites

The known spawning sites in the region were described by Rose-Taylor (2006) at different spatial scales. The first site, Cracker Rock (CR), is the most northerly site in the study area. It is located 1.5 km from the shore at a location called Middle Bill. Gull Island 1 (GI1) is located 600 m south-southeast of Gull Island (Gull Island is 2.5 km from the coast of Newfoundland). Close to GI1 is Gull Island 2 (GI2), 200 m south-southwest of the shore of Gull Island. Further south, Turr Island (TI) is 850 m west-northwest of Turr Island and 2.7 km from the Straight Shore. The most southerly site, Hincks Rock (HR), is located 2 km northeast of Pouch Island and 4.5 km southeast of the community of Newtown. The sites are at water depths ranging from 18 to 35 m. The locations of these spawning sites are identified on Figure 3-1 and described in Table 3-1.

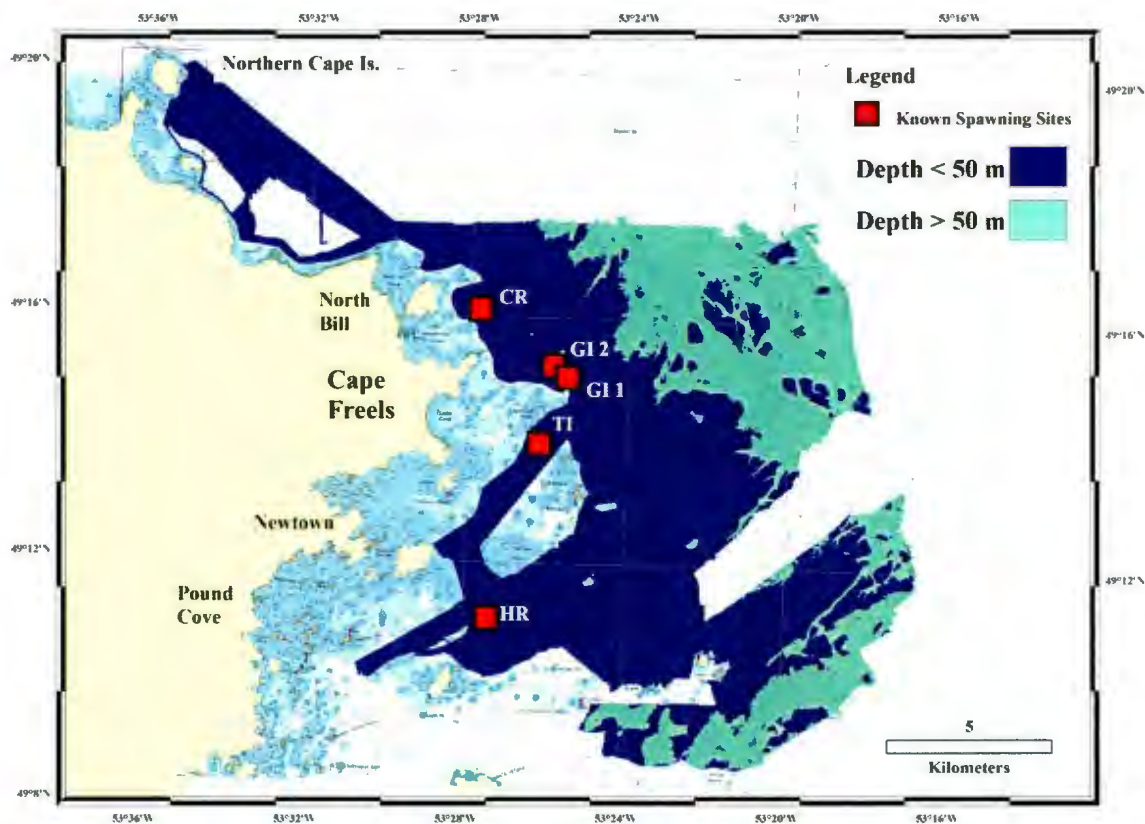


Figure 3-1: Map showing the multibeam survey area. Dark blue indicates water depth of less than 50 m; green indicates water depth greater than 50 m. Each spawning site is identified by a red square with its abbreviated name. This information is superimposed on Canadian Nautical Chart no. 4857.

3.3 Substrate characteristics of known spawning sites

Bottom grabs were collected, processed, and reported by Rose-Taylor (2006) on all known spawning sites to identify their substrates. The seafloor of all five sites can be characterized as hard. No mud is present at any of the sites and only a limited amount of sand was found. All sites have pebbles except HR; all sites have a wide range of grain sizes. Most sites had moderately sorted sediments as one of their main substrate characteristics.

Rose-Taylor (2006) conducted a supervised classification of the known spawning sites that determined the substrate type, extent, and distribution within the 1 km² area centred around the sampled location. The classification was determined from the analysis of single-beam echosounder acoustic data with the QTC Impact software. The supervised classification generated four classes. The largest class in terms of area was named “gravel” and was composed of sediment grain size ranging from sand to pebbles, which is considered the substrate on which spawning occurs (Carscadden et al., 1989; Rose-Taylor, 2006); the second largest substrate class was named “cobble-boulder-bedrock” (Table 3-2). These two classes contribute to the hard nature of the seafloor of the study area. The two other classes were named “fine sand” and “vegetation.”

Table 3-1: List of the known capelin demersal spawning sites, including location and depth.

NAME	ABBREVIATION	LATITUDE ° (N)	LONGITUDE ° (W)	DEPTH
Crackers Rock	CR	49.2687	53.4625	20.3 m
Gull Island I	GI1	49.2508	53.4253	35.5 m
Gull Island II	GI2	49.2538	53.4312	28.8 m
Turr Island	TI	49.2325	53.4362	18.0 m
Hincks Rock	HR	49.1849	53.4564	24.1 m

Table 3-2: Result of a supervised classification of the substrate for the known spawning sites from Rose-Taylor (2006).

SPAWNING SITE	SUPERVISED CLASSIFICATION		
	Substrate	Seafloor %	depth (m)
CR	Sand	0.7	> 18
	Macroalgae	16.3	10 to 18
	Gravel	55.8	> 20
	cobble-boulder-bedrock	27.2	> 18
G11 & G12	Sand	9.4	> 20
	Macroalgae	8.1	10 to 18
	Gravel	45.8	<25
	cobble-boulder-bedrock	36.6	20 to 25
TI	Sand	0.0	-
	Macroalgae	31.7	10 to 20
	Gravel	61.3	> 20
	cobble-boulder-bedrock	7.2	18
HR	Sand	7.1	> 20
	Macroalgae	8.3	10
	Gravel	35.3	< 18
	cobble-boulder-bedrock	49.3	> 20

3.4 Geologic setting

The surficial geology of the study area is a legacy of the last glaciation with subsequent modification by marine processes (Shaw et al., 2006). The study area and its surroundings were glaciated during the late Wisconsinan (Jayasinghe, 1978; Shaw et al., 2006). The Notre Dame Ice Stream covered the study area at 14 ka BP (thousands of radiocarbon years before present). The ice stream retreated inland between 13 ka and 12 ka BP (Shaw et al., 2006), exposing the study area to marine processes. Glacial features left on the landscape indicate that the ice was moving from west to east (Jayasinghe, 1978). The shore adjacent to the study area is a landscape of subdued topography with fields of

erratic boulders, and ponds and bog infilling depressions in bedrock or till (Jayasinghe, 1978). A succession of Devonian bedrock composed of Cape Freels granite, Hare Bay gneiss, and Deadman's Bay granite underlies the area. The Cape Freels granite is exposed on islands within the study area and extends under Bonavista Bay (Jayasinghe, 1978). Most of the seafloor rock outcrops within the survey area are likely composed of Cape Freels granite.

The area occupies a zone dominated by waves and wind-driven currents, which have eroded the glacial sediments. The seafloor is rough; its surface is composed of exposed granite and poorly sorted sand and gravel. Isolated boulders occur on the seafloor across the area. The sand and gravel are actively reworked by wave and current action (Shaw et al., 1999). The currents arrange the gravel into ripples, which have an average wavelength of 2.3 m and a northwest-southeast orientation. The ripples were observed in water depths of 29 m to 73 m (Shaw et al., 1999). Sand sheets, terminated by sand dunes of wavelengths of 8 m and overlying gravel, were observed (Shaw et al., 1999). The sand and gravel substrate is marked by iceberg pits and furrows, although the existence of these pits and furrows is ephemeral due to the sediment transport taking place in the area (Shaw et al., 1999). The majority of the study area lies within the depth zone of wave and current action, which is 60 m and shallower (Shaw et al., 1999). Those areas of the seafloor covered by a coarse gravel lag (pebbles-cobbles-boulders) are more stable, since these grain sizes are only occasionally affected by wave and current action. The gravel lag creates a covering layer over the finer sediments which protects them from wave action (Shaw et al., 1999).

3.5 Oceanography

The waters of the study area are influenced by a westerly component of the Labrador Current that follows the coast (Figure 3-2). The Labrador Current carries cold and fresh water from Hudson Bay and the Arctic Ocean. The cold water transported by the current is trapped in a Cold Intermediate Layer (CIL) between warmer surface water and the bottom continental slope water (Colbourne et al., 1997). Along the coast, the CIL is located in depths greater than 50 m, which keeps the water at a temperature below 0°C (Colbourne et al., 1997). Throughout the study area, this contour line has an orientation NW-SE and depicts the roughness of the seafloor. The contour line changes its orientation by 90° at the southeast portion of the study area and runs toward the coast (Figure 3-1). The Labrador Current carries icebergs (Colbourne et al., 1997) that can ground in the study area, leaving scours and furrows on the seafloor (Shaw et al., 1999).

In an average year, the northeast coast of Newfoundland is covered with sea ice from January to April. Most of this ice drifts down from the north (Zhang et al., 2004), carried by the Labrador Current, keeping the water temperature below 1°C at 30 m depth from January to May (Colbourne et al., 1997). This water temperature is less than the minimum 2°C necessary for spawning. The water temperature peaks at >12 °C in August, but quickly decreases thereafter (Colbourne et al., 2012).

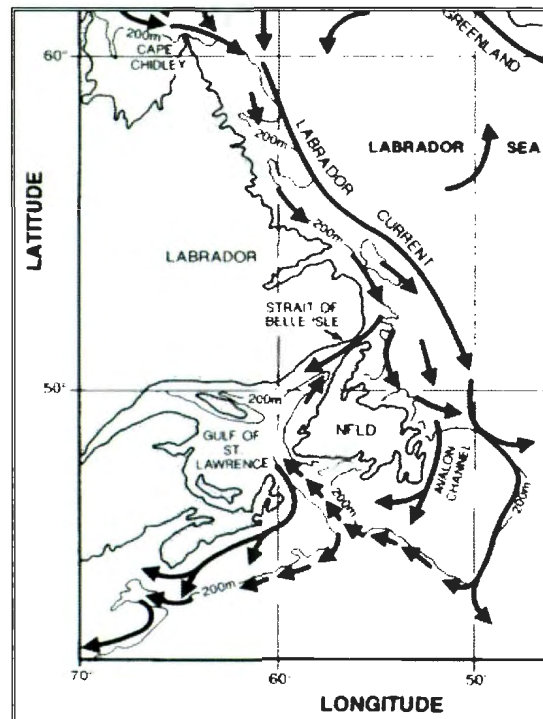


Figure 3-2: Map of the Northwest Atlantic region showing the Labrador Current and its branches. Adapted with permission from E. Colbourne (Colbourne et al., 1997)

3.6 Marine ecosystem

The marine ecosystem of the study area is described as boreal (Livingston and Tjelmeland, 2000) and diverse. The main food web species of the ecosystem are plankton, shrimp, capelin, cod, seal, whale, and many seabirds like gulls, common murre, gannets, and puffins (Carscadden et al., 2002). Capelin is considered a key species of the northeast coast ecosystem, situated between the trophic levels of small species and the larger predator species (Davoren et al., 2006). The ecosystem is sensitive to variations in water temperature. The region experienced fluctuations in water temperature in the 1990s (Davoren and Montevecchi, 2003), which impacted the ecosystem through species growth and food availability (Carscadden et al., 2002). The region's ecosystem sustains a fishery as well as ecotourism activities such as whale and seabird watching.

4 DATA SOURCES AND METHODS

Chapter 4 presents the data used in this habitat mapping project, as well as an overview of the data acquisition and quality assurance processes. Following an introduction to the basic principles of sonar data acquisition, the processing steps required to extract relevant information for habitat mapping from multibeam data are described and illustrated schematically in Figure 4-1. Data analysis began by determining the appropriate spatial scale with which to analyze the spawning site characteristics on the seafloor. Next, the morphologic characteristics of the spawning sites were identified, followed by the definition of the substrate classes used to describe the seafloor. Finally, the steps involved in the production and validation of spawning habitat maps from a supervised classification are outlined.

Data Analysis Flow Chat Demersal Capelin Spawning Sites

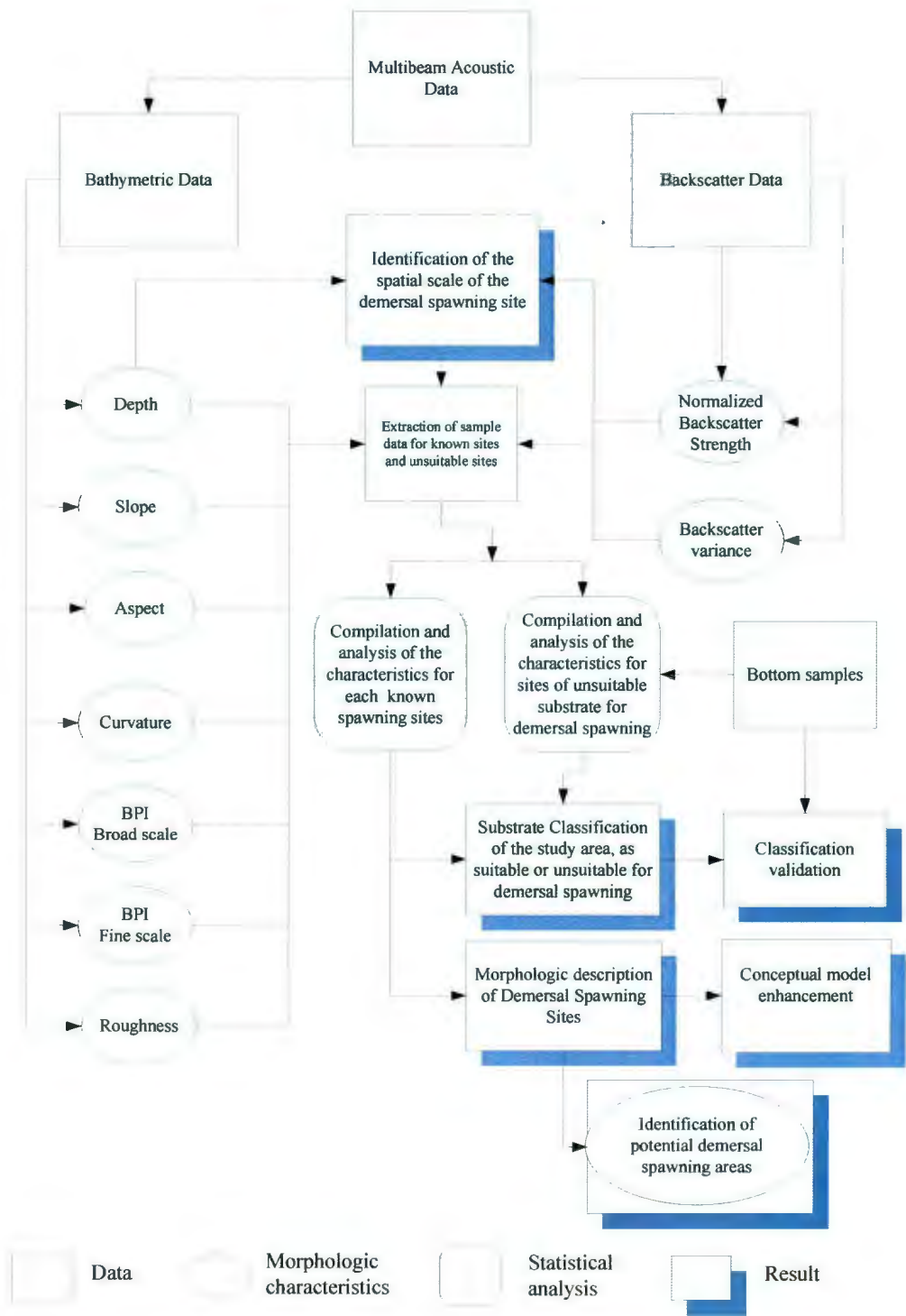


Figure 4-1: Flow chart of the operations to describe and classify demersal capelin spawning sites from multibeam sonar data.

4.1 Data acquisition and processing

Data from the multibeam echosounder cannot be analyzed until it is properly processed and formatted. This section summarizes the acquisition of acoustic data and outlines some mandatory processing steps that must occur before the data can be validated and analyzed.

4.1.1 Multibeam dataset

During the summers of 2006 and 2007, the Canadian Hydrographic Service (CHS) collected the hydro-acoustic dataset analyzed in this study. The dataset was collected using two hull-mounted Kongsberg EM3002 multibeam echosounders. The echosounders were hull mounted on two 9.4 m-long hydrographic launches, called the *Plover* and the *Pipit* (Figure 4-2). The system operates at a frequency of 300 KHz, and can record up to 254 soundings per ping. The maximum across-track opening angle is 130° and the along-track opening angle is fixed at 0.5°. The echosounders can achieve a depth resolution of 1 cm (Kongsberg, 2009). From the acoustic data collected, two specific data layers were produced: (1) the bathymetry and (2) the intensity of the acoustic return (i.e. backscatter). During the execution of the survey, a line pattern was run by the hydrographic launches to cover the entire study area. One acoustic file was created for each survey line (Figure 4-3). The multibeam echosounders produced binary files from which the backscatter and bathymetric data could be extracted.

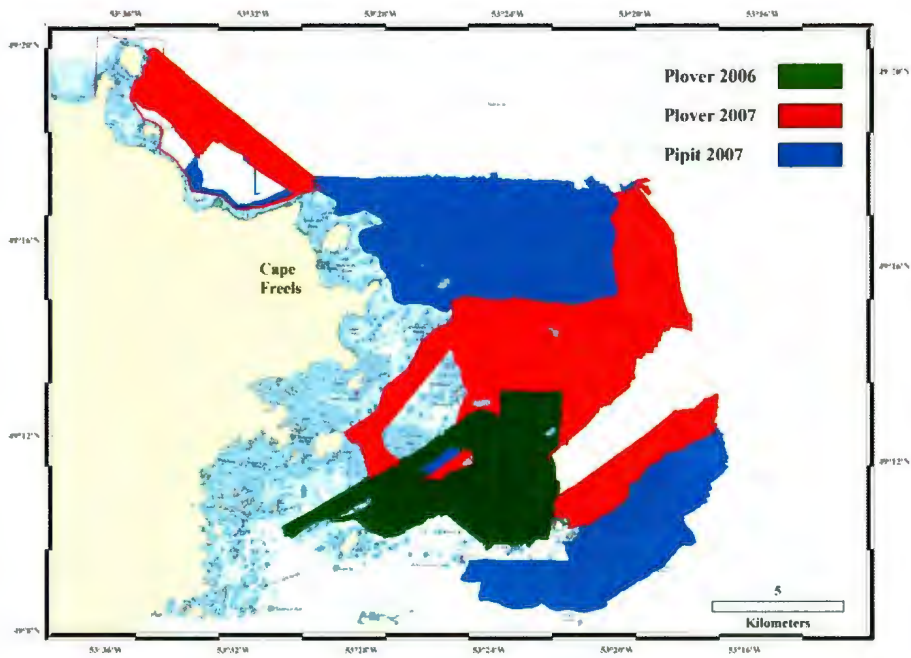


Figure 4-2: Map showing the spatial and temporal multibeam coverage by the launches *Plover* and *Pipit* across the study area.

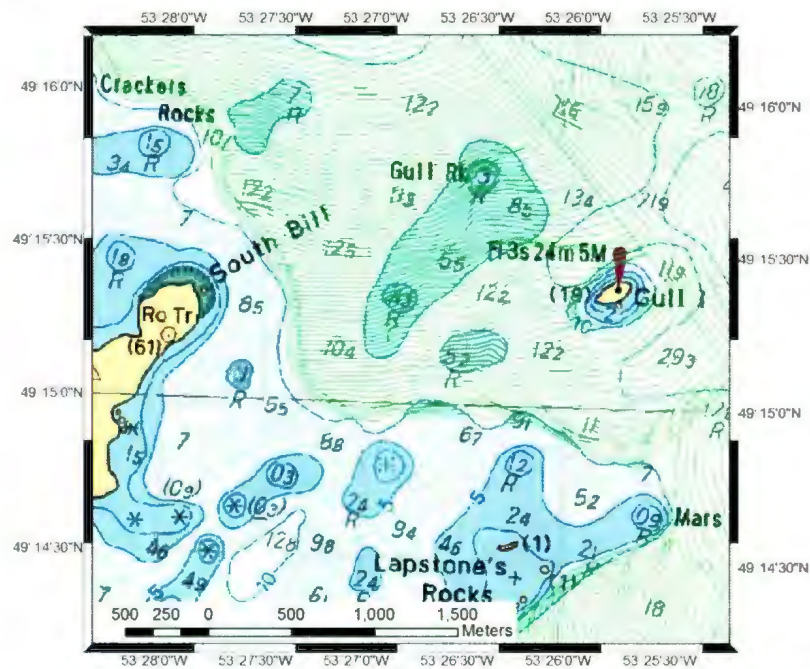


Figure 4-3: Map showing the survey lines (in green) over a portion of the study area. The survey lines are superimposed on the Canadian nautical chart 4857 which depicts depth in metres.

4.1.2 Bathymetric data and its processing

The bathymetric data were processed with the software CARIS HIPS/SIPS 6.1 (www.caris.com). Corrections were applied to compensate for vessel motion and tides, and to flag any echoes that did not appear to be reflected from the seafloor. This process is known as data cleaning. During this step, acoustic data that could be associated with noise or benthic flora were rejected; the remaining dataset reflects only the bottom of the seafloor. Due to this data cleaning process, no values were associated with noise or the presence of aquatic flora during later backscatter processing.

The manufacturer of the echosounders certifies that the data collected meets the special order of the S-44 depth accuracy requirement of the International Hydrographic Organization (www.iho.int) for bathymetric surveying (www.km.kongsberg.com). The requirement varies with depth. For example, depths surveyed in 20 m should have a precision of +/- 0.3 m. The bathymetric data were processed for quality assurance and standard compliance according to the standards of the Canadian Hydrographic Service. The statistical accuracy of the multibeam data in three dimensions (xyz) was assessed by creating an uncertainty surface at a resolution of 5 m, using the CARIS Total Propagated Error (TPE) algorithm (Figure 4-4). The software generated a predicted uncertainty value, which combined the vertical and horizontal predicted error (Calder, 2003). The algorithm was incorporated into the HIPS/SIPS data processing software as part of the Combined Uncertainty and Bathymetry Estimator (CUBE) algorithm (Calder, 2003; www.caris.com). The surface showed that most of the data had a positional uncertainty of

less than 0.5 m. Only the data deeper than 100 m on the edges of the survey had uncertainty values above 1 m (Figure 4-4) due to the larger beam spreading.

A 1 km² subset of bathymetric data, centred over each of the five known capelin spawning sites, was extracted and analyzed. This particular areal dimension was selected because Rose-Taylor (2006) demonstrated that such an area provided an effective representation of seafloor substrates in and around spawning sites in the study area. The spatial resolution of the grid used to generate these subsets was 1 m. These high-density datasets were specifically used to accurately capture the morphology and substrate character of the spawning sites, including percent coverage of each substrate class. Working with a contained area had the added benefit of keeping the digital data files manageable. A 5 m resolution grid covering the entire study area was produced for the bathymetry. This resolution captured the detailed habitat features that were expected to range from 10 to 20 m in size (Anderson, 2001). The 5 m grid was also chosen to keep the amount of data manageable. Regular grids at 1 m and 5 m resolution were created in HIPS using all of the soundings. ASCII files were used to transfer the grids from HIPS to ArcGIS. All datasets used the WGS 1984 datum and the Universal Traverse Mercator (UTM) projection, zone 22N.

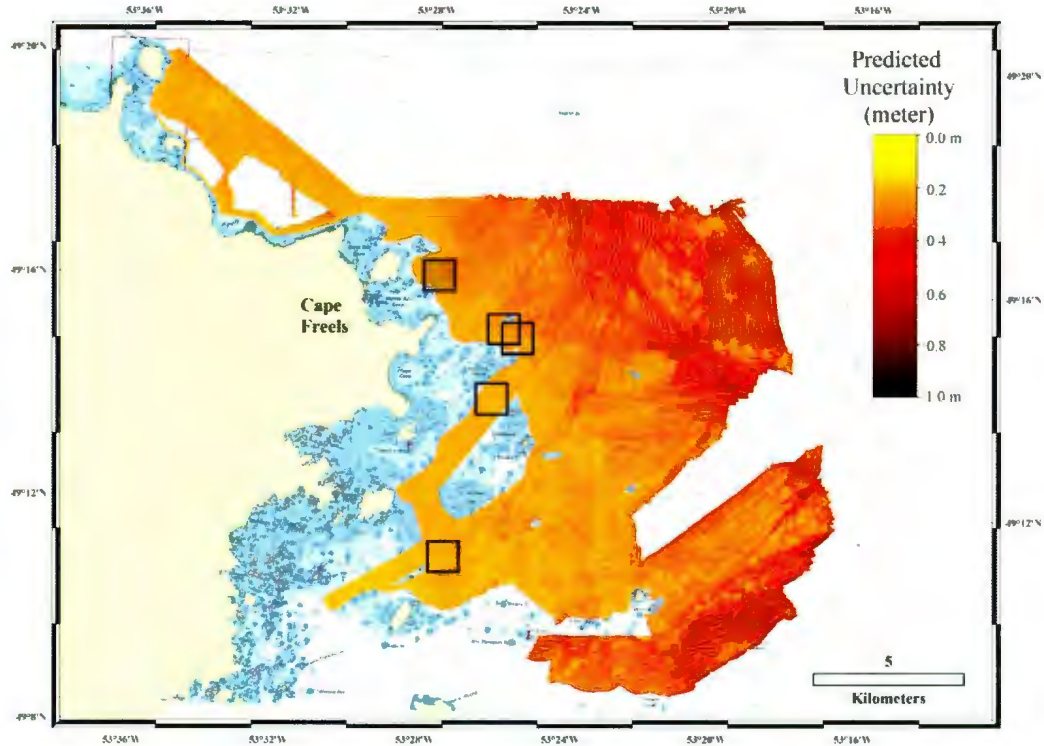


Figure 4-4: Map showing the uncertainty associated with bathymetric multibeam data. Most of the study area has a predicted bathymetric uncertainty below 0.4 m. The black squares show the location of the 1 km² grid cells surrounding the known spawning sites.

4.1.3 Compensation of backscatter data

Backscatter is the amount of acoustic energy returned from an acoustic echo reflected by the seafloor. It is commonly used as a proxy for the grain size of surficial sediments (Collier and Brown, 2005; Fonseca and Mayer, 2007). A complication in quantifying this parameter arises, however, because most of the energy of the sound wave, once reflected by the seafloor, is deflected away from the transducer due to the angle of incidence. In fact, only a fraction of the energy is returned to the transducer. As the angle of incidence grows, the proportion of energy reflected back to the transducer gets smaller. This

relationship is represented by Lambert's Law (Hammerstad, 2000) and needs to be compensated for when using backscatter data. Additional loss of energy comes from the spreading and attenuation of the acoustic signal in the water column; the greater the distance between an object and the transducer, the greater the energy loss. Due to these characteristics of sound propagation, it is important to normalize the backscatter intensity for angle and range (Tang et al., 2005).

A Time Variable Gain (TVG) correction was used to compensate for the loss of energy caused by range and angle of incidence. This compensation renders targets of the same nature with a similar backscatter value, regardless of their distance and angle in relation to the acoustic transducer (Marszal, 2007). In the case of the EM3002, the TVG values were calculated, logged, and applied in real time. During post-processing, however, this compensation was reversed and a new one applied with a different algorithm. Post-processed TVG are more accurate than real time ones, due to the availability of the complete returned signal.

After normalization and TGV correction, the strength of the returned acoustic energy depends on two variables: density difference and angle of incidence with the seafloor. The density difference between the ambient water and the seafloor substrate will vary depending on the characteristics of the substrate. For example, a rocky ledge reflects more sound than a muddy bottom. The second variable, the angle of incidence with the seafloor, causes the backscatter imagery to reflect the shape of the seafloor and is not to be confused with the compensation correction above. Sand waves, for example, produce a

continuous variation in the angle of incidence between the sound wave and the seafloor, which causes a continuous variation in signal intensity. By removing the amplitude variation caused by the angle of incidence on the seafloor, the backscatter values attributed solely to the substrate grain size can be isolated. The swath of bathymetry obtained from the multibeam system is used to calculate a tangent plane at the backscatter location. The subtraction of the tangent plane angle from the beam angle (Figure 4-5) gives the true angle of incidence of the backscatter value (De Moustier and Matsumoto, 1993; Preston, 2009).

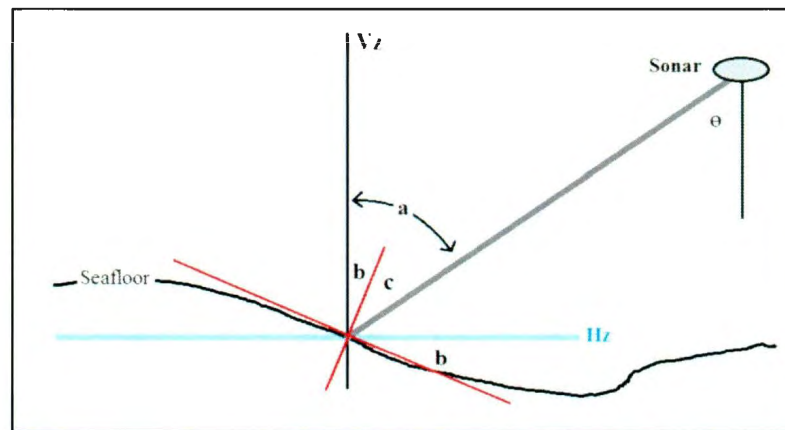


Figure 4-5: Image depicting the correction for angle of incidence. Angle a is the angle of incidence given by the beam angle θ . The red line is the tangent at the backscatter point giving the slope of the seafloor, angle b. The equation $a-b=c$ gives the corrected angle of incidence between the beam and the seafloor. Hz identifies the horizon and Vz the vertical to the horizon.

The two EM3002 transducers that were used during the survey were not calibrated for backscatter values, allowing relative comparison of backscatter intensities, but not actual decibel intensities that could be compared between the two systems. As a consequence, the exact amplitude of the signal transmitted and received by the multibeam transducers is not known. Thus, acoustic strength cannot be determined, and the backscatter cannot be

expressed as an absolute value (Preston, 2009). The compensated backscatter value is relative and dimensionless. The values are encoded on 8 bits ranging from 0 to 255 and have no unit. The backscatter data for this study was encoded such that values start at 0 and grow linearly to a maximum possible value of 255. A separate compensation tables must be created for each transducer, and for any changes in transducer settings for pulse length. The tables created are an empirical compensation (Preston, 2009) and therefore acoustic strength cannot be directly compared with other locations.

4.1.4 Processing of backscatter data

QTC MultiView (Version 400-718) software was used to produce the compensated backscatter dataset from the echosounder raw data files. The method used for processing the backscatter from the multibeam echosounder with QTC MultiView is described in Preston (2009). The first step was to convert the Kongsberg data files into QTC MultiView format. During this process, the compensation table for range and angular response was built. Limits for the grazing angles were established between 10° and 85° . Data captured from grazing angles that were too small or from angular artefacts close to the nadir zone of the multibeam swath were considered unacceptable and discarded (Preston 2008). Values below 10° had an amplitude too high to calculate angular correction; values above 85° were outside the opening angle of the swath of the multibeam system and therefore identified as erroneous.

The backscatter data located in the nadir zone as well as the echoes identified as noise during the bathymetry cleaning were flagged as not suitable for seabed classification and were not used after data conversion. This information was imported from HIPS/SIPS into the MultiView software automatically. The full resolution, compensated backscatter was segmented in ASCII format for each survey line and then amalgamated into one large file for each 1 km² area surrounding the known spawning sites. For each point file imported into the GIS, a series of raster images were created at 1 m resolution.

It was not technically possible to create a backscatter grid at full resolution for the entire study area. The ASCII files generated by MultiView were too big to be loaded and aggregated into the ArcGIS software. To keep the file size manageable, a series of ASCII files containing all the backscatter point data was created for the two multibeam systems. MultiView does not properly export files exceeding 2 GB, therefore the point files had to be limited to that size. For each point file imported into the GIS, a series of raster images were created at 5 m resolution. A mosaic was created from the raster files within the GIS using the mean value as a solution for overlapping cells.

The backscatter data from the *Pipit* and *Plover* echosounders had to be processed separately, even though the instruments were very similar and operated at the same frequency. After processing, it was necessary to evaluate the significance of any differences between the two systems. A comparison of overlapping data in both datasets was conducted by subtracting the two raster images, compiled at 5 m resolution. The

results determined whether the two backscatter datasets could be analyzed together or had to be examined separately.

4.1.5 Bottom samples

A series of bottom samples (appendix B) were collected by DFO in Newfoundland from 2001 to 2005 and were processed by Rose-Taylor (2006). The samples were collected over areas of known spawning sites as well as in a grid pattern in the vicinity of Gull Island (Figure 4-6). A higher density of samples was taken in the spawning areas of Gull Island 1 and 2. Due to the impossibility of collecting rock outcrop samples with a Petersen Grab, the sites of obvious bedrock on the seabed were identified from the multibeam image within each spawning area at 1 m resolution. The morphological characteristics of these locations were then determined as if they were bottom sampling sites. This also increased the number of samples available within the spawning areas. The bottom samples collected by DFO were used to supervise and validate the classification of the spawning areas as well as the study area. Not all samples were used to supervise the classification. Due to the high volume of samples, significant quantities were only taken from within the spawning areas to extract the morphologic characteristics at 1 m and 5 m resolution (appendix C).

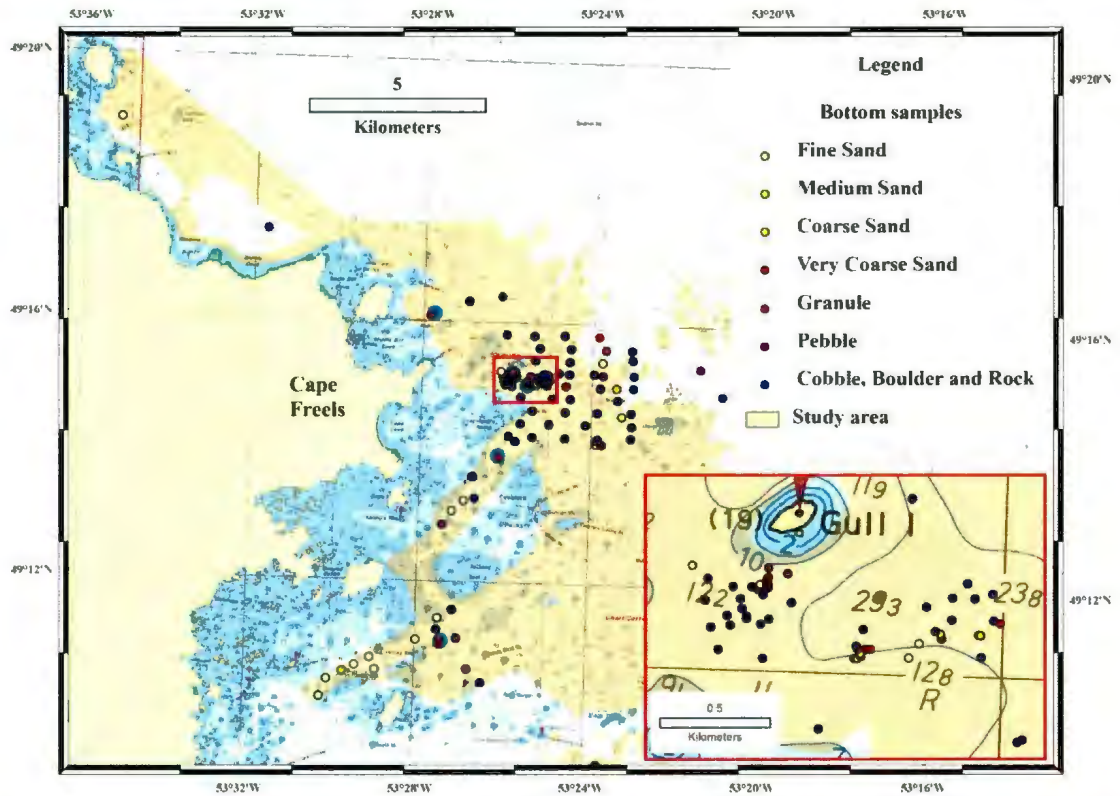


Figure 4-6: Location and nature of the bottom samples used to validate the classification of substrate suitable for demersal capelin spawning. A brown shadow outlines the study area. An inset depicts an area having a high density of samples. It is located at the Gull Island 1 and 2 spawning areas.

4.2 Data analysis

Data analysis began by determining the spatial scale of the phenomenon observed, and then finding the best resolution in which to depict them. Once these determinations were made, data in the bathymetric and backscatter datasets were separated into a series of layers.

4.2.1 Spatial scale and resolution

The data collected for the study area as a whole and the demersal spawning sites specifically had to be analyzed at several spatial scales. The choice of spatial scale was driven by the size of the benthic features under study, the technical limitations of the echosounder resolution, and the limitations imposed by the size of the digital dataset. Details of the spatial scales used throughout the study follow.

4.2.1.1 Data resolution for the known spawning sites and spawning areas

Each spawning site and its surrounding area was defined by a 1 km² area, with the position of the known spawning sites at the centre. The resolution for the data was set to 1 m. This is the optimal data resolution with respect to the density and accuracy of the full resolution point dataset. A higher resolution would render a raster representation with many empty cells as some of the cells would not include any acoustic sounding. Those areas studied at a 1 m resolution will be referred to as “spawning areas” throughout the remainder of this thesis.

4.2.1.2 Definition of spawning site spatial scale

The spawning sites were defined as areas of optimum size in which variances for the backscatter and bathymetric values reached a threshold. To determine this spatial dimension, data variability within circles of different radii centred on the known spawning sites was analyzed (Figure 4-7). The statistical variables plotted for the backscatter and bathymetric data were the range, mean, and standard deviation. The size

of the radius prior to a sizeable change of variance — one which produced an inflection point on the graph — was identified as the best one to represent that spawning site. This analysis was performed for each of the five known spawning sites. The smallest overall radius from the five sites was chosen as the best area to represent demersal spawning sites in the study area. Those sites are referred to as “spawning sites” throughout the remainder of this thesis.

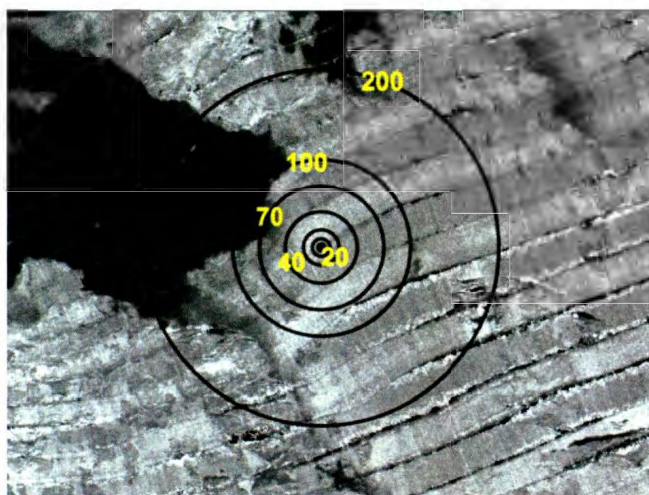


Figure 4-7: Example showing the circles used for the variance study at the Hincks Rocks spawning site, superimposed on a greyscale backscatter image. The black circles are centred on the known spawning site and the yellow numbers are the associated radius values in metres.

4.2.1.3 Data resolution for study area

All the morphologic characteristics of the study area were depicted at 5 m resolution, which provides a higher resolution than the seabed morphology known to be between 10 and 20 m in size (Anderson, 2001). This area portrayed at 5 m resolution is referred to as “the study area” throughout the remainder of this thesis.

4.2.2 Backscatter

The compensated backscatter data layer acts as a proxy for seafloor grain size (Collier and Brown, 2005; Fonseca and Mayer, 2007). The delineation of the spawning substrate was determined from the backscatter values. The backscatter data were binned at the layer resolution (Table 4-1). Each cell represents a small portion of seafloor. From the backscatter point data binned into cells, three layers, listed below, were produced. All the backscatter data were displayed in the GIS using a greyscale range of 0 to 255.

Mean backscatter value

The value for each cell of this layer is the statistical mean of the backscatter values present within that cell. As the proxy for the substrate grain size, this value was used to delineate an area that corresponded to the spawning substrate identified in the conceptual model.

Backscatter standard deviation

The value for each cell of this layer is the standard deviation of the backscatter values present within that cell. The standard deviation is a measure of variance, which was used to characterize the variation in backscatter within each cell. Standard deviation is expressed using a relative scale ranging from 0 to 255.

Backscatter count

This layer records the number of backscatter points present within each cell grid. The value represents n for each cell from which a backscatter value was calculated. The backscatter count was used to ensure an adequate number of points for statistical analysis; no substrate characteristics were extracted from this layer.

Backscatter data range

For each ground truthing site, delineated by a 20 m radius circle, the usable range for the mean and standard deviation backscatter values was determined by distribution of the backscatter data. The limits were set at ± 1.5 times the standard deviation on each side of the mean (Figure 4-8). This removed any remaining outliers due to false echoes and angular compensation artefacts. Additionally, by setting a narrower range of accepted backscatter values in relation to the standard deviation tolerance, the possibility of ambiguity between the range of backscatter values and the substrate associated with it was reduced.

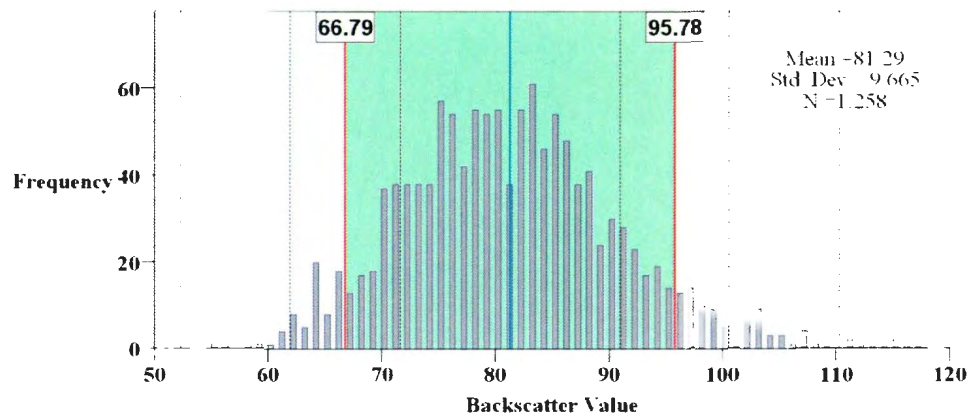


Figure 4-8: Distribution of the mean backscatter values for each cell in the 20 m circle centred on the Hincks Rock spawning site. The vertical blue line indicates the mean value. The dashed lines show the standard deviation intervals. The shadowed green area delimited with red lines indicates the range of values chosen to represent the mean backscatter value for this spawning site. Backscatter is expressed in dimensionless units on a scale of 0-255.

4.2.3 Bathymetry

In the study area, bathymetry was identified as a proxy for bottom temperature (Rose-Taylor, 2006). The minimum temperature necessary for successful demersal spawning corresponds with the 50 m isobath (Rose-Taylor, 2006). Taking this into account, a raster layer corresponding to 50 m water depth and shallower was created to contain the dataset within the temperature range necessary for capelin spawning.

The bathymetry layer is the basis from which the other layers representing the morphology were extracted. Specifically, four morphologic characteristics were derived from the bathymetric dataset: slope, aspect, curvature, and roughness (Wilson et al., 2007). These four layers were created for the entire study area, and again for each of the five 1 km² the spawning areas. The range of values for the morphologic characteristics associated with the five spawning sites was determined from a sample of data collected within a 20 m radius circle centred on the known spawning location. The data were

extracted from the 1 km² layer. Table 4-1 shows the resolution at which each layer was calculated.

- Slope: the steepness of the seafloor in degrees.
- Aspect: the direction in which the slope faces, measured in degrees azimuth.
- Curvature: the rate of change of the slope (Lanier et al., 2007) expressed as the radius of curvature in metres.

The Benthic Terrain Modeller (BTM) tool, available as an extension to ArcGIS (Wright et al., 2005), was used to generate the layers for rugosity and bathymetric position index (BPI) at a broad and fine scale. The National Oceanic and Atmospheric Administration (NOAA) produced the BTM.

- Rugosity: the expression of the ratio between the surface area and the surface of its corresponding plane (Jenness, 2002)
- Bathymetric Position Index (BPI): a measure of the local variation of the seafloor morphology (Wilson et al., 2007).

BPI can be used for seabed classification (Wilson et al., 2007). It gives a relative indication of the seafloor morphology at a point as it can indicate a peak, a trough, a transition between a peak and a trough (a slope), or a flat area (Figure 4-9). Two spatial scales, a broad scale and a fine scale, were used to describe the BPI. This method uses an annular shape to exclude the region too close to the centre of the cell. Two annulus values

are necessary to calculate the broad and fine-scale BPI. The values are determined by the user and depend on the spatial scale of the phenomenon that they are intended to describe. The first value is the radius of the inner annulus, reflecting the spatial scale of the phenomenon in relation to its surroundings. The second value is the radius of the outer annulus, representing the region to which the centre point will be compared. The bathymetric data between the inner and outer annulus are compared to the value at the centre of the annulus and the algorithm determines the BPI value of a given raster cell (Lanier et al., 2007; Erdey-Heydorn, 2008).

The BPI values were used to investigate the relationship between the steepness of seafloor depressions and the water depth of the spawning sites. A Pearson's correlation was calculated between the broad-scale BPI and depth to address this relationship. The broad-scale BPI is a measure of steepness; a larger number represents a more accentuated change in the bathymetry (Lanier et al., 2007; Erdey-Heydorn, 2008).

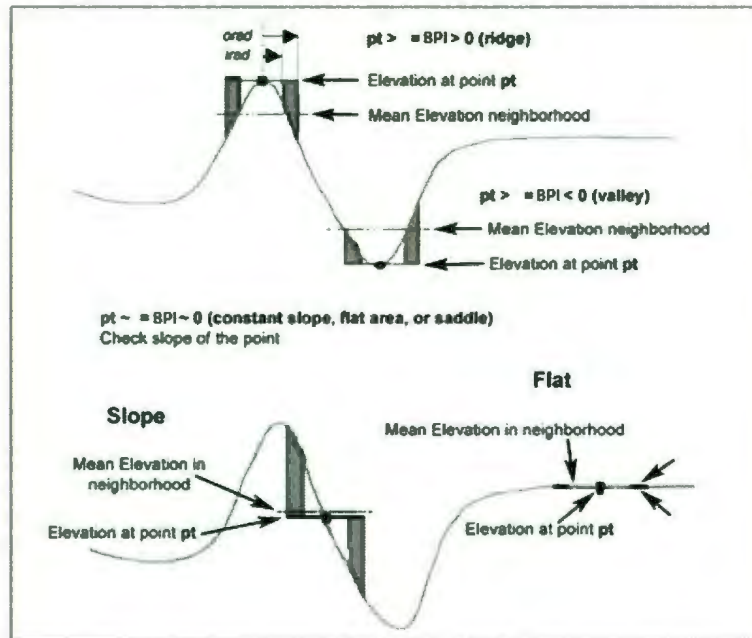


Figure 4-9: Graphic depicting the BPI and how it determines if a point is located on a peak, trough, slope, or flat (Partial Weiss, 2001). In the figure, irad is the inner radius of annulus in cells and orad is the outer radius of annulus in cells.

Table 4-1: List of the layers and their resolutions created into GIS for analysis.

Layers	Area and Resolution		
	Spawning sites	Spawning areas	Study area
	20 m circle (1 m)	1 km ² square (1 m)	(5 m)
Backscatter intensity			
Mean	X	X	X
Standard Deviation	X	X	X
Count		X	
Morphology			
Bathymetry		X	X
Slope	X	X	X
Aspect	X	X	X
Curvature	X	X	X
Roughness	X	X	X
BPI small scale	X	X	X
BPI large scale	X	X	X

4.3 Data classification

Two types of seafloor classification were performed. First, a supervised classification was completed from all the compiled seafloor characteristics. All the data were analyzed by integrating them into different layers of a GIS (Valavanis et al., 2008). The data layers consisted of the physical characteristics of capelin spawning habitat and its surroundings. Second, an automated unsupervised classification was performed using QTC MultiView software.

4.3.1 Supervised classification

For the substrate study, the acoustic reflectivity and morphologic characteristics of the substrate were compiled and analyzed, allowing the seafloor to be designated as one of three classes. The first class included substrate texture varying from sand to pebbles (Rose-Taylor, 2006) that shared the morphologic characteristics of existing spawning sites and was deemed “suitable” for spawning. The two other classes of substrate were unsuitable for spawning: cobble, boulder, and rock, termed “unsuitable coarse substrate”; and substrate finer than sand, termed “unsuitable fine substrate.”

It has already been determined that an area of a certain radius would represent the substrate and morphology of the known spawning sites. This same area was used to sample backscatter and bathymetric data, ensuring phenomena were compared at the same spatial scale. The data sampling sites of the different substrate classes corresponded

to bottom samples collected during previous studies (Rose-Taylor, 2006). The position of some of the samples had to be adjusted with the bathymetric imagery to conform to its morphology. This discrepancy can be attributed to positioning errors inherent in bottom sampling methods.

For each seafloor characteristic for which a layer was created (e.g. backscatter, slope, BPI) a sample of data at 1 m resolution was taken. The size of the sample was dictated by the variance study (cf. section 4.2.1.2). For the suitable spawning substrate, the samples were taken at the known spawning sites. For the two classes unsuitable for spawning, data samples were taken from locations corresponding to the unsuitable bottom samples previously gathered. The minimum and maximum values for each layer were compiled for the three classes. Areas of seafloor that had characteristic values within the range for all layers of a specific class were assigned to that class. If an area had morphological and backscatter characteristics relating to more than one of the three classes, it was classified according to Table 4-2. The seabed was classed as suitable if all conditions were fulfilled, giving priority to suitable over unsuitable. If there was ambiguity between fine and coarse substrate, preference was given to fine, as a low backscatter value is more likely to identify fine substrate. The classification was executed for the five known spawning areas at 1 m resolution, and then at 5 m resolution for the entire study area.

Table 4-2: Classifications decision chart for areas that correlate to more than one class. An x is marked when all the characteristics of a specific category were met.

Category			Classification
Suitable	Unsuitable fine substrate	Unsuitable coarse substrate	
X	X	X	Suitable
X	X		Suitable
X		X	Suitable
	X	X	Unsuitable fine
		X	Unsuitable coarse
			Unclassified

4.3.1.1 Validation of the classification

The substrate classification was compared with bottom samples. The samples provided the ground truthing necessary to quantify the accuracy of the seafloor classification (Collier and Brown, 2005). The bottom samples had been collected for a previous study (Davoren et al., 2007) to obtain a representation of the seafloor substrates.

4.3.1.2 Spawning areas classification (1 m resolution)

Validation was performed by comparing the distribution of the substrate for the combined five spawning areas, obtained from the classification, to the substrate distribution observed through the bottom samples. The five areas represented a sample of 5 km² over the area containing the ground truthing data, which was sampled over 120 km². A valid classification should demonstrate a substrate distribution correlated to the distribution of bottom samples over the study area.

4.3.1.3 Study area classification (5 m resolution)

All bottom samples were compared to the spawning substrate classification (Table 4-3) for the study area. A valid classification should demonstrate a good rate of accordance between the bottom samples and the corresponding classes. The recorded bottom sample positions are affected by inherent errors, due to the differences between the position of the grab on the seafloor and the GPS receiver antenna on the survey vessel. It is reasonable to associate a bottom sample with its corresponding substrate that is located within the margin of error of the sample. To assess the impact of those errors, a search for substrate corresponding to the bottom samples was executed within radii of 10, 20, 30, and 40 m (Figure 4-10). The best estimate of positioning errors of the bottom samples provided the most accurate validation of the classification.

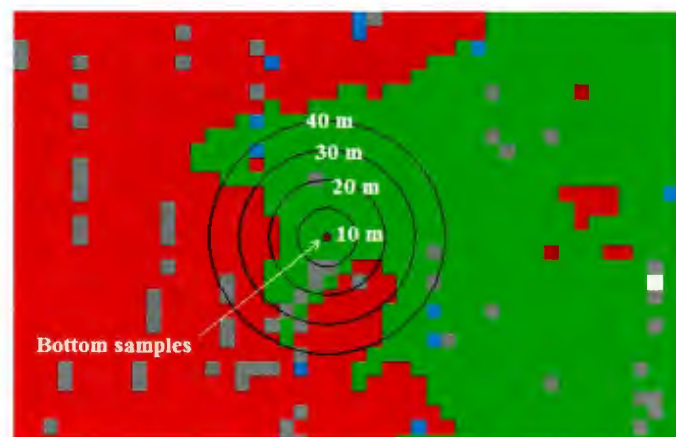


Figure 4-10: Display of error circles around a coarse substrate bottom sample, superimposed on a portion of the study area classification, depicting the different classes it can be associated with, depending on its position error.

Table 4-3: Spawning substrates defining the corresponding classes.

Correspondence of substrate to class	
Bottom sample	Classes of spawning substrate
Fine sand	Unsuitable substrate, fine
Medium sand	Suitable substrate
Coarse sand	
Very coarse sand	
Granule	
Pebble	
Cobble, Boulder	Unsuitable substrate, coarse

As a second check for accuracy, the same method used for the validation of the 1 m resolution data was employed. The distribution of the classes was compared to the substrate distribution observed through the bottom samples.

5 RESULTS

Two technical uncertainties needed to be resolved prior to data analysis: first, the compatibility of the data produced by the two echosounders needed to be established; and second, the characteristics of fine substrate had to be defined using data gathered outside of the five spawning areas. This chapter begins with a resolution of these issues, followed by a description of the seafloor imagery. Next, the representative size of a spawning site is determined. The morphological characteristics and backscatter values associated with each substrate class (unsuitable coarse, unsuitable fine, or suitable for capelin demersal spawning) were then defined and summarized.

Habitat classification maps of all five spawning sites, as well as a classification of the entire study area, are included. The proportion of habitat covered by each substrate classification is shown at both data resolutions used in the study, and the relationship between the two resolutions is established. Bottom samples were compared to the classification results, and a Pearson correlation was used to evaluate the accuracy of the mapping by comparing it with bottom samples. These validation results were presented.

5.1 Similarity of backscatter datasets

Before analyzing the backscatter data, it was necessary to determine if the datasets collected by the *Pipit* and the *Plover* could be combined into one single dataset. To do so, the overlapping backscatter values from the two collections were compared.

Both the mean and the standard deviation backscatter data were compared by determining the difference in values in the overlapping sections of the two backscatter datasets. No visual artefacts attributable to the two different instruments were observed on the combined datasets (Figure 5-1). The mean value of the difference between the two acoustic systems was very close to 0 (Figure 5-2) for both the mean and standard deviation backscatter. The comparison showed that 35% of the data have a difference of less than 5 units across a relative scale from 0 to 255 and 59% are less than 10 for the mean layer. The data were centred on the most frequent zero value, suggesting that both systems were properly calibrated (Figure 5-2). The comparison also revealed that 48% of the data have a difference of less than 5 and 74% are less than 10 for the standard deviation layer (Table 5-1). Given that the less reliable data at the nadir and extremities of the swath were included in this comparison, it was concluded that the two backscatter datasets were similar enough to be combined. The backscatter datasets were merged and considered homogeneous for the data analysis.

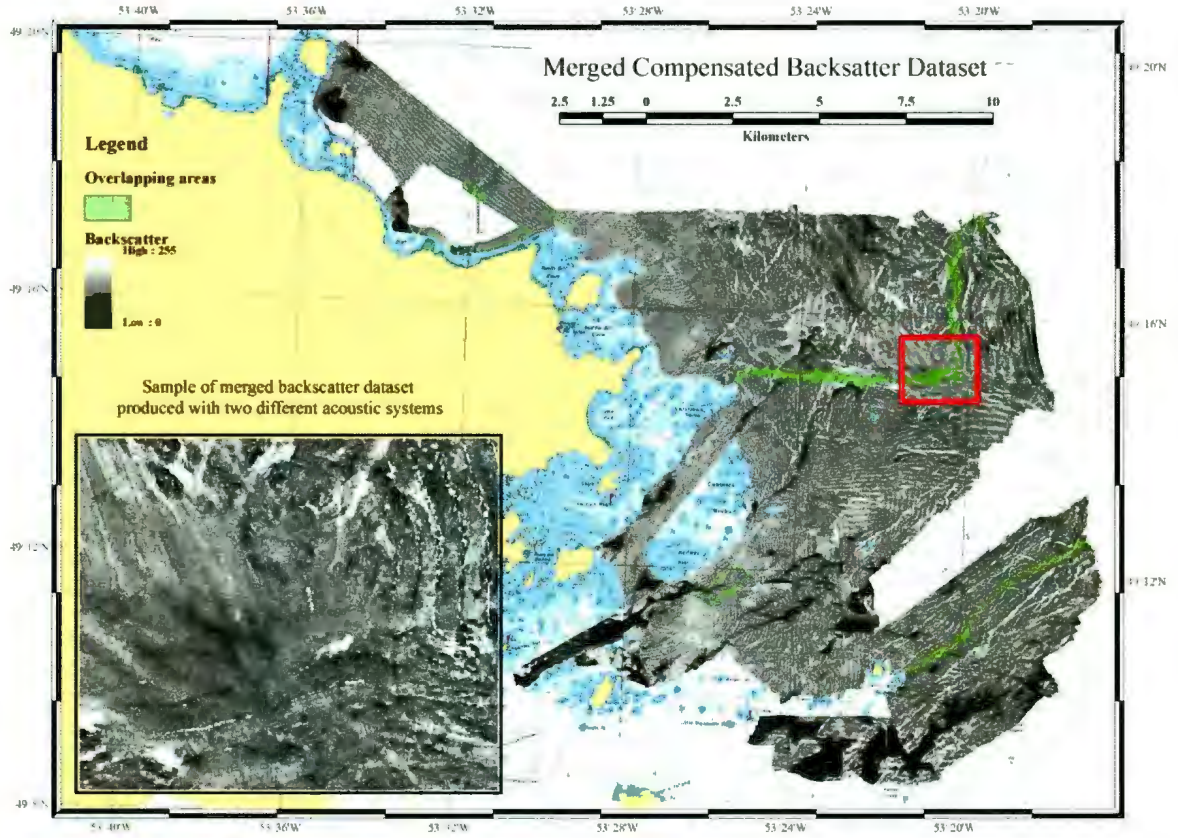


Figure 5-1: Map of the mean compensated backscatter at a spatial resolution of 5 m. Backscatter is expressed in dimensionless units on a scale of 0-255. The dataset is superimposed onto Canadian nautical chart 4857. The areas in which the two datasets overlap are also shown on the map. The enlargement shows the homogeneity of the data.

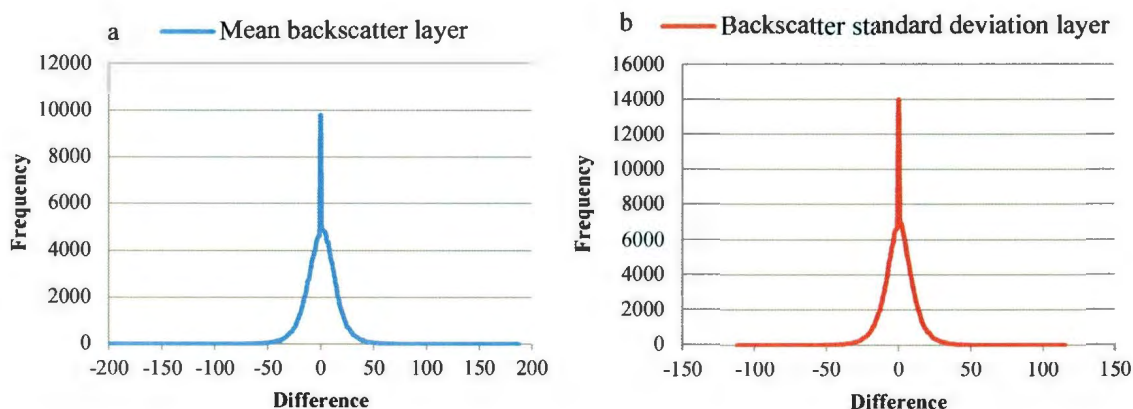


Figure 5-2: Distribution of the difference between the backscatter data from the *Pipit* and from the *Plover*, where both datasets overlap spatially, showing a) the difference in mean backscatter, and b) the difference in the backscatter standard deviation. Backscatter is expressed in dimensionless units on a scale of 0-255.

Table 5-1: Statistics of the differences between the two backscatter datasets. Backscatter is expressed in dimensionless units on a scale of 0-255.

Differences statistics				
Backscatter layer	Mean	Standard Deviation	+/- 5	+/- 10
Mean difference	0.72	15.76	35%	59%
Standard Deviation difference	0.18	11.27	48%	74%

5.2 Definition of fine-grained substrate characteristics

The only spawning area that contained a fine sand substrate bottom sample was the Gull Island 2 site; this was not enough to extract representative acoustic characteristics of fine-grained substrate. In general, the number of fine sand bottom samples available within the study area was very limited. One area at the southwest extremity of the study area, however, provided data of a manageable size for the 1 m resolution, and also contained six fine sand bottom samples (Figure 5-3). In total, seven samples were available for the definition of fine sand substrate at 1 m resolution.

Table 5-2: Number of samples (n) included in the circular areas of a given radius.

Radius (m)	2	4	10	20	40	70	100	200
N	13	51	315	1259	5033	15300	31022	123875

5.3.1 Backscatter results

Analysis of the backscatter variance revealed different curve patterns for each site and each backscatter measure. The variance indicated by the backscatter standard deviation (Figure 5-4a) converged at 20 m and 40 m radii. The only site that yielded an inflection point for backscatter was Hincks Rocks, where the standard deviation values (Figure 5-4a) showed an inflection at 40 m radius. At 20 m radius, the backscatter variance decreased for GI1 and TI, and increased for the other sites. This indicates a change in seabed environment at about this distance. The convergence of the standard variation values for all sites around 40 m indicates that the variance in the spawning areas has been captured at this point. This indicates that spawning sites have a radius smaller than 40 m. The maximum backscatter variance (Figure 5-4b) shows an inflection point at 10 m for Gull Island 1 and 2. Those backscatter values were lower than the smallest maximum backscatter value at the Turr Island site, and so did not represent a realistic limit for the maximum backscatter value attributable to spawning substrate. Other inflection points were observed at 40 m and 70 m.

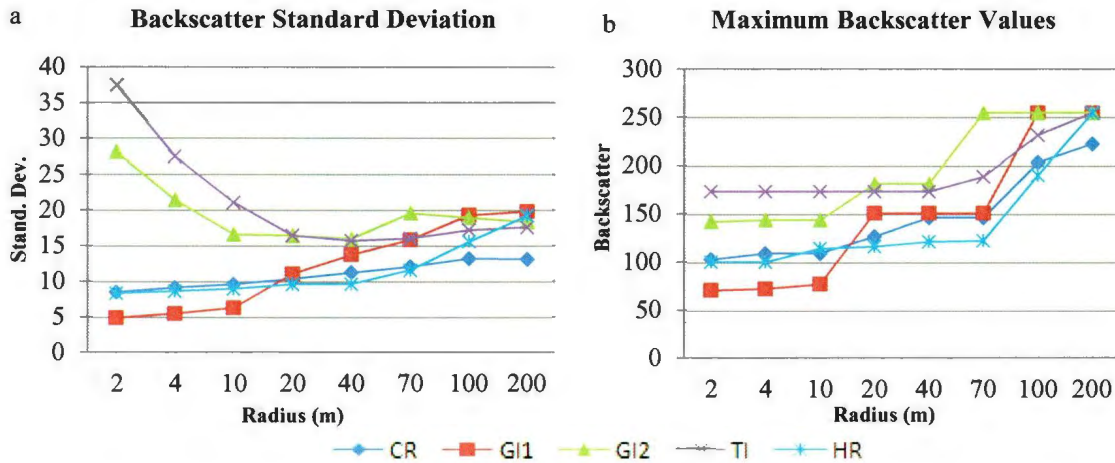


Figure 5-4: Results of the variance study for backscatter values from the five known demersal spawning sites. Backscatter is expressed in dimensionless units on a scale of 0-255. The sites are labelled by their abbreviations. The graphics show: a) standard deviation, and b) maximum variance of backscatter values for a circular area of a given radius.

5.3.2 Bathymetry results

The analysis of bathymetric values revealed a clearer depiction of the rate of change in the variance than the backscatter values. The curves for bathymetry standard deviation (Figure 5-5a) show an inflection point at 40 m radius for all sites. A smaller inflection point was also noticeable at 20 m for the Crackers Rocks site. The bathymetric mean (Figure 5-5b) shows a moderate inflection point at 40 m for all sites, except Crackers Rocks, which displayed a weak inflection point at 20 m. This is consistent with the observation made for bathymetric standard deviation. The bathymetric minimum graphic (Figure 5-5c) shows an inflection at 40 m for all sites, except Crackers Rocks, which shows an inflection at 20 m. This is also consistent with the observation made for bathymetric standard deviation. The mean and minimum values indicate that the water surrounding spawning sites get shallower beyond 40 m radius. The maximum depth

curves (Figure 5-5d) show that spawning sites remain the deepest point of the surrounding area.

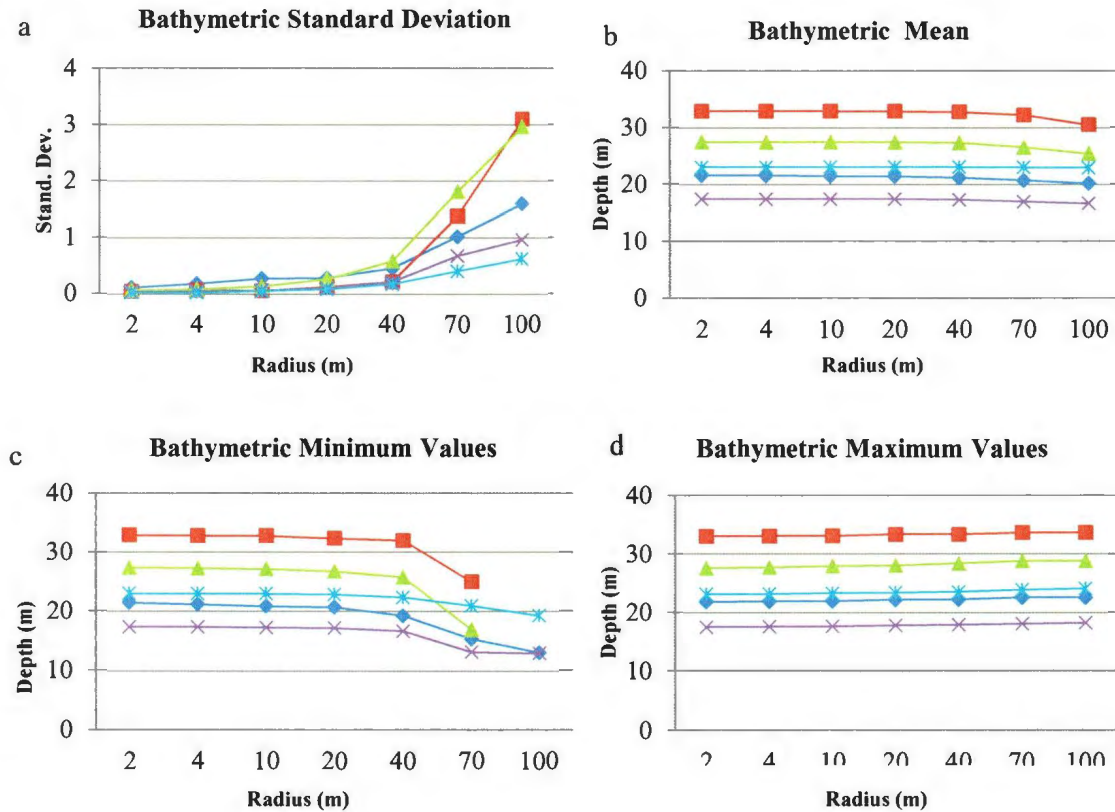


Figure 5-5: Results of the variance study for depth values from the five test demersal spawning sites. The sites are labelled by their abbreviations. The graphs depict the a) standard deviation, b) mean, c) minimum, and d) maximum variance of bathymetry values for a circular area of given radius.

In summary, the analysis of backscatter variance across circular areas of given radius did not clearly define a representative minimum area for demersal spawning sites. The only valuable information was a common standard deviation value at 20 m and 40 m radii for all sites. The analysis of bathymetry data clearly showed the lowest inflection point at 20 m radius. As the 20 m radius value ensured a sufficient number of samples (Table 5-2) and a low variance, it was selected to represent spawning sites in subsequent analysis.

5.4 Morphologic characteristics

5.4.1 Backscatter

The minimum and maximum backscatter values were compiled from the 1 m resolution backscatter datasets at the location of the available bottom samples. They were tabulated separately for each category of substrate mapped (Table 5-3). The frequency in Figure 5-6 and Figure 5-7 was normalized so all substrates could be displayed on a common y axis.

Table 5-3: Compilation of the minimum and maximum values for the mean and the standard deviation observed from the 1m backscatter data. The values were compiled for the three categories of substrate. Backscatter is expressed in dimensionless units on a scale of 0-255.

Category		Mean backscatter layer	Standard deviation backscatter layer
Suitable substrate	Min	56	18
	Max	103	47
Unsuitable, coarse substrate	Min	49	13
	Max	99	47
Unsuitable, fine substrate	Min	32	3
	Max	63	20

Analysis of the mean backscatter data (Figure 5-6) clearly shows that the fine substrate backscatter signature is distinct from that of the spawning substrate. The bivariate distribution of the fine substrate data may indicate two distinct substrates. Only fine sand was identified from the bottom samples. This may suggest that a substrate finer than fine sand is present in the study area. The backscatter data also shows that backscatter values cannot be used to accurately differentiate between spawning substrate and coarse substrate. Similar results were obtained when standard deviation backscatter data were

compared (Figure 5-7). Backscatter data indicate therefore that fine substrate has less variance than other substrates. Because a clear distinction was observed between the suitable substrate and the fine substrate, the mean backscatter was identified as a key measure of distinguishing these two classes.

In summary, analysis of the backscatter values established that the compensated backscatter dataset contained the information necessary to classify fine substrate unsuitable for capelin spawning. Unfortunately, the same analysis also established that it was not possible to detect the difference between suitable spawning substrate (pebble size) and coarse substrate (larger than pebble size and bedrock) unsuitable for spawning (Rose Taylor, 2006). In fact, some of the areas identified as bedrock from their morphology and bottom sampling had lower backscatter values than the known spawning sites (Figure 5-6 and Figure 5-7)

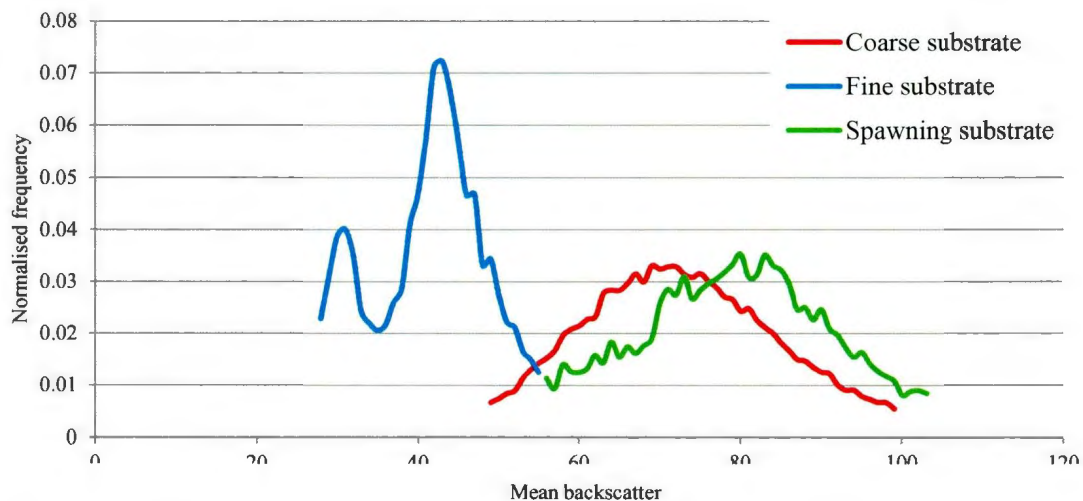


Figure 5-6: Normalized frequency distribution of the mean backscatter values. Backscatter is expressed in dimensionless units on a scale of 0-255.

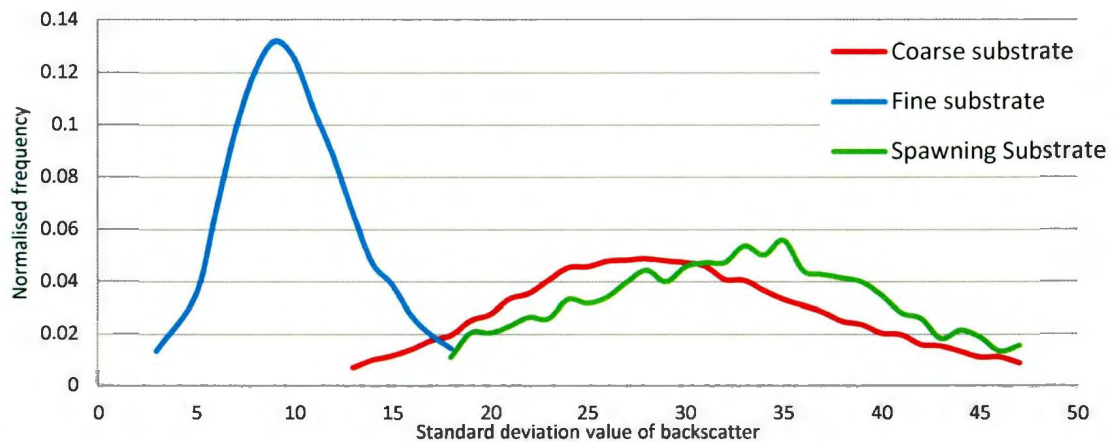


Figure 5-7: Normalized frequency distribution of the standard deviation backscatter values. Backscatter is expressed in dimensionless units on a scale of 0-255.

5.4.2 Bathymetry of the study area and the spawning areas

The morphology of the seafloor offers the first, most accessible insight into the benthic habitat types present in the study area. Large morphologic features like bedrock outcrops or flat plains can be visually identified. The water depth of the study area varies from 5 m to 115 m but most of the area is shallower than 50 m. The geomorphology portrays smooth rounded surfaces in the flat areas that are likely covered by sediment and surrounded by rough angular surfaces that are bedrock outcrops. The seafloor gently slopes on a plateau that extends 8 km to 10 km from shore. The plateau presents a network of trenches between the bedrock outcrops, with the most obvious ones oriented from southwest to northeast. The preeminent flat areas are located at the end of the plateau and are about 40 m deep. The main trenches present depressions that are 20 m deep as the rock outcrop mostly lie in depths of 20 m. Beyond the plateau is the deepest

part of the study area, which shows large tracts of flat bottom with numerous rocky outcrops; these tracts are about two-thirds flat bottom to one-third outcrop. The rocky outcrops are in the order of 60 m above the surrounding depth of 100 m.

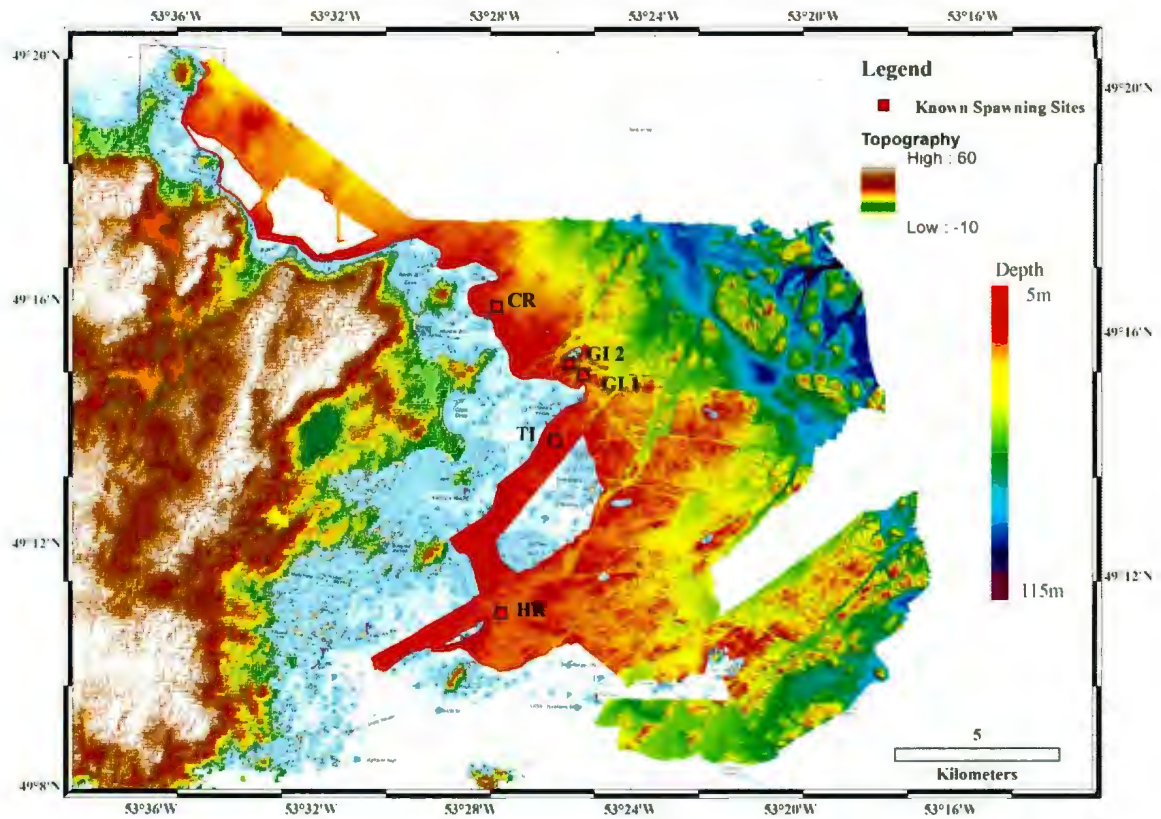


Figure 5-8: Map showing the multibeam survey areas with the corresponding known capelin demersal spawning sites.

The bathymetry of the five spawning areas is described starting from north with **Cracker Rock** (Figure 5-9). The water depth ranges from 7 m to 29 m. The seafloor is generally rough but limited in relief over the 1 km². The area deepens toward the northeast. The spawning site is located in a small depression of only a few metres deeper

than the surrounding low relief bedrock outcrops. The area presents a surface texture suggesting sediments of various sizes.

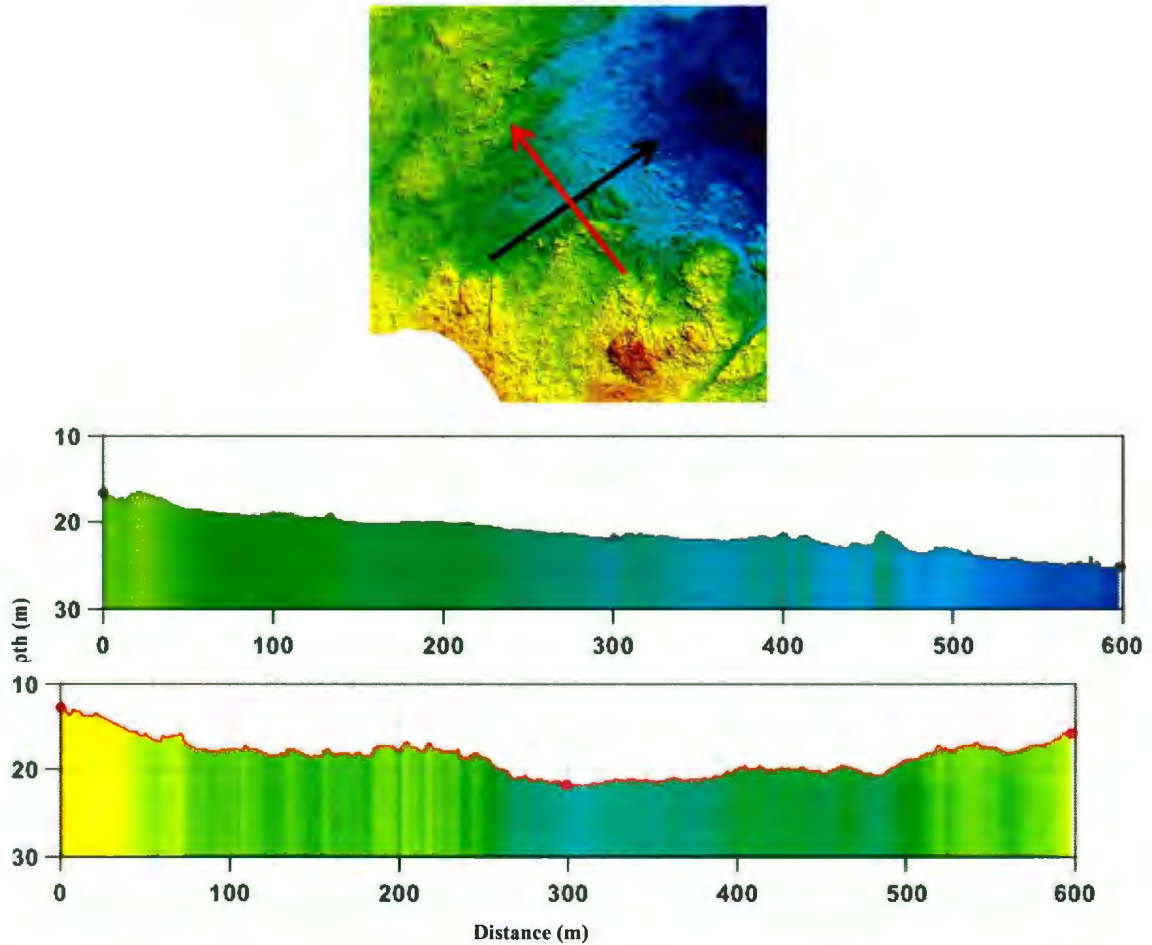


Figure 5-9: One km² subset of the multibeam bathymetric data centred on the known capelin demersal spawning site at Cracker Rock. The images present a 4x vertical exaggeration; the colour represents the depth. The shallowest parts are coloured in red and gradually move toward dark blue as the depths increase. An artificial sun illumination from the northeast at an elevation of 45° enhances the texture of the image. Two cross sections of the spawning site are also presented. The arrows in the top image identify the cross sections by colour and orientation. The dot at the centre of the profile marks the known spawning site.

Gull Island 1 (Figure 5-10): The depth ranges between 7 m and 38 m. The seafloor at the site has flat areas surrounded by bedrock outcrop over the 1 km². This site is the deepest of the five and is located in the middle of a trench that is 10 m deep and 100 m wide, with

an east-west orientation. The trench can be followed eastward to the deepest water of the study area. This area is composed of a network of trenches dissecting the bedrock outcrops. The seafloor of the trenches seems covered by sediment.

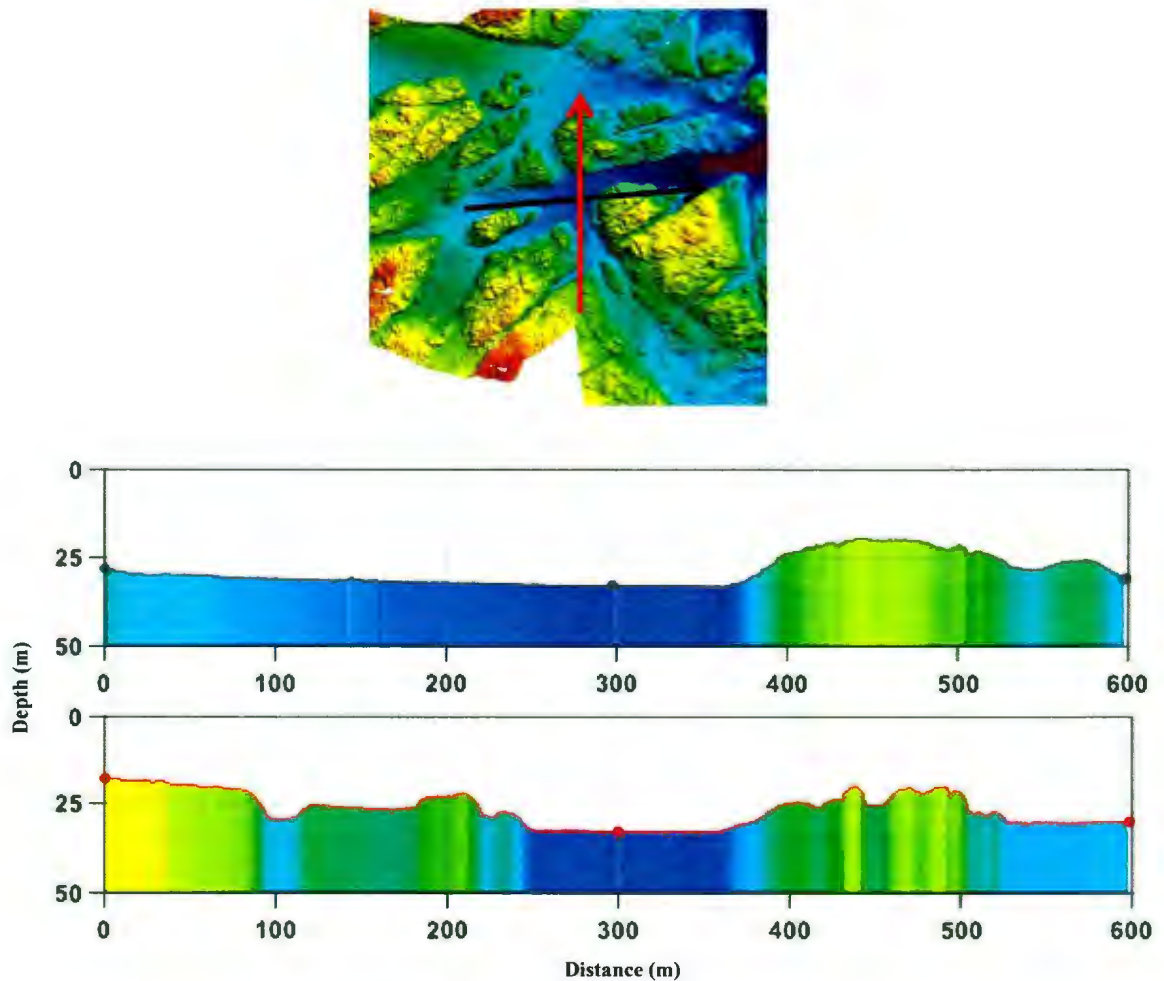


Figure 5-10: One km² subset of the multibeam bathymetric data centred on the known capelin demersal spawning site at Gull Island 1. See Figure 5-9 for explanation of figure details.

Gull Island 2 (Figure 5-11): The depth varies from 6 to 33 m. This site is located just south of Gull Island on a wide flat sea bottom, surrounded by bedrock outcrop. Ripples of

2 m wide by 0.2 m deep can be observed near the site, suggesting sediments. The morphology of the surrounding area is similar to the area of GI1 and shows large rock outcrops rising 10 m from the flat areas.

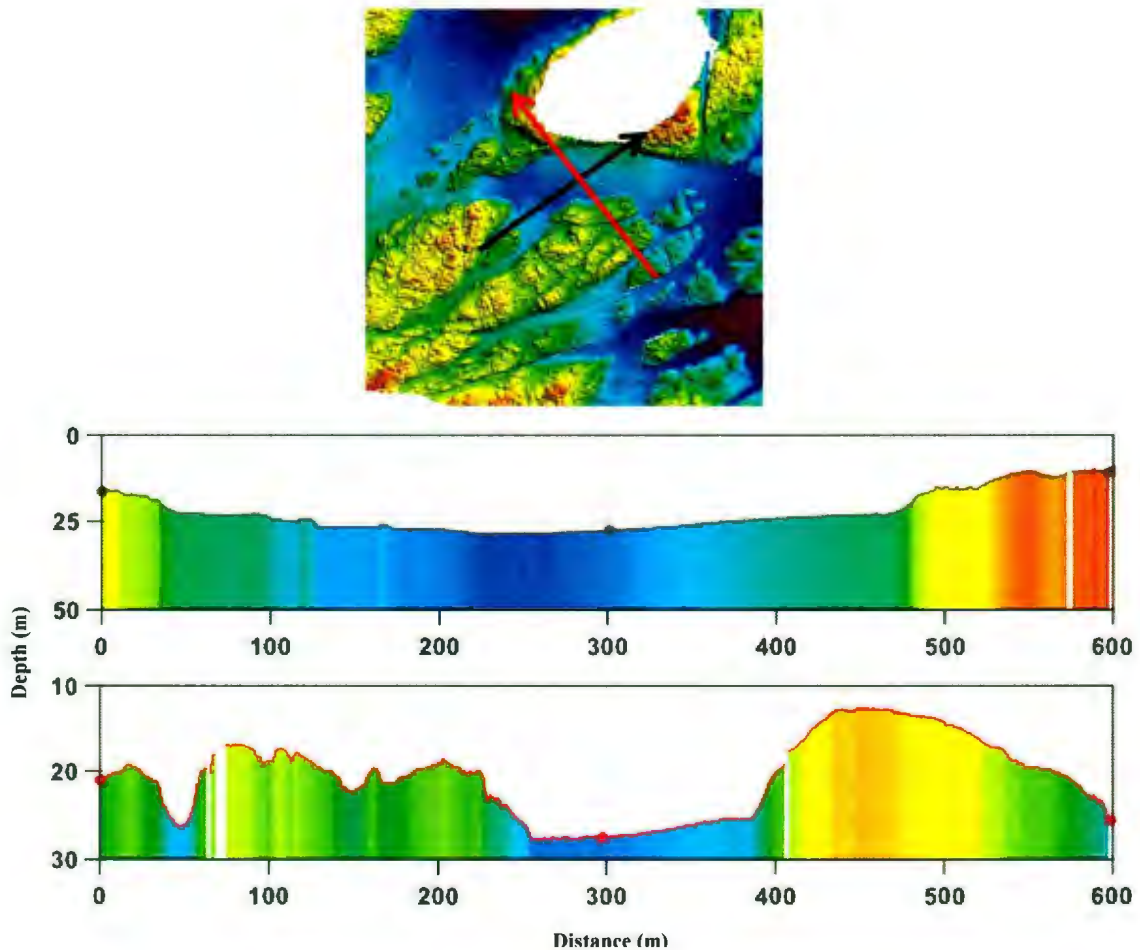


Figure 5-11: One km² subset of the multibeam bathymetric data centred on the known capelin demersal spawning site at Gull Island 2. See Figure 5-9 for explanation of figure details.

Turr Island (Figure 5-12): The depth varies between 5 m and 22 m. This site is the shallowest of the five and is located on a slope leading to an elongated depression that is 5 m deep and 150 m wide and oriented to the northeast. It is surrounded by bedrock outcrop on two sides. The site is located at the shallow end of a trench that is connected to

the deepest part of the study area. Sediments appear to cover the seafloor surrounding the rock outcrop over the 1 km² area.

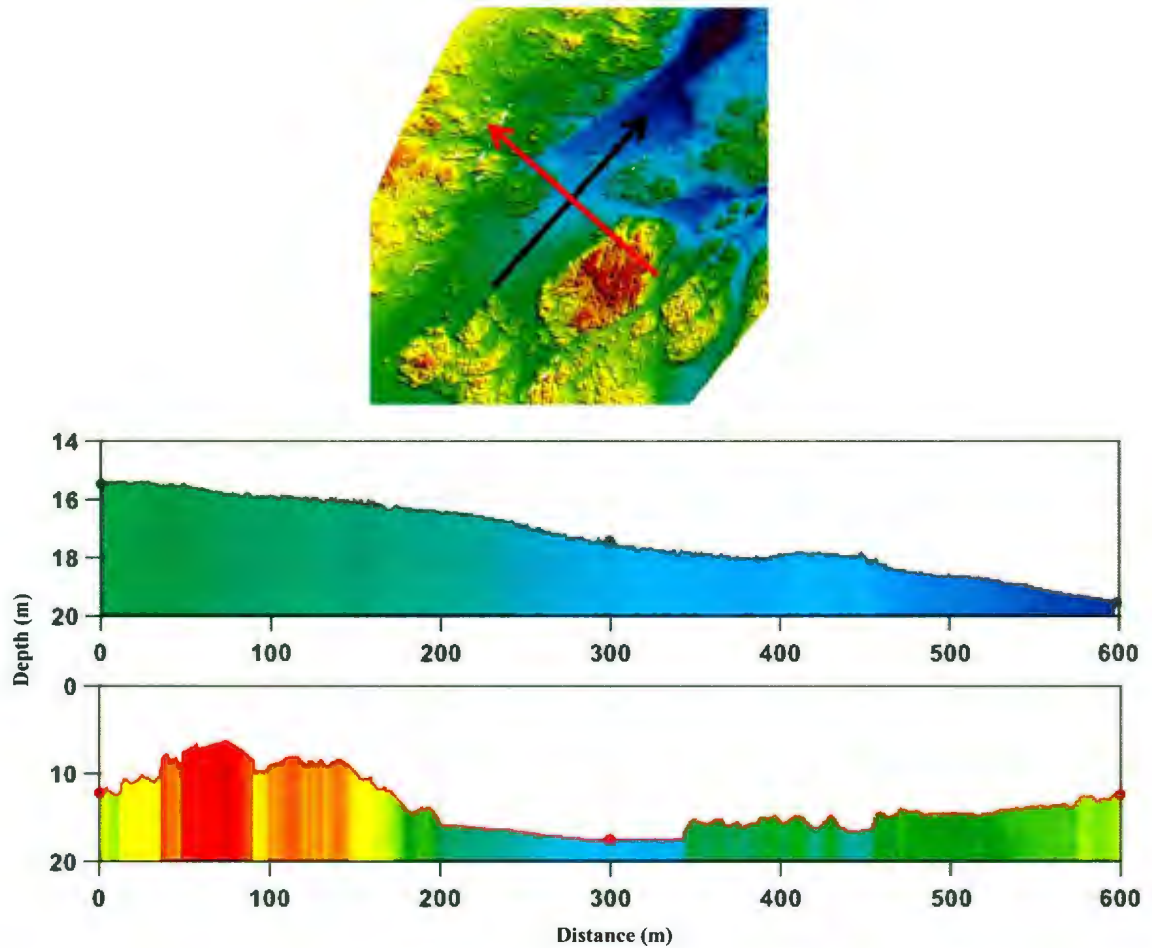


Figure 5-12: One km² subset of the multibeam bathymetric data centred on the known capelin demersal spawning site at Turr Island. See Figure 5-9 for explanation of figure details.

Hincks Rock (Figure 5-13): The depth varies from 5 m to 24 m. This site is located in the middle of a broad depression of 400 m diameter and 2 m depth. The area is surrounded by isolated rock outcrops 8 m high. Most of the 1 km² is flat, with a few shallow rock surfaces that crop out 1-2 m above the sediment surface. Unlike the last three sites

described, no networks of trenches were observed. The relief is less accentuated by comparison.

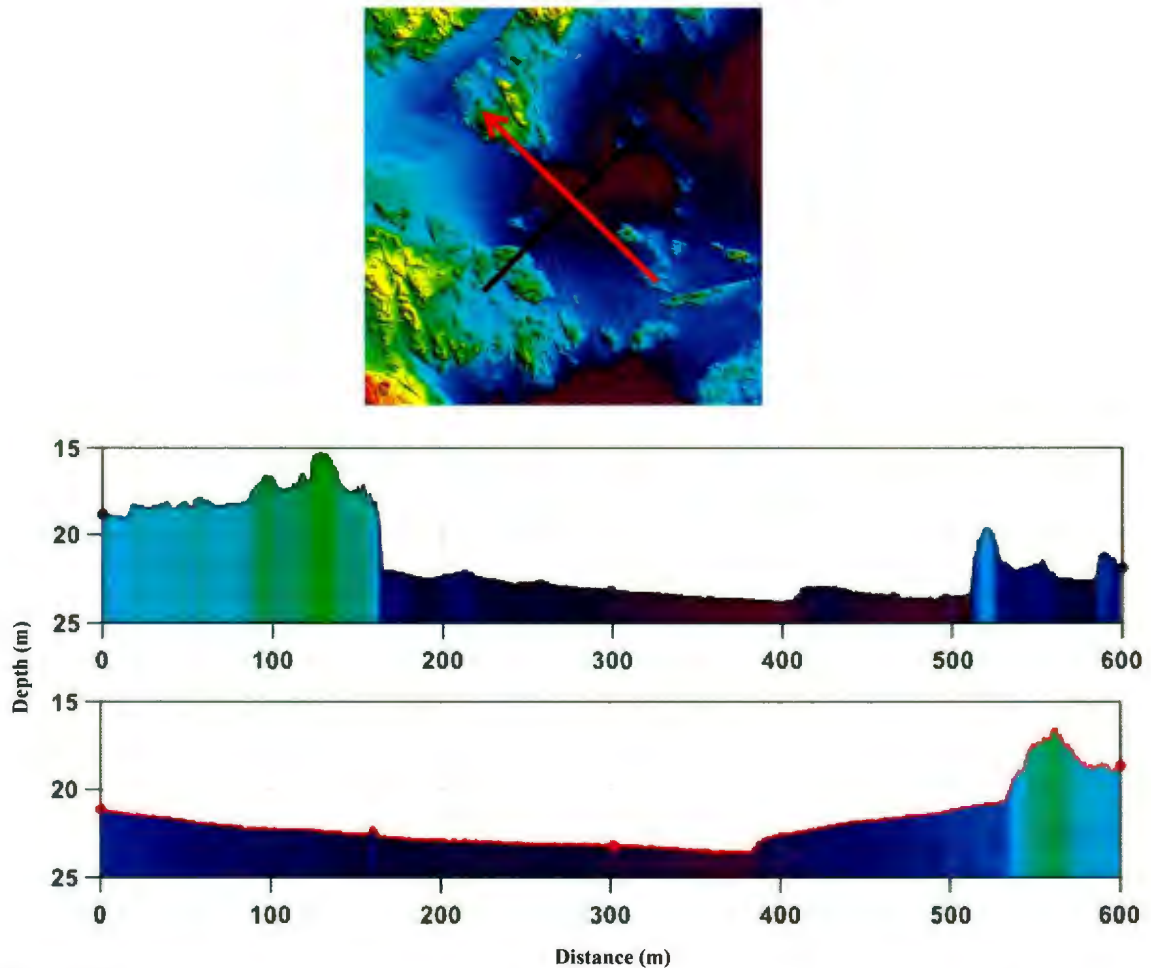


Figure 5-13: One km² subset of the multibeam bathymetric data centred on the known capelin demersal spawning site at Hincks Rock. See Figure 5-9 for explanation of figure details.

Together, the seafloor profiles show that the spawning sites are consistently located in the middle of a roughly flat-bottomed depression partially surrounded by moderate bedrock slopes on at least two sides. Depressions range in minimum width from 100 to 300 m (Figure 5-14).

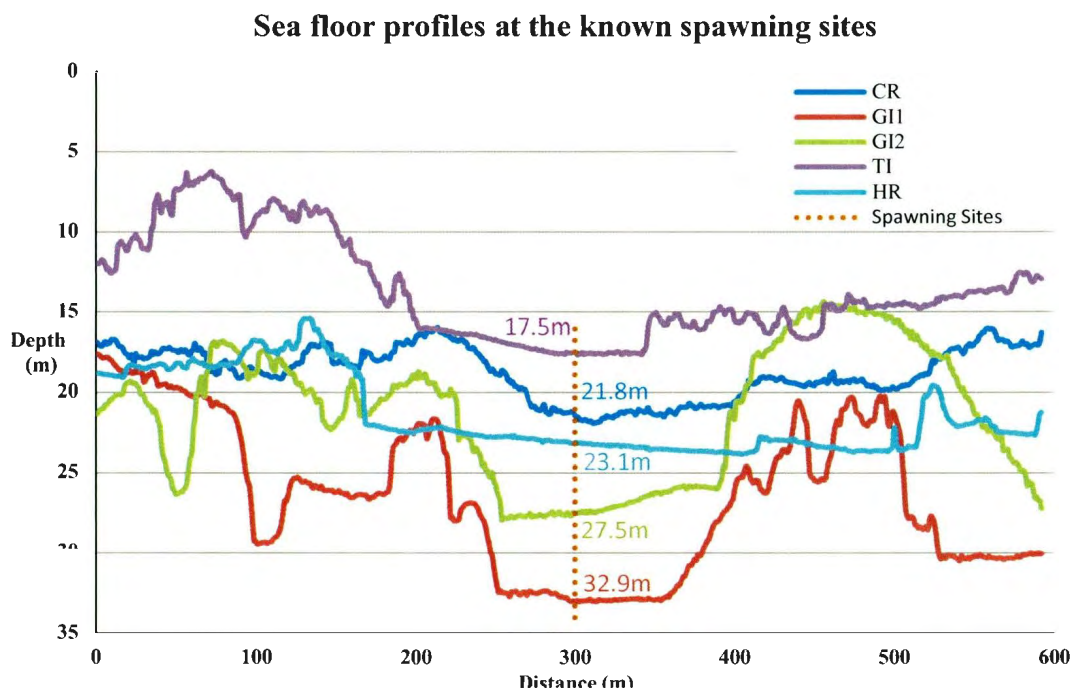


Figure 5-14: Superimposed depth profiles of the five known spawning sites, shown at a 10X vertical exaggeration.

5.4.3 Morphology derived from depth

The morphological characteristics and surface roughness of each substrate class were derived from the bathymetry of bottom sampling sites. Five measures were calculated: slope angle, curvature, rugosity, broad-scale bathymetric position index (BPI), and fine-scale BPI. The minimum and maximum values of these morphologic characteristics were compiled for each class of bottom substrate (Table 5-4).

Table 5-4: Compilation of the minimum and maximum values for the slope, curvature, rugosity, broad scale BPI, and fine-scale BPI for each of the three substrate types. They were extracted from the sampling of the bathymetric data produced at 1 m resolution.

		Slope (Degrees)	Curvature (Radius, m)	Rugosity (Ratio)	Broad- scale BPI	Fine-Scale BPI
Suitable substrate	min	0.01	-196	1.00	1	0
	max	18.89	134	1.19	7	1
<hr/>						
Unsuitable substrate grain size too large (Coarse)	min	0.03	-541.20	1.00	-12	-3
	max	63.42	604.30	2.47	2	3
<hr/>						
Unsuitable substrate grain size too small (Fine)	min	0.01	-97.20	1.00	0	0
	max	8.78	101.40	1.05	4	1

5.4.3.1 Slope, curvature, rugosity, and aspect

From the slope angle (Figure 5-15), slope curvature (Figure 5-16), and rugosity (Figure 5-17) data ranges, a narrow spread of values was observed for both the unsuitable fine and suitable substrates compared with the unsuitable coarse substrate. There is a direct correlation between grain size and the maximum value for each of the three morphologic characteristics. The same was not true for the minimum values. This is explained by the fact that the data resolution is larger than the sediment grain size of the unsuitable fine and suitable substrates and therefore cannot capture the minimum variance attributable to the grain size. This is not the case for the large boulder and rock outcrops present in the unsuitable coarse substrate.

The slope, curvature, and rugosity data (Figure 5-15, Figure 5-16 and Figure 5-17) showed a similarity between fine and suitable substrate. The morphology of those substrates is similar since the difference in grain size is not large enough to be part of different spatial scale phenomenon. It was also observed that the coarse substrate data spread to the entire value range. The coarse substrate was the only category that had high slope values. The coarse substrate ranges of values are related to the curved shape and steepness of the large rock outcrops already described from the bathymetry. The slope, curvature, and roughness values described the spawning sites as very flat. From these data it was determined that the aspect characteristic (i.e. the orientation of the slope) added no information that could help differentiate the classes of substrate. Therefore no values related to the slope aspect were compiled or considered for further analysis and mapping.

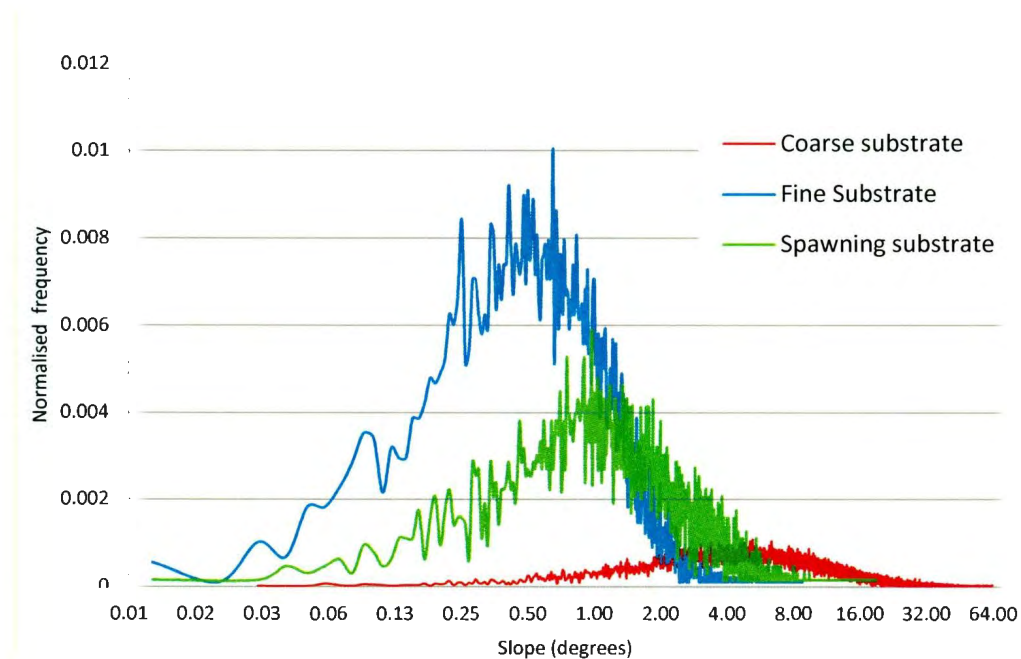


Figure 5-15: Normalized frequency distribution of the slope values. The x axis is displayed as a logarithmic scale of base 2 to show the differences for the small values.

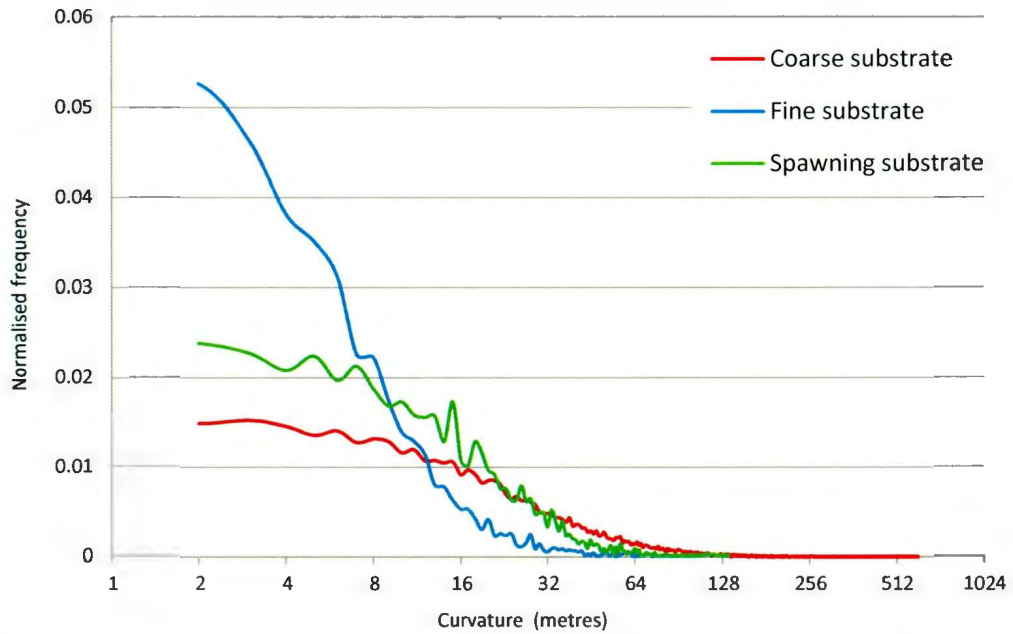


Figure 5-16: Normalized frequency distribution of the curvature values. The x axis is displayed as a logarithmic scale of 2 to show the differences for the small values.

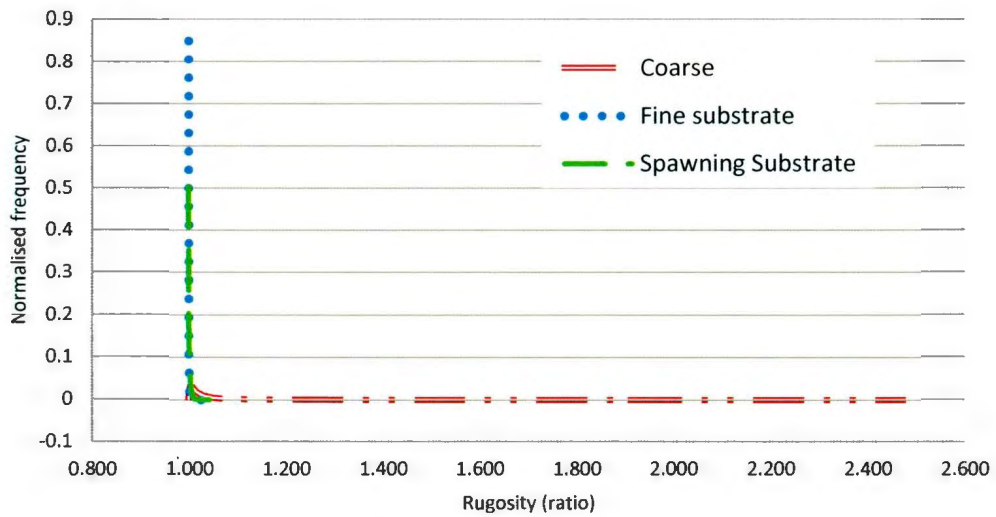


Figure 5-17: Normalized frequency distribution of the rugosity values.

5.4.3.2 Bathymetric Position Index (BPI)

The use of different parameter values when computing BPI — a measure of the local variation of the seafloor — allowed the seafloor morphology to be examined at different scales. The values for the broad-scale parameters were adopted from previous studies (Erdey-Heydorn, 2008; Lanier et al., 2007) and empirical results, whereas those used for the fine-scale parameters were based on the variance analysis of spawning sites in this study.

For the broad-scale BPI, many values for the inner and outer radius were tested to determine the one that would best suit the broad-scale morphology of the study area. For the 1 m resolution data, values of 25 m and 125 m for the inner and outer radius respectively (Figure 5-18a) failed to identify the bedrock outcrops as peak areas and many small-scale features that were not desirable in a broad-scale context were displayed. The same values at 5 m resolution failed to clearly identify the trenches that were easily identifiable in the bathymetric dataset and there were too many flat areas for a broad-scale context. Only small differences were observed between the three other calculations of broad-scale BPI (Figure 5-18a, c, d). The range of index values resulting from the computation (Table 5-5) was similar. The three sets of BPI values captured the rock outcrop described in Shaw et al. (1999). The centre values of the three valid broad scales (Figure 5-18) used for this study were an inner radius of 50 m and an outer radius of 250 m at 1 m resolution. Those values are cell quantities and were changed, therefore, to 10 and 50 for the 5 m resolution data computation. This translated into a description of the

bathymetric index for a seabed feature having a 5 m radius within a 250 m radius area.

The chosen values were similar to the range used in Lanier et al. (2007).

Table 5-5: Variation of the range of the BPI index resulting from different values used for a broad-scale BPI calculation. Sets of BPI values correspond to the inner and outer annulus values.

BPI values (in m)	25 / 125	40 / 200	50 / 250	60 / 300
Minimum index	-13	-14	-15	-15
Maximum index	10	12	12	12

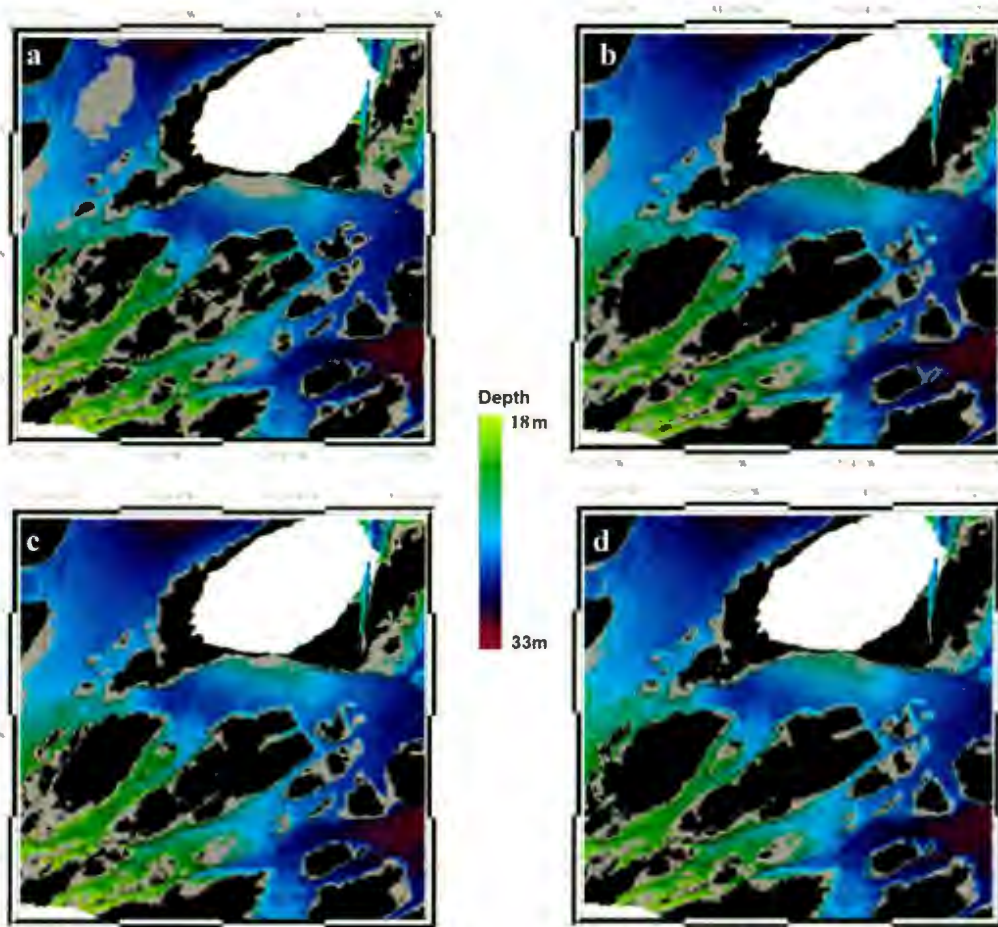


Figure 5-18: Results of broad-scale BPI computation at Gull Island 2 for a) 25, 125 m b) 40, 200 m c) 50, 250 m and d) 60, 300 m. Each pair of values presents the inner and outer distances of the annulus used for the calculation of BPI. The black areas represent peaks and the grey areas are the transition from peak to trough. The trough areas have been made transparent to display the colour-coded bathymetry in the background. The blank area represents Gull Island.

The values used for fine-scale BPI at 1 m resolution were an inner radius of 5 m and an outer radius of 20 m. These values were cell quantities; therefore they were changed to 1 m and 4 m for the data at 5 m resolution. These values were chosen to approximate the spatial scale of the spawning site determined by the variance study of the spawning sites. The smaller annulus value corresponded to the largest resolution used in this study.

The BPI values proved to be quite useful. As the backscatter data did not allow differentiation between suitable and unsuitable coarse substrates, only the morphologic characteristics were used to establish the difference between these two classes. The morphologic characteristics of the coarse substrate were spread over the entire range of values, with the exception of the broad-scale BPI (Figure 5-19). This meant the broad-scale BPI was the only factor that could help differentiate the coarse substrate from the spawning substrate. It also showed that the broad-scale BPI values could not be used to distinguish between the spawning substrate and the unsuitable fine substrate. The spread of BPI values for the coarse substrate was an unfortunate effect of the very high data resolution, as demonstrated in the spatial scale analysis. The overwhelming occurrence of zero values for the fine-scale BPI highlighted that there was only a small variation in morphology within a 20-metre circle (Figure 5-20). The low variation supported the choice of a 20 m radius circle to represent one type of seafloor at this spatial scale. No differences could be established between the substrate classes using the fine-scale BPI.

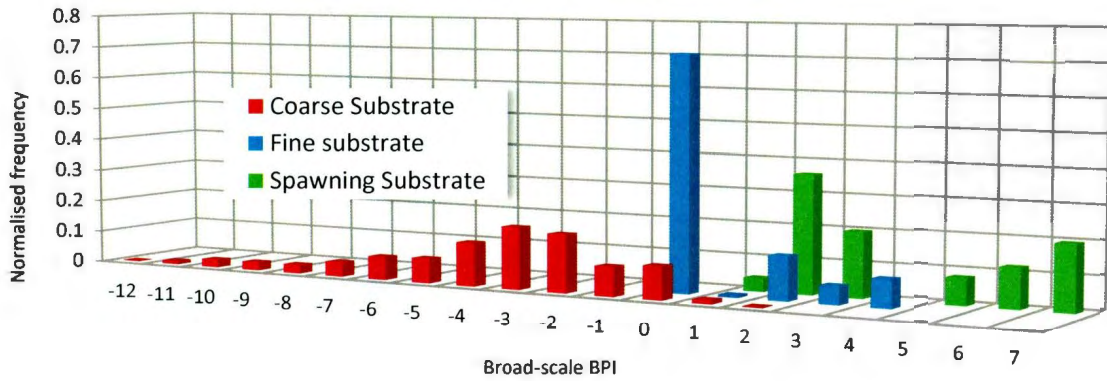


Figure 5-19: Normalized frequency distribution of the broad-scale BPI values.

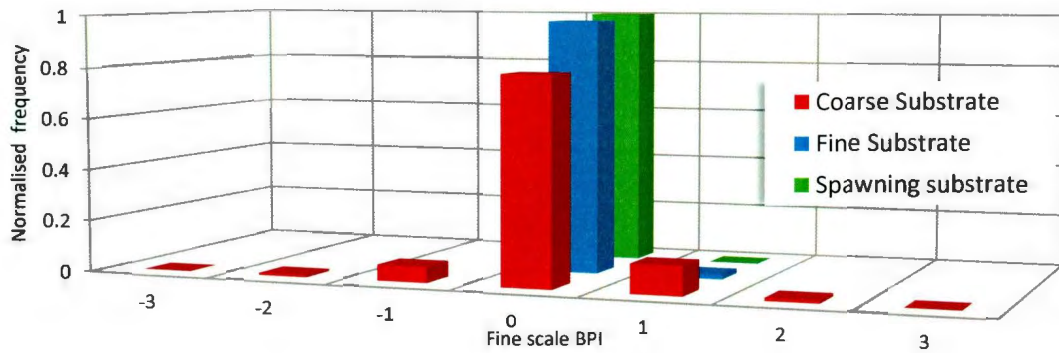


Figure 5-20: Normalized frequency distribution of the fine-scale BPI values.

5.4.4 Unclassified area

The range of values for the seven characteristics observed through data sampling for each substrate was smaller than the range of those characteristics compiled for the entire study area (Figure 5-21). The pixels associated with those out-of-range values were not part of any of the three identified substrates.

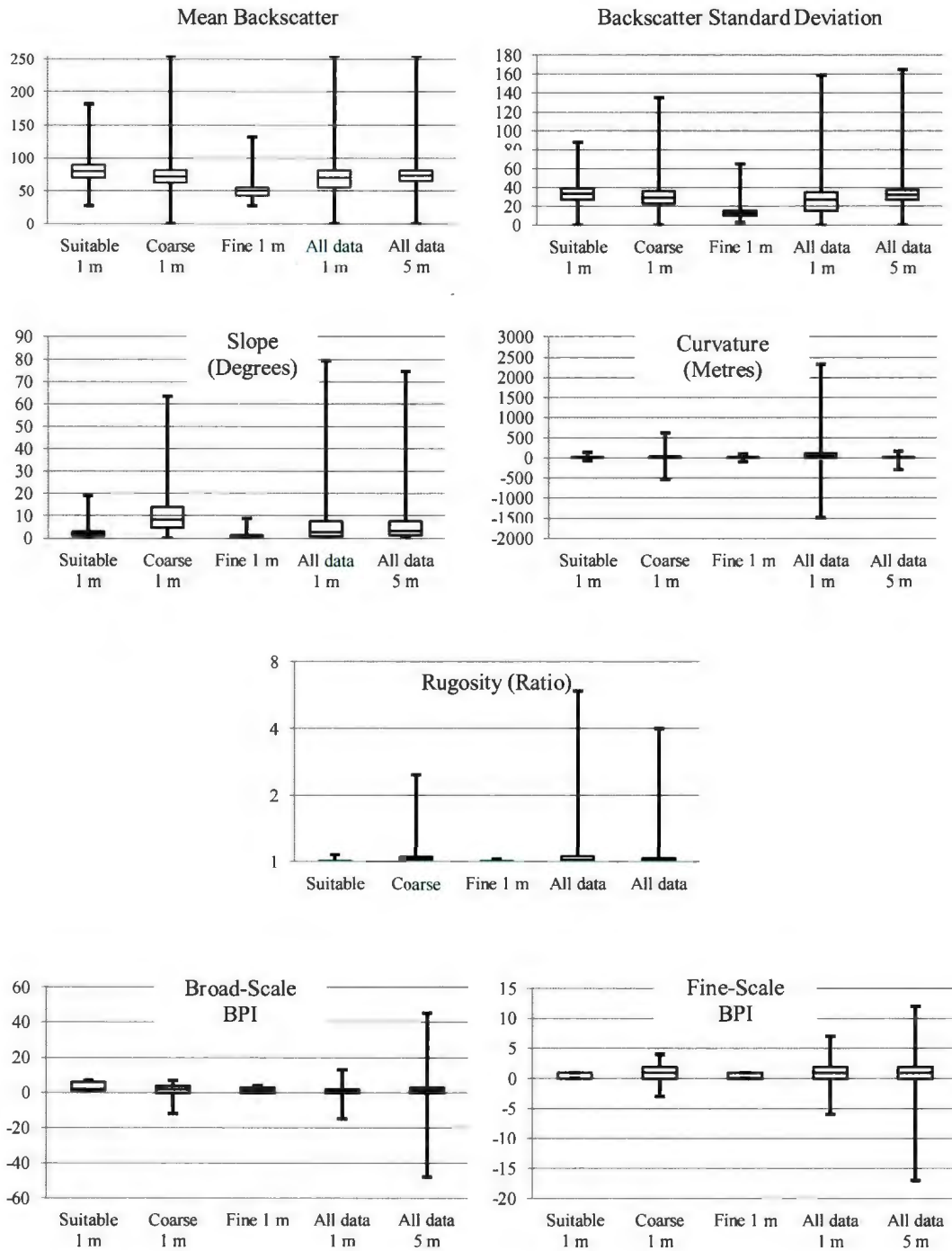


Figure 5-21: Distribution of values for seafloor characteristics. The first three boxplots on each graphic show the data distribution for the three substrate classes from all the spawning areas, whereas the last two boxplots show the distribution of all the data compiled at 1 m and 5 m resolutions. Backscatter is expressed in dimensionless units on a scale of 0-255.

5.5 Relief of spawning sites in relation to depth

A possible correlation between the steepness of seafloor depressions and the depth of the spawning sites was suggested by Rose-Taylor (2006) and investigated in this study. There was a positive correlation between the broad-scale BPI and the depth of the spawning sites, with an $R^2 = 0.89$ (Figure 5-22). The small number of spawning sites render the analysis inconclusive, but the results suggest a trend. Nothing specific was observed in the morphologic characteristics that would differentiate the deeper spawning sites from the others. More spawning sites are needed to obtain a conclusive answer to this question.

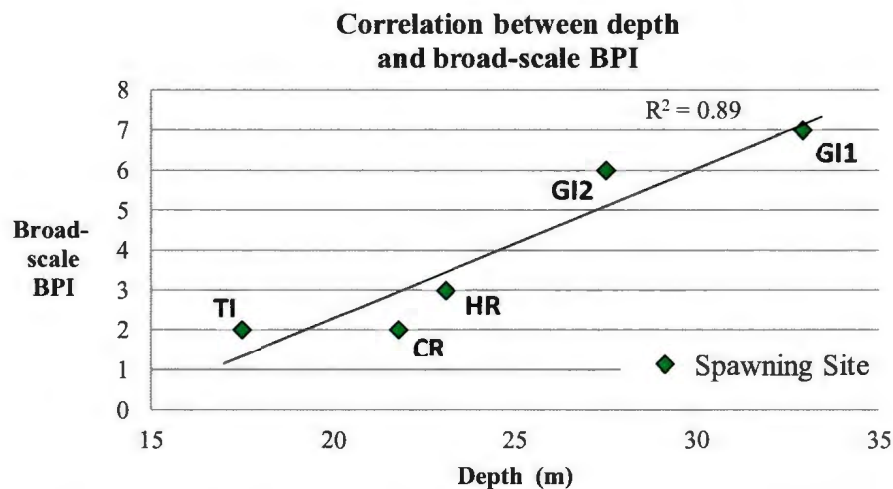


Figure 5-22: Pearson correlation between depth and broad-scale BPI. Spawning sites are indicated by green squares and a linear trendline shows the best-fit linear relationship. The R^2 value indicates the strength of the correlation.

5.6 Supervised classification

Classification maps were created using the characteristics identified for each substrate class. Maps created from data at 1 m resolution for each of the spawning sites are described first, followed by those created using 5 m resolution. The items shown on the spawning area maps are the same for all studied areas, and the symbols used to depict them are shown in Figure 5-23. Classification samples were used to establish the characteristics of the three classes and are shown on the 1 m resolution maps. The bottom samples shown on the 5 m resolution maps provide a test of the supervised classification.

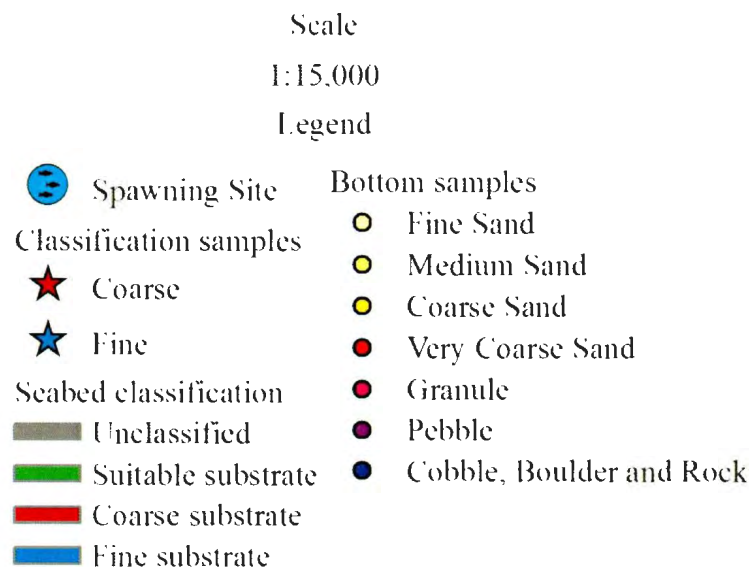


Figure 5-23: Legend for the classification maps of the five known spawning sites.

In all spawning areas (Figure 5-24 to Figure 5-28), coarse substrate occupied approximately half of the seafloor and the percentage of substrate that had physical characteristics suitable for spawning was roughly one-third. The amount of fine substrate

in each area varied, but it occupied the smallest percentage of seafloor in each area. The coverage percentage by substrate type in each spawning area is provided in Figure 5-29.

The area of unclassified data varied for all sites and was created by two principal situations. In the first, the broad and fine-scale BPI values were outside of the range compiled for the three classes. This was caused by narrow trenches or areas of transition between the suitable and unsuitable coarse substrates. In the second, the noisy backscatter data had values outside of the range compiled for the three classes. Most of that data was located on the edge of the survey lines. The white stripping on all classification maps (Figure 5-24 to Figure 5-28) was caused by the removal of backscatter data during processing (cf. section 4.1.4).

5.6.1 Crackers Rocks classification

The classification maps created for Crackers Rocks (Figure 5-24) correspond well with the bathymetry. Only one bottom sample, composed of pebble, fell within the suitable substrate area, which is in accordance with the suitable grain size for spawning. The area of suitable substrate varied in size and shape, though the predominant shape was elongated with an east-northeast orientation. Only very small amounts of fine substrate were located in a single narrow trench in this area.

Suitability of Substrate for Demersal Capelin Spawning at Crackers Rocks Site

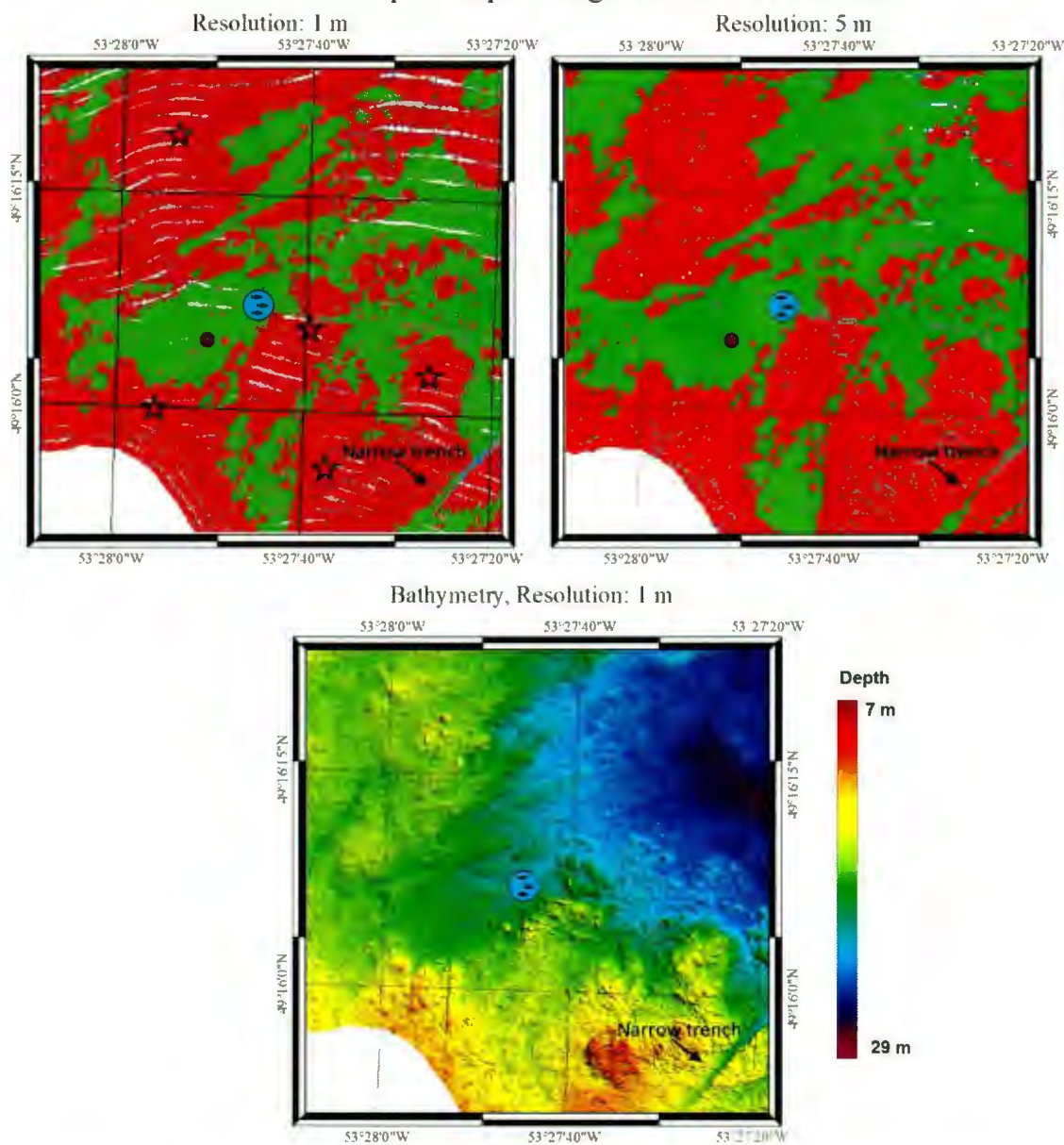


Figure 5-24: Maps of the suitable substrate for demersal capelin spawning at the Crackers Rocks site displayed with the bathymetry. See Figure 5-23 for legend details.

5.6.2 Gull Island 1 classification

The classification maps created for Gull Island 1 (Figure 5-25) show a correspondence between the suitable substrate and the trenches outlined by rock outcrop displayed by the bathymetry. There were 39 bottom samples available for this area, with many concentrated at the spawning site (Figure 4-6). Only three samples, all of them fine sand, did not match the classification on the map: one of these samples was on an area labelled unclassified; one on suitable; and one on coarse substrate. The other samples correlated with the substrate of their seafloor class. Only very small amounts of fine substrate were located in a trench in this area. This spawning area had the highest percentage of unclassified data.

Suitability of Substrate for Demersal Capelin Spawning at Gull Island 1 Site

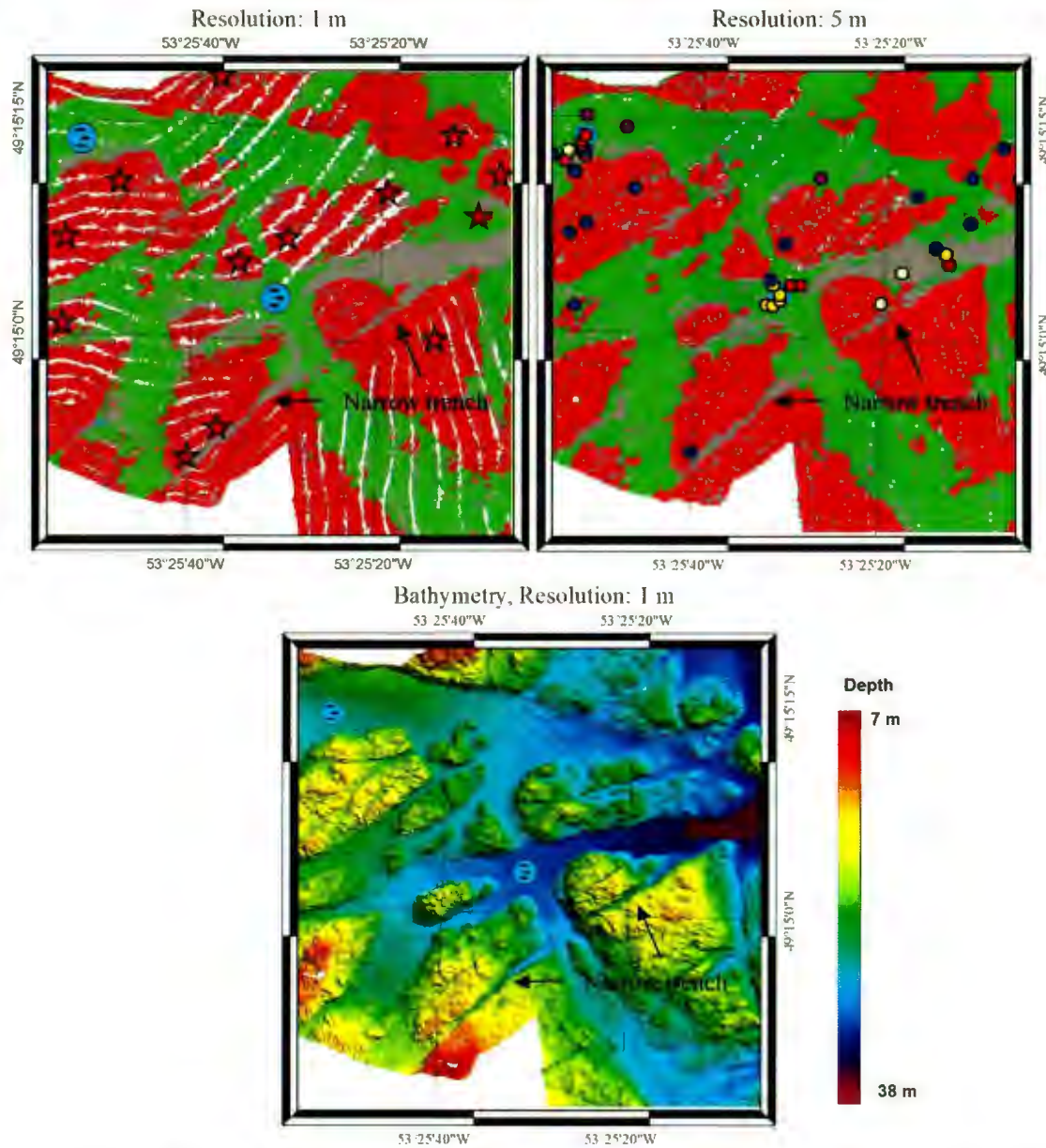


Figure 5-25 : Maps of the suitable substrate for demersal capelin spawning at the Gull Island 1 site displayed with the bathymetry. See Figure 5-23 for legend details.

5.6.3 Gull Island 2 classification

The classification maps created for Gull Island 2 (Figure 5-26) are similar to those for the Gull Island 1 area, with a network of suitable substrate located between rock outcrops. These features compared well with the bathymetry. There were 39 bottom samples available in this area, which were mostly concentrated close to the spawning site. Only one fine sand bottom sample did not match the classification as shown on the map. The other samples correlated with the substrate of their seafloor class. A significant deposit of fine substrate was located on the northwest corner of the Gull Island 2 site.

5.6.4 Turr Island classification

The classification maps created for Turr Island (Figure 5-27) show that the bottom of the NE-SW elongated trench was classified as suitable substrate. Only very small amounts of fine substrate were located in a trench in this area. Only two bottom samples were available for this site, one composed of granule and pebble, and one indicating rock. Both were in accordance with the classified substrate.

Suitability of Substrate for Demersal Capelin Spawning at Turr Island Site

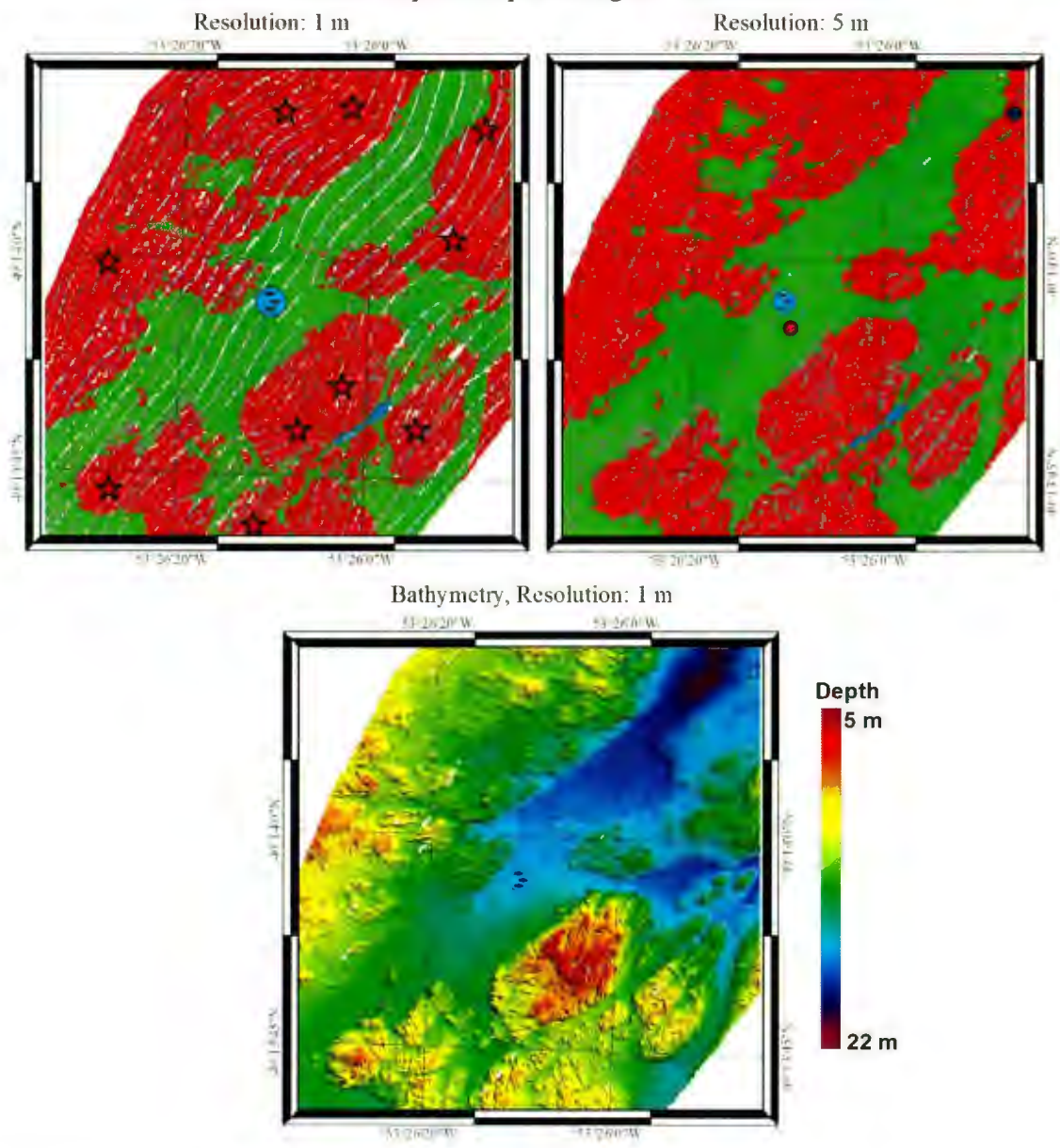


Figure 5-27: Map of the suitable substrate for demersal capelin spawning at the Turr Island site displayed with the bathymetry. See Figure 5-23 for legend details.

5.6.5 Hincks Rock classification

The classification maps created for Hincks Rocks (Figure 5-28) for the fine and suitable substrate compared well with the bathymetry. The coarse substrate, however, appeared to agree only in the western half of the zone. The bathymetry and one bottom sample showed the eastern half of the zone has sediments with dispersed rock outcrops, while the classification map showed a large area of coarse substrate. This classification was caused by the 0 value of broad-scale BPI, which indicates that the area is not a depression and therefore unsuitable for spawning. Three other bottom samples were available to evaluate this site. Two were composed of granules and fell within the suitable substrate area; the third, composed of rock, fell within the coarse substrate area. All samples were in accordance with the grain size of the class indicated by the substrate map. The suitable substrate was found on large patches of seafloor randomly distributed across the zone. The spawning site and the surrounding suitable substrate were located at the end of a long trench that reached a depth of 50 m (Figure 5-8). A significant deposit of fine substrate was located on the north and northwest portions of the Hincks Rocks site. This was the highest percentage of fine substrate of the five areas.

Suitability of Substrate for Demersal Capelin Spawning at Hincks Rocks Site

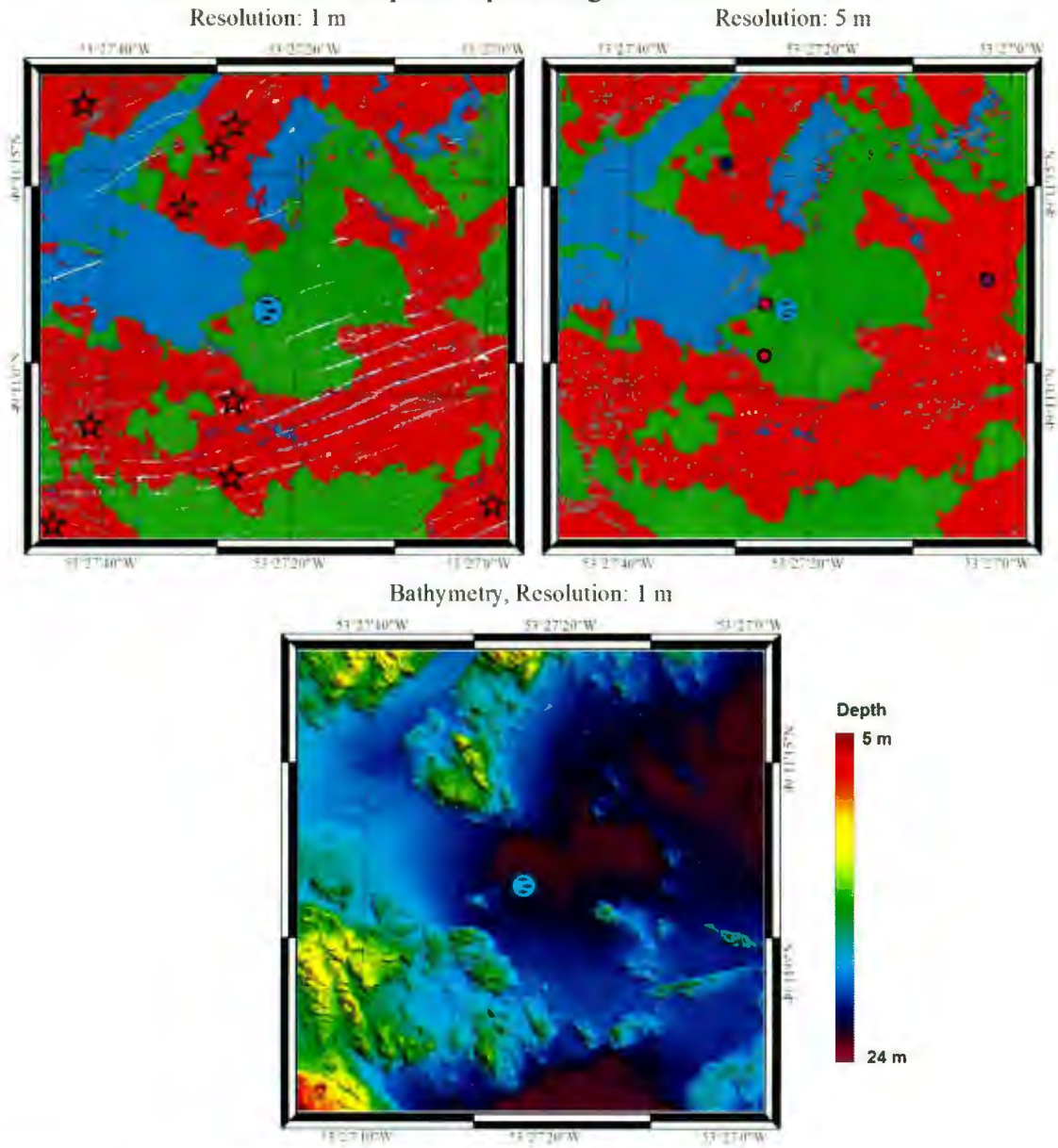


Figure 5-28: Map of the suitable substrate for demersal capelin spawning at the Hincks Rock site displayed with the bathymetry. See Figure 5-23 for legend details.

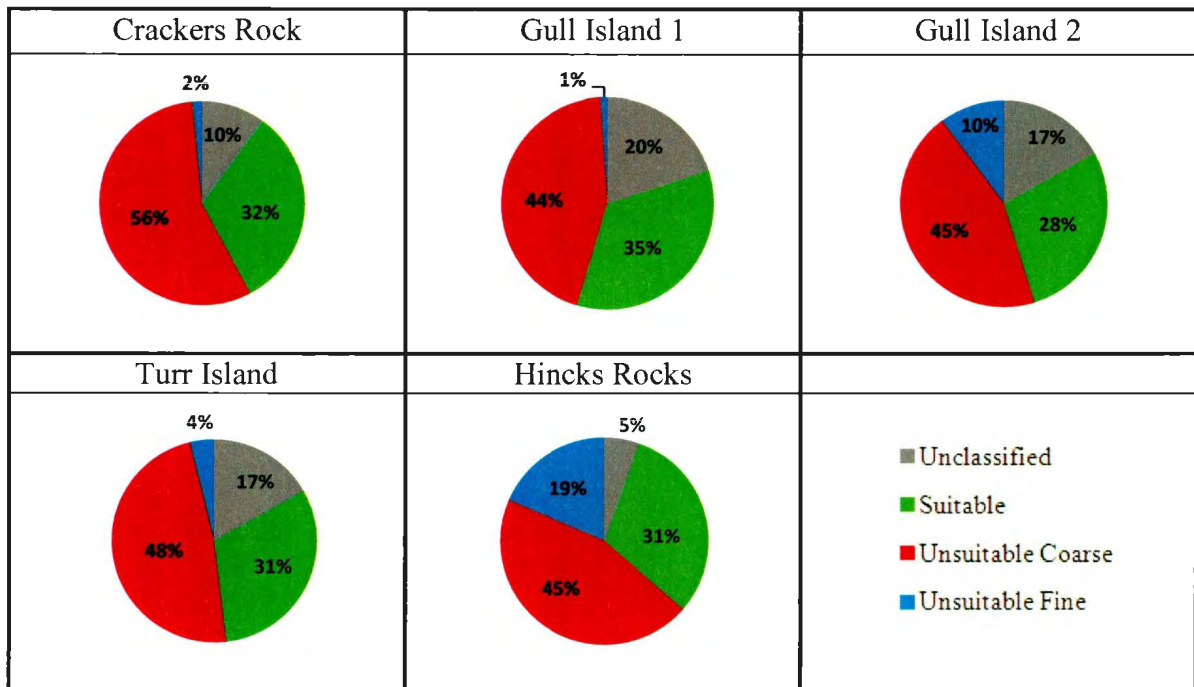


Figure 5-29: Pie charts depicting the percentage of seafloor occupied by each class of substrate within the 1 km² spawning area for each of the five known spawning sites.

5.6.6 Classification of the study area and resolution

A major constraint for classifying large geographic areas at high resolution is the huge size of the datasets. One way to overcome this is to evaluate a range of resolutions to determine if they will adequately depict phenomena of a certain spatial scale. The cumulative area for each substrate class for the five spawning sites were used to validate that the 1 m and 5 m classifications could adequately represent spawning grounds at the same spatial scale.

The greatest difference observed between the classifications executed at 1 m and 5 m resolutions was 7% for unclassified substrate. The largest difference among the three classified substrates was 6% for the suitable substrate. The small differences between the

classifications created using data at 1 m and 5 m resolutions indicated that the morphologic characteristics observed at these two resolutions were of the same spatial scale. The seafloor phenomena captured by both resolutions was essentially the same (Figure 5-24 to Figure 5-28) and are consistent with a spawning site footprint of 20 m diameter (cf. section 5.3). Pearson’s correlation (Figure 5-31) gives an R^2 of 0.96, which indicates that the results from the two classifications are similar enough to be deemed equivalent. The two spatial scales were compatible enough to perform a classification of the entire study area at a 5 m resolution.

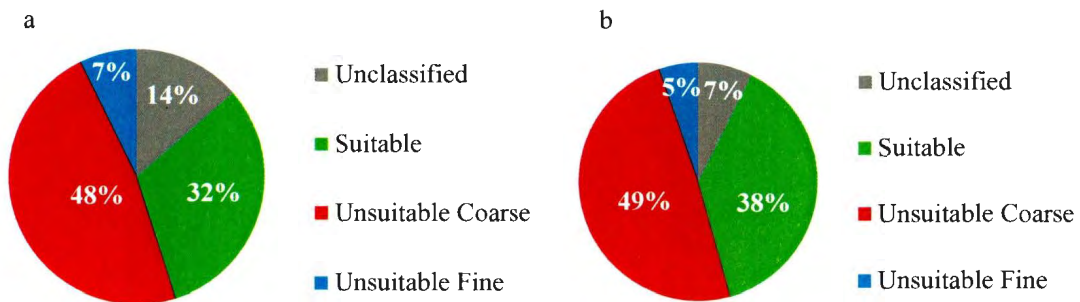


Figure 5-30: Pie charts depicting the percentages of each class for the five known spawning areas. The values are compiled separately for the two spatial resolutions used: a) 1 m and b) 5 m using the 1 m resolution characteristics values.

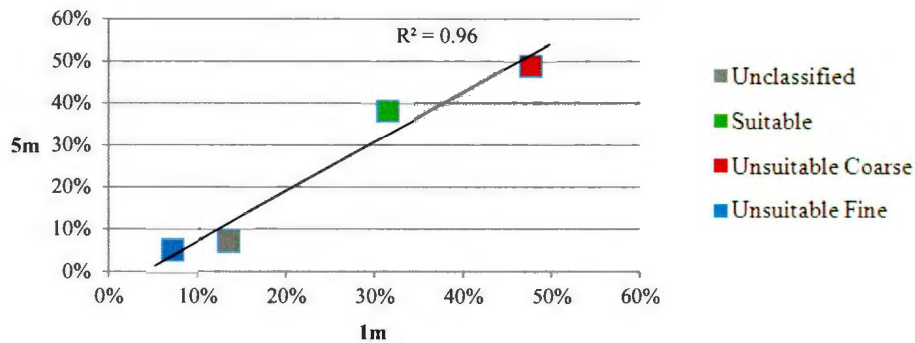


Figure 5-31: Pearson correlation between the percent coverage of the substrate classes for the five known spawning areas at a resolution of 1 m (Figure 32 a), compared to those at a resolution of 5 m (Figure 32 b). The values for the characteristics determined at 1 m resolution were used for both classifications.

5.6.7 Study area classification

The classification map for the study area (Figure 5-32) is dominated by coarse substrate.

The abundance of bedrock is obvious from the bathymetry (Figure 5-8) and correlates well with the classification. A series of fissures on the bedrock form a network of depressions where sediment accumulates; suitable substrate is located in these depressions. Three of the spawning areas, Gull Island 1, Gull Island 2, and Turr Island, present the same pattern. The northern portion of the study area presents a more even distribution of suitable and coarse substrates. The fissures are less predominant on the morphology, putting less restriction on the distribution of the suitable substrate. Two spawning areas, Crackers and Hincks Rock, present this same pattern. Fine substrate comprised a small proportion of the seafloor and was concentrated within only a few regions, mainly in the southern portion of the study area.

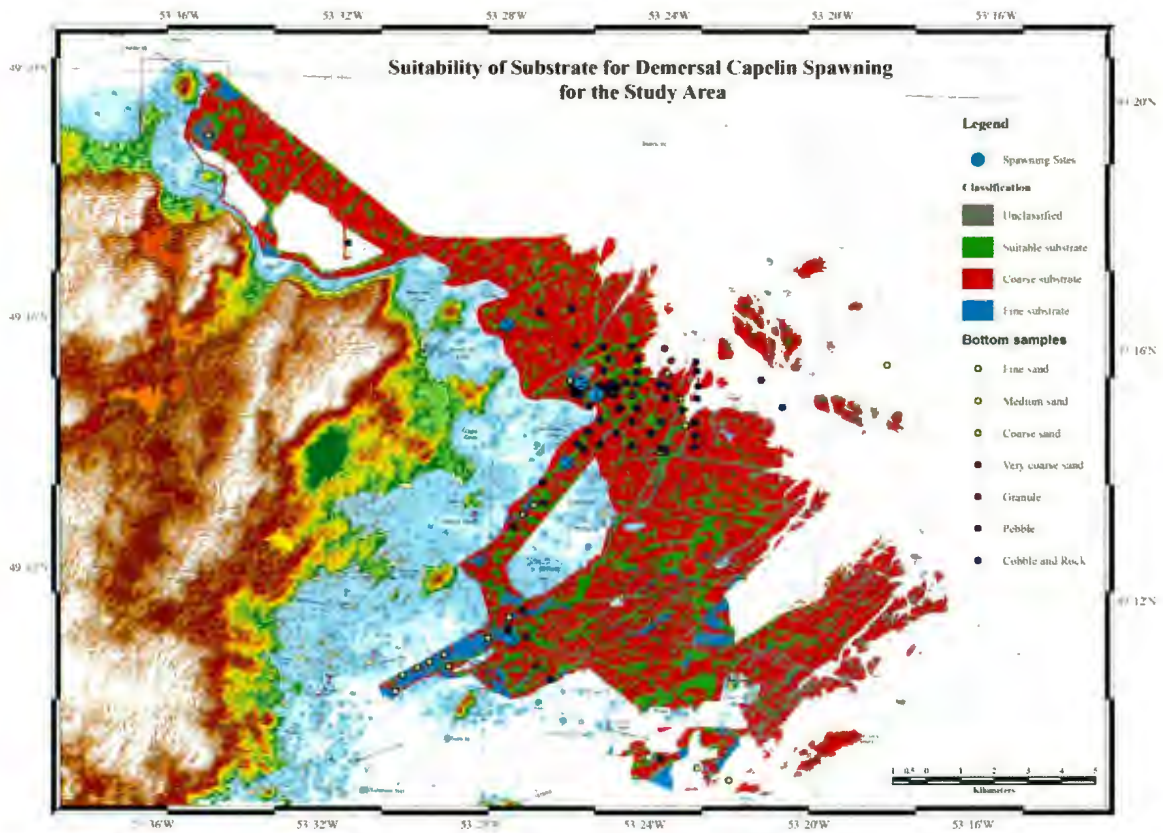


Figure 5-32: Map depicting the seafloor suitability for demersal capelin spawning for the whole study area. The bottom samples are overlaid over the classification.

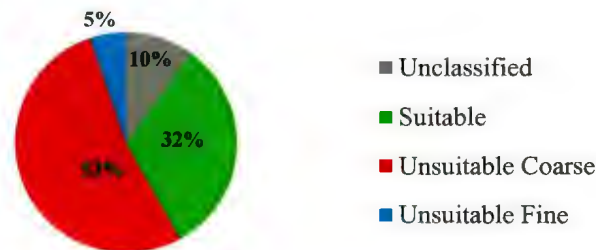


Figure 5-33: Percentage of seafloor occupied by each substrate class within the study area.

5.6.8 Substrate distribution

The substrate study, performed at two resolutions, showed consistent results for the three substrate classes (Table 5-6). One-third of the seafloor offered a substrate potentially

suitable for demersal capelin spawning; just over half of the area was composed of an unsuitable coarse substrate. Unsuitable fine substrate was present only in specific areas and covered about 5% of the seafloor. About 10% of the seafloor could not be classified.

Table 5-6: Numerical results and differences between the classifications at 1 m and 5 m.

		1m resolution			5m resolution			Difference (1m – 5m)	
Site	Class	Pixel	%	m ²	Pixel	%	m ²	%	m ²
CR	Unclassified	93 725	10%	93 725	880	2%	22 000	8%	71 725
	Suitable	302 550	32%	302 550	16 754	44%	418 850	-12%	-116 300
	Unsuitable Coarse	528 021	56%	528 021	20 347	53%	508 675	3%	19 346
	Unsuitable Fine	15 223	2%	15 223	103	0%	2 575	1%	12 648
GI 1	Unclassified	177 752	20%	177 752	4 311	12%	107 775	8%	69 977
	Suitable	308 342	35%	308 342	15 208	41%	380 200	-6%	-71 858
	Unsuitable Coarse	394 509	44%	394 509	17 696	47%	442 400	-3%	-47 891
	Unsuitable Fine	10 023	1%	10 023	138	0%	3 450	1%	6 573
GI 2	Unclassified	143 901	17%	143 901	4 478	13%	111 950	4%	31 951
	Suitable	241 702	28%	241 702	12 372	35%	309 300	-6%	-67 598
	Unsuitable Coarse	379 788	45%	379 788	15 758	44%	393 950	0%	-14 162
	Unsuitable Fine	87 084	10%	87 084	2 988	8%	74 700	2%	12 384
TI	Unclassified	149 041	17%	149 041	2 914	8%	72 850	9%	76 191
	Suitable	278 508	31%	278 508	14 214	38%	355 350	-7%	-76 842
	Unsuitable Coarse	427 407	48%	427 407	19 480	53%	487 000	-5%	-59 593
	Unsuitable Fine	34 408	4%	34 408	349	1%	8 725	3%	25 683
HR	Unclassified	53 353	5%	53 353	1 192	3%	29 800	2%	23 553
	Suitable	307 968	31%	307 968	13 474	34%	336 850	-3%	-28 882
	Unsuitable Coarse	448 494	45%	448 494	18 927	47%	473 175	-2%	-24 681
	Unsuitable Fine	184 226	19%	184 226	6 396	16%	159 900	3%	24 326
5 sites	Unclassified	617772	14%	617772	13775	7%	344375	6%	273397
	Suitable	1439070	32%	1439070	72022	38%	1800550	-7%	-361480
	Unsuitable Coarse	2178219	48%	2178219	92208	49%	2305200	-1%	-126981
	Unsuitable Fine	330964	7%	330964	9974	5%	249350	2%	81614

5.7 Classification validation

The classification of the seafloor was validated using ground truthing as demonstrated in Mayer and Fonseca (2007). A series of bottom samples were taken prior to the multibeam survey or any seafloor classification. The samples were distributed across the study area (Figure 4-6) and were collected without knowledge of the spatial distribution of the different substrates (Rose-Taylor, 2006). The sampling was of a higher density at the spawning sites.

5.7.1 Classification of spawning areas

The distribution of the samples (Figure 5-34) was used as a measure of accuracy for the classification at 1 m resolution by correlating the percentage of seafloor covered by each class with the corresponding sample distribution for each substrate. The cumulative values of the five known spawning areas were used to maximize the covered area.

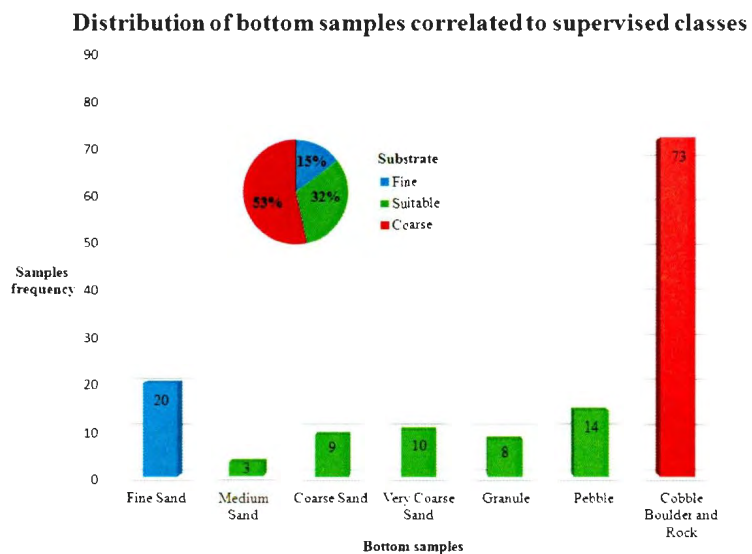


Figure 5-34 : Distribution of the bottom samples from each the study area.

The proportion of the bottom sample types correlated well with the proportion of the corresponding substrate. Despite the low number of samples, a good correlation was assessed (Figure 5-35). This confirms the success of the classification performed. From this result, it can also be interpreted that there is homogeneity between the seafloor of the individual spawning sites and the entire study area. The known spawning sites (1 km²) were a good representation of the study area.

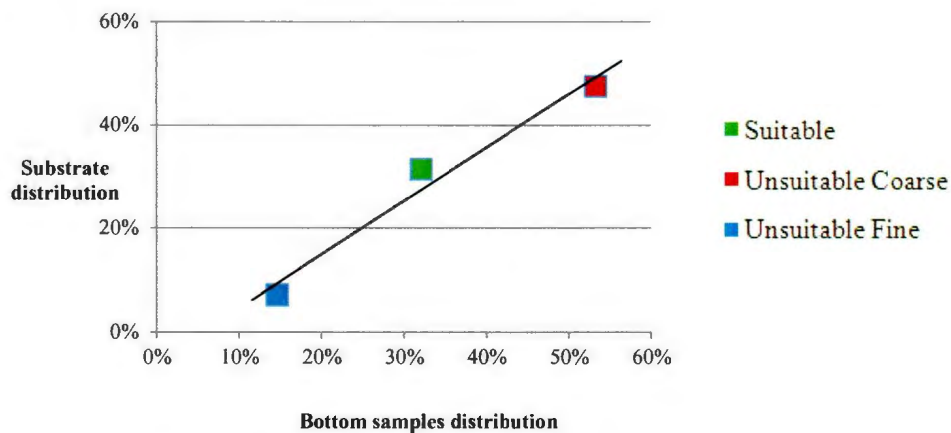


Figure 5-35: Display of the correlation evaluating the validity of the substrate classification of the five known spawning areas as compared to the distribution of bottom samples throughout the study area. The three classes are represented by squares and a linear trendline showed the strength of the correlation.

5.7.2 Classification of the study area

The classification of the study area at a resolution of 5 m was evaluated using the same method as the classification at 1 m resolution. In addition, all the bottom samples were compared to their corresponding classifications (Figure 5-32). For each sample that did not correlate to its corresponding class, the classification data within a radius of 10 m, 20 m, 30 m, and 40 m were compared to the bottom samples. This accounted for the effect of

the samples' positioning error on the relationship between the class and the bottom samples. Taking into consideration the drift of the vessel, the accuracy of the position given by the GPS, and the offset between its antenna and the location of the grab, the value at 20 m was most representative of the accuracy of the samples. This value also correlated to the spatial scale determined for the spawning sites. Despite the low number of samples, a good correlation could be assessed (Figure 5-36), and 87% of the bottom samples were correctly classified (Table 5-7). Those numbers validate the seafloor classification presented. All results from the different validation methods indicated a high rate of success for the classification.

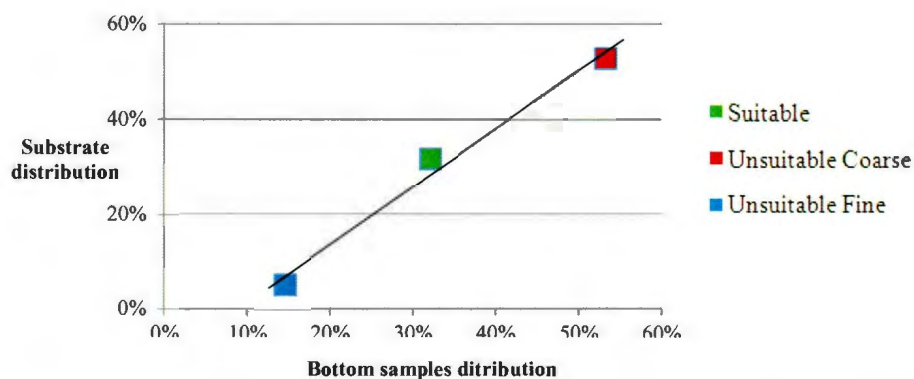


Figure 5-36: Display of a correlation evaluating the validity of the substrate classification of the study area (5 m resolution) in comparison with the distribution of bottom samples throughout the entire study area.

Table 5-7: Variability in the correlation between the seafloor classification and the bottom samples, based on the presence of samples corresponding to the classified substrate within a radius of 10 m, 20 m, 30 m, and 40 m.

Correlation between bottom samples and classified substrate					
Radius around samples	On site	10 m	20 m	30 m	40 m
Correlation percentage	0.61	0.76	0.87	0.92	0.94

6 DISCUSSION AND CONCLUSION

This chapter reviews the results of this research project and addresses some of the questions that arose during its execution. After a summary of the study results, there is a discussion of the morphologic characteristics of capelin demersal spawning sites and spawning areas, and the supervised classification of the study area. The discussion is structured around the research questions posed in Chapter 2. During the study, a number of issues and unexpected results were identified and addressed. These points are discussed below, within the relevant sections, and serve to explain the study's shortfalls and limitations. This chapter concludes by suggesting avenues for further research, with a view to resolving known issues and pursuing better knowledge of capelin and their demersal spawning sites.

6.1 Study results

This study found that the demersal spawning sites had a minimum radius of 20 m and were located at the bottoms of seabed depressions. In order to accurately identify areas that have the appropriate substrate texture for spawning, morphologic characteristics extracted from the bathymetry, as well as backscatter data, are required to distinguish between the spawning substrate, predominantly pebble gravel, and coarser unsuitable gravel, typically cobble to boulder, gravel and bedrock. Once it was determined that a coarser resolution of 5 m for the multibeam backscatter data was as representative of the seafloor as the 1 m resolution dataset, it was possible to map potential capelin spawning

substrate for the entire study area. This study determined that, in the region of Cape Freels on the northeast coast of Newfoundland, up to one-third of the seafloor between water depths of 5 and 50 m offers potentially suitable substrate for capelin demersal spawning.

6.1.1 Spawning sites

6.1.1.1 What is the minimum footprint of a spawning site?

The variance study carried out to determine the minimum footprint of a spawning site resulted in a circular radius of 20 m. This represents an area of 1256 m², about the size of a large building lot. This footprint provides a minimum spatial scale for the characterization of the substrate on which capelin spawn and is in accordance with Anderson (2001), who estimated that benthic habitat heterogeneity occurs at spatial scales less than 40 m.

6.1.1.2 What backscatter characteristics define a demersal capelin spawning substrate?

Fonseca and Mayer (2007) identified backscatter as a proxy for substrate texture. The backscatter standard deviation value was used as a proxy for small-scale roughness (Fonseca and Mayer, 2007) and proved to have a distribution similar to the mean backscatter. These backscatter measures were readily able to distinguish unsuitable fine substrate from suitable spawning substrate in the spawning sites. In contrast, there was complete overlap in mean and standard deviation backscatter signatures for suitable and

unsuitable coarse substrates. Part of the explanation for this unexpected result may be the low backscatter values observed for bedrock. A common assumption is that a hard bottom should generate a higher backscatter return than a softer bottom (Bachman, 1985). Further investigation of this apparent discrepancy was not possible within the current study; however, three possible explanations are proposed, which may be tested in follow-up research. (1) Vegetation: bedrock outcrops in the study area may be covered with marine vegetation (e.g. seaweed) that increases scattering of the acoustic signal. Rose Taylor (2006) describes the presence of macrophytes in the spawning areas. The echosounder frequency of 300 kHz would typically return a low backscatter value from vegetation growing on the shallow bedrock (Dartnell et al, 2008). (2) Sediment: fine sediment (mud or fine sand) may be infilling outcrop crevices and depressions, which would return lower backscatter values at the spatial scale used in this study. (3) Smoothness: the surface of the bedrock rock outcrops may have very low roughness, perhaps due to polishing and fine-scale erosion by glaciers (Shaw et al., 2006); these flat surfaces would return a low backscatter value as most of the energy would be deflected away from the receiver with increased grazing angles. This explanation is corroborated by the roughness measures interpreted from the high-resolution bathymetric data (Figure 6-1). The same phenomenon was observed offshore of the bedrock-dominated coastlines of Grand Manan Island, New Brunswick, where bedrock outcrops displayed lower backscatter values than surrounding gravel substrates (Hughes Clarke, 2011).

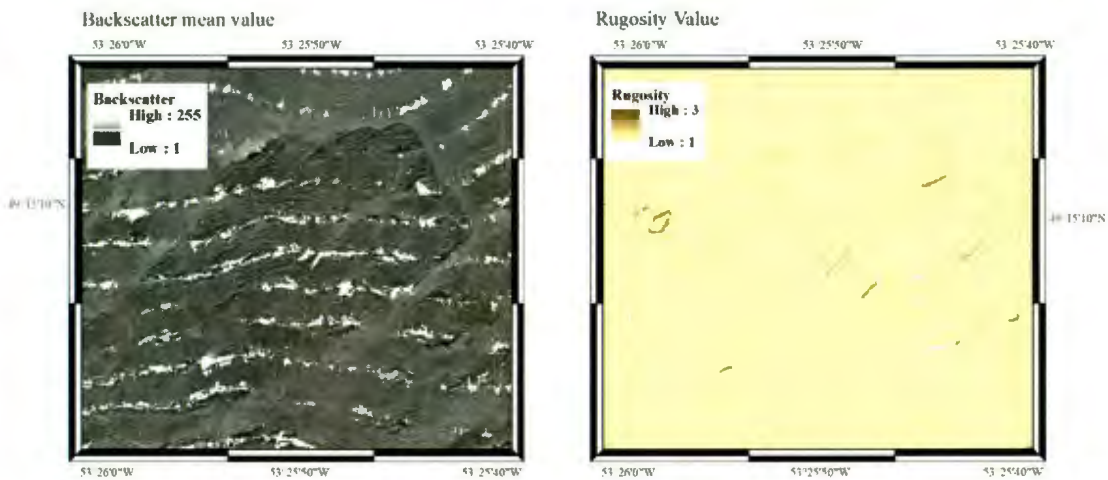


Figure 6-1: Images of a rock outcrop close to the GI2 spawning site at 1 m resolution. The backscatter image (left) depicts low values for rock outcrops. Backscatter is expressed in dimensionless units on a scale of 0-255. The rugosity layer (right) shows low values on the peaks and edges of the rock outcrops.

6.1.1.3 What morphological characteristics define a demersal capelin spawning site?

A series of potentially relevant morphological parameters for spawning sites was derived from the multibeam dataset. They were slope, rugosity, curvature, broad-scale BPI, fine-scale BPI, and aspect. Depth was used to determine slope, rugosity, curvature, and aspect. Slope was identified as relevant, as all spawning sites had a slope value of less than 8° — in other words, a relatively flat seabed. This was consistent across the five spawning sites. Rugosity was extracted from the bathymetric dataset at a resolution of 1 m. This characteristic was used to characterize surface roughness at a larger scale than grain size. It contributed to the definition of the spawning site but was not a critical factor in the classification of spawning areas. All of the study sites had a rugosity value of around 1.0, which is consistent with flat seafloor spawning sites. Curvature was highly variable between spawning sites and determined to be unimportant in characterising spawning

sites. Similarly, aspect values contributed little value towards characterizing spawning sites. At 1 m and 5 m resolutions, aspect values were randomly distributed across all quadrants. This was not surprising considering that spawning sites had low slopes and rugosity. BPI values proved to be quite valuable in characterizing spawning sites, especially broad-scale BPI, differentiating between suitable and unsuitable coarse substrate on spawning sites.

In the spawning areas (analyzed at 1 m and 5 m resolution) and the entire study area (analyzed at 5 m resolution), the location of suitable substrate is consistent with the distribution of glacial sediment described by Shaw et al. (1997) that accumulated between the rock outcrops. The classification was mostly driven by the geological characteristics of the study area. The overview of bathymetric data (Figure 5-8) corresponds with the seafloor model described by Shaw et al. (1999).

6.1.1.4 Were spawning sites located in topographic depressions?

BPI values clearly indicated that all five spawning sites were located within topographic depressions. Both broad- and fine-scale BPI indices indicated this morphology, with positive values ranging from 0 to 7. This can also be observed from the bathymetric analysis (Figure 5-5d) and images provided by the multibeam data (Figure 5-8), indicating that BPI values should be a descriptive measure for identifying demersal capelin spawning sites. This is consistent with Rose-Taylor's (2007) conclusion that spawning sites lie in bathymetric depressions.

6.1.1.5 Do spawning sites occur in gravel ripple troughs on the seafloor?

By observing the images provided by the multibeam data and the slope images, it was determined that spawning sites were not located at the bottom of gravel ripples. Such ripples, which average 2.3 m in wavelength (Shaw et al., 2009), would be visible as recurring patterns of parallel, crest-aligned ridges on the seafloor and should clearly stand out on bathymetric data at 1 m resolution. Such a pattern was not observed within the spawning sites.

6.1.2 Demersal capelin spawning site conceptual model

This study has identified two important contributions to the conceptual model of demersal capelin spawning. Overall, the slope and rugosity for all capelin demersal spawning sites are very low, and both broad-scale and fine-scale BPI indicate that spawning takes place in a topographic depression. Therefore, in summary, the five spawning sites were located on areas of relatively flat seafloor and situated at the bottom of broad topographic depressions or in steep-sided, rock-walled valleys or troughs. These characteristics of spawning sites are consistent with the observations of Carscadden et al. (1989) and Rose-Taylor (2006).

6.1.3 Identification of potential spawning habitat

A seafloor classification identifying the substrate suitable for demersal capelin spawning was successfully compiled for the area surrounding the spawning sites, and for the entire

study area. This classification showed an excellent correlation with the substrate recovered from bottom samples. It was estimated that up to one-third of the study area displayed seafloor characteristics potentially suitable for capelin demersal spawning. This is consistent with Rose-Taylor (2006) who, using gravel substrate as a proxy for suitable spawning ground, determined that one-third of her surveyed area had substrate suitable for spawning. To further test the effectiveness of this multibeam-based classification, however, it will be necessary to locate new spawning sites based on the interpretation of the classification maps. To date only a few spawning sites have been identified (Davoren et al., 2006) over a rather large area of suitable substrate. This raises the question of why there are so few sites. What are the biological factors that influence the choice of a spawning site? If it was only the substrate and morphological characteristics of the seafloor that determined spawning, many more spawning sites would have been expected. Even the possibility that capelin demersal spawning only takes place on ancient submerged beaches (Carscadden et al., 1989) would not explain such a low number of sites. In the eventuality that there are indeed only a few spawning sites, it is clear that there are factors other than seabed characteristics and water temperature (Rose Taylor, 2006) that predispose the choice of a site.

As mentioned in the geologic setting (cf. section 3.4), most of the seafloor rock outcrops within the survey area are likely composed of Cape Freels granite. They display a network of linear fissures or troughs, most likely structurally controlled and tentatively interpreted as joint controlled. These structural features correlate well with the topographic setting of suitable substrate for capelin spawning offshore (Figure 6-2). For

comparison, 10 fissures were randomly selected and measured from both satellite images of the land and seafloor images. The troughs on land varied in width between 15 m and 80 m and had an orientation from 10° to 100°. On the seafloor, their widths varied from 25 m to 100 m and their orientation from 25° to 100°. From this rough comparison it can be tentatively concluded that the same structural pattern extends from the coast into the nearshore (Figure 6-3).

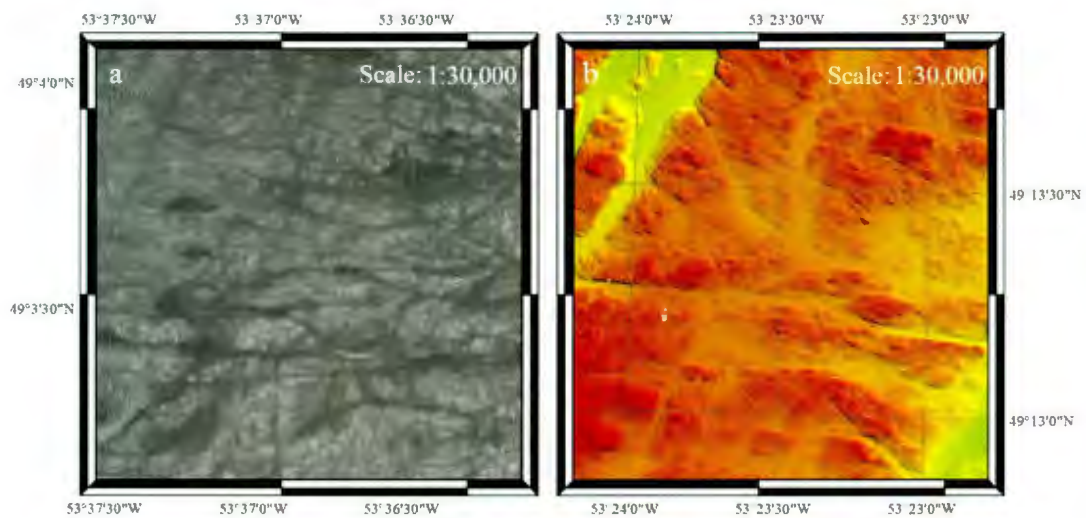


Figure 6-2: Images of bedrock in the vicinity of Newtown a) on land from a 2008 SPOT (www.geobase.ca) image at 10 m resolution and b) on the seafloor from a 5 m resolution multibeam image.

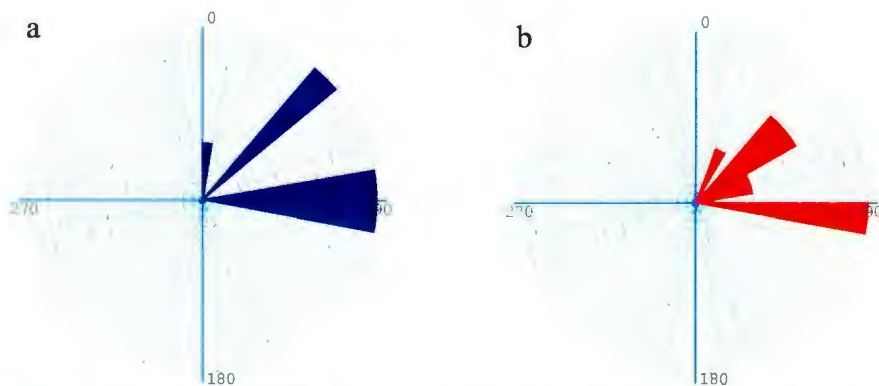


Figure 6-3: Rose diagram of the orientation and frequency of observed faults a) on land and b) on the seafloor. Every three concentric rings represent one observation.

6.2 Study limitations and data constraints

6.2.1 Supervised classification validation

Some uncertainty remains about the positional accuracy of the bottom samples used in the supervised classification. The drift of the vessel and of the grab influence the position of each sample as it sinks across the water column during data acquisition. The samples are accurate; the potential problems come from the interpretation of an unsuccessful attempt to recover a sample. As an example, it was assumed that the seafloor was composed of rock when the Petersen grab was observed to be empty of any sediment while another cause could be possible. It was also noted that the correlation values for the areas of fine substrate were somewhat low. The lower proportion and lower number of fine substrate samples may explain this.

6.2.2 Backscatter

The backscatter data collected from the nadir data beam were not suitable for analysis (Preston, 2009). The removal of the nadir data created gaps and linear artefacts along the edges of the data gaps. The linear artefact consisted of unreliable backscatter values close to the nadir of the survey lines. The multibeam echosounder used in this study was mounted on a 31-foot launch and may have created ambient noise that diminished the clarity of the backscatter signal.

The higher the acoustic frequency, the smaller the objects that returned an echo (Medwin and Clay, 1997). A higher frequency is also more sensitive to ambient noise and would return signals from vegetation or other objects present in the water column, therefore reducing the quality of the substrate observation. The backscatter quality may have also contributed to the inability to distinguish between gravel and coarse substrates (Figure 6-4).

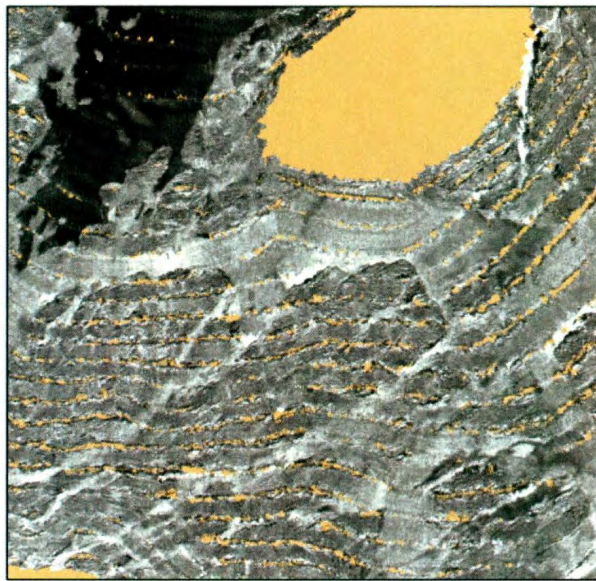


Figure 6-4: Backscatter image at 1 m resolution of the GI2 spawning area. The brown background highlights the area that has no data. This image displays the linear artefact at nadir as well as the higher backscatter value (brighter areas) surrounding the lower backscatter values for bedrock (darker areas).

For substrates of smaller grain size, the backscatter information seems to have been less hampered by quality issues. The low scattering of the backscatter from these soft bottoms may have reduced artefacts. In these cases, the backscatter data successfully delineated those areas where grain size became too small for spawning. The areas of low backscatter

values were well defined through the entire study area and matched well with the available bottom samples.

6.3 Further research

6.3.1 Study of other known spawning sites

There are additional known spawning sites in the vicinity of this study (Table 6-1) (Davoren et al., 2007). It would be beneficial to acquire and analyze multibeam acoustic data from these sites and add the results to this study. Studying an increased number of known sites would enhance the knowledge of their characteristics and make the evaluation of suitable spawning substrate more accurate. The extension of the multibeam coverage and analysis of water column data could also help address questions such as whether capelin are following trenches on the seafloor as a route to reach their spawning location (Davoren et al., 2006). Another related aspect to consider would be the use of trenches by developing larvae. The trenches and the prevailing wind during the hatching seasons (Leggett et al., 1984), having a similar orientation, may present a combined positive effect for the migration of the larvae toward deeper water. The trenches that are believed to be a way in (Davoren et al., 2006) for the spawning capelin may also be a way out for the larvae. If this is the case, the presence of trenches and their orientation could be incorporated in the spawning substrate prediction model. This would significantly reduce the area potentially available for demersal spawning on the northeast coast of Newfoundland.

Table 6-1: Locations and names of other known demersal spawning sites on the Straight Shore (Davoren et al., 2007).

Spawning Site	Latitude ()	Longitude ()
Wadham Island	49.4985	-53.7601
Northern Penguin Island	49.4560	-53.7988
Deadman's Bay II	49.3564	-53.6437
Deadman's Bay I	49.3526	-53.6486

6.3.2 Demersal spawning vs. beach spawning

Work has been done in regards to archaeological shoreline reconstruction from multibeam data (Bell et al., 2009). The reconstruction of ancient shorelines from multibeam data would permit researchers to evaluate the possibility that demersal spawning sites were once on, or in the proximity of, beaches. This could provide evidence for the hypothesis that capelin demersal spawning originates from beach spawning, such as the southeast shoal on the Grand Banks of Newfoundland (Carscadden et al., 1989).

6.3.3 Water temperature change model

Currently, on the northeast coast of Newfoundland, the depth at which demersal spawning may take place is influenced by water temperature. In the event of a change in the water temperature pattern, the available mapped distribution of suitable spawning substrate should be modified. A change in the prevailing water temperature may make some

potential habitat areas unsuitable due to suboptimal temperatures. From multibeam acoustic data, a model could be built to evaluate the available spawning substrate for the depth that correlates to the optimal water temperature for spawning to be successful. In the event of warmer water temperatures near beaches, would capelin move their spawning location to demersal sites? A model would provide a tool to identify and manage the potential demersal spawning areas on the northeast coast of Newfoundland.

6.3.4 Low backscatter value over bedrock

The unexpected result of lower backscatter values over bedrock could be studied further. An explanation would contribute to a better interpretation of backscatter datasets, and may lead to a greater understanding of the relation between frequency, roughness, and backscatter direction and intensity.

6.4 Conclusions

The two main objectives of this study — to identify the morphologic characteristics of demersal spawning sites and to identify potential spawning grounds — were addressed by the available multibeam dataset. This study confirms that demersal spawning is taking place in topographic depressions. It also suggests that spawning is taking place in areas with a flat seafloor. The analysis and correlation of the different layers of data collected provided the basis for the production of habitat maps, which contributed to a better understanding of the demersal spawning sites used by capelin on the northeast coast of Newfoundland.

As a note of caution, the study was only based on five known spawning sites. A larger sample may reduce the area potentially available for demersal spawning. In the process of making habitat maps, more was learned about the strengths and limitations of multibeam technology. Existing assumptions regarding the spatial scale of seafloor characteristics was reinforced and all previous knowledge of capelin spawning substrate was reiterated. There are many more aspects of demersal spawning to study, including, for example, an investigation of the factors that may have triggered the capelin's choice of spawning site. The research conducted for this study contributes new information which may serve as the base for further research on capelin spawning sites and their environment.

References

- Anderson, J. T., 2001. Classification of marine Habitats Using Submersible and Acoustic Techniques. 17th Lowell Wakefield Symposium, Spatial Processes and Management of Marine Population. 377-393.
- Bachman, R. T., 1985. Acoustic and physical property relationships in marine sediment. *Journal of the Acoustical Society of America*, 78, 616-621.
- Bell, T.; Westley, K.; Plets, R.; Quinn, R.; Forsthe, W.; and Renouf, M.A.P., 2009. The Submerged Landscape Archaeology Network—A landscape approach to the investigation of prehistoric marine archaeology. 44th Annual Meeting of the Northeastern Section, Geological Society of America.
- Brown, C. J., Collier, J. S., 2008. Mapping benthic habitat in regions of gradational substrata: An automated approach utilising geophysical, geological, and biological relationships. *Estuarine, Coastal and Shelf Science*, 78, 203-214.
- Calder, B. R., 2003. Automatic Statistical Processing of Multi-beam Echo-sounder Data. *The International Hydrographic Review*, 4, 53-68.
- Carscadden, J. E., Frank, K. T., Miller, D. S., 1989. Capelin (*Mallotus villosus*) spawning on the southeast shoal: influence of physical factors past and present. *Canadian Journal of Fisheries and Aquatic Sciences*, 46, 1743-1754.
- Carscadden, J. E., Montevecchi, W. A., Davoren, G. K., Nakashima, B. S., 2002. Trophic relationships among capelin (*Mallotus villosus*) and seabirds in a changing ecosystem. – *ICES Journal of Marine Science*, 59, 1027-1033.
- Colbourne, E., Craig, J., Fitzpatrick, C., Senciall, D., Stead, P., Bailey, W., 2012. An assessment of the physical oceanographic environment on the Newfoundland and Labrador Shelf during 2011. DFO Can. Sci. Advis. Sec. Res. Doc. 2012/044. iv + 33.
- Colbourne, E., deYoung, B., Narayanan, S., Helbig J., 1997. Comparison of hydrography and circulation on the Newfoundland Shelf during 1990-1993 with the long-term mean. *Canadian Journal of Fisheries and Aquatic Sciences*. 54 (Suppl. 1), 68-80.
- Colbourne, E., deYoung, B., Rose, G. A., 1997. Environmental analysis of Atlantic cod (*Gadus morhua*) migration in relation to the seasonal variations on the Northeast Newfoundland Shelf. *Canadian Journal of Fisheries and Aquatic Sciences*. 54 (Suppl.1), 149-157.
- Collier, J. S., Brown, C. J., 2005. Correlation of sidescan backscatter with grain size distribution of surficial seabed sediments. *Marine Geology*, 214, 431-449.

Dartnell, P., Collier, R., Buktenica, M., Jessup, S., Girdner, S., Triezenberg, P., 2008. Multibeam sonar mapping and modeling of a submerged bryophyte mat in Crater Lake, Oregon. U.S. Geological Survey Data Series 366, <http://pubs.usgs.gov/ds/366/>.

Davoren, G. K., Montevecchi, W. A., 2003. Signals from seabirds indicate changing biology of capelin stocks. *Marine Ecology Progress Series*, 258, 253-261.

Davoren, G. K., Anderson, J. T., Montevecchi, W. A., 2006. Shoal behaviour and maturity relations of spawning capelin (*Mallotus villosus*) off Newfoundland: demersal spawning and diel vertical movement patterns. *Canadian Journal of Fisheries and Aquatic Sciences*, 63, 268-284.

Davoren, G. K., May, C., Penton, P., Reinfort, B., Buren, A., Burke, C., Andrews, D., Montevecchi, W. A., Record, N., deYoung, B., Rose-Taylor, C., Bell, T., Anderson, J. T., Koen-Alonso, M., Garthe, S., 2007. An Ecosystem-Based Research Program for Capelin (*Mallotus villosus*) in the Northwest Atlantic: Overview and Result. *Journal of Northwest Atlantic Fishery Science*, 39, 35-48.

De Moustier, C., Matsumoto H., 1993. Seafloor Acoustic Remote Sensing with Multibeam Echo-Sounders and Bathymetric Sidescan Sonar Systems. *Marine Geophysical Researches*, 15, 27-42.

Dodson, J. J., Carscadden, J. E., Bernatchez, L., Colombani, F., 1991. Relationship between spawning mode and phylogeographic structure in mitochondrial DNA of North Atlantic Capelin *Mallotus villosus*. *Marine Ecology Progress Series*, 76, 103-113.

Edsall, T. A., Poe, T. P., Nester, R. T., Brown, C. L., 1989. Side-Scan Sonar Mapping of Lake Trout Spawning Habitat in Northern Lake Michigan. *North American Journal of Fisheries Management*, 9:3, 269-279.

Ellis, D. V., 2001. A Review of Some Environmental Issues Affecting Marine Mining. *Marine Georesources and Geotechnology*, 19, 51-63.

Erdey-Heydorn, Mercedes D., 2008. An ArcGIS Seabed Characterization Toolbox Developed for Investigating Benthic Habitats', *Marine Geodesy*, 31:4, 318-358.

Ferrini, V. L., Flood, R. D., 2005. The effects of fine-scale surface roughness and grain size on 300 kHz multibeam backscatter intensity in sandy marine sedimentary environments. *Marine Geology*, 228, 153-172.

Fonseca, L., Mayer, L., 2007. Remote estimation of surficial seafloor properties through the application Angular Range Analysis to multibeam sonar data. *Marine Geophysics Researches*, 28, 119-126.

Hammerstad, E., 2000. Backscattering and Seabed Image Reflectivity. EM Technical Note,
[http://www.km.kongsberg.com/ks/web/nokbg0397.nsf/AllWeb/226C1AFA658B1343C1256D4E002EC764/\\$file/EM_technical_note_web_BackscatteringSeabedImageReflectivity.pdf?OpenElement](http://www.km.kongsberg.com/ks/web/nokbg0397.nsf/AllWeb/226C1AFA658B1343C1256D4E002EC764/$file/EM_technical_note_web_BackscatteringSeabedImageReflectivity.pdf?OpenElement).

Hughes Clarke, J. E., Mayer, L. A., Wells, D. E., 1996. Shallow-Water Imaging Multibeam Sonars: A New Tool for Investigating Seafloor Processes in the Coastal Zone and on the Continental Shelf. *Marine Geophysical Researches*, 18, 607-629.

Hughes Clarke, J. E., 2011. Coastal Sediment Lecture, GGE5033 Marine Geology for Hydrographers, University of New Brunswick.

ICES, 2007. Acoustic seabed classification of marine physical and biological landscapes. ICES Cooperative Research Report No. 286, 183.

Jayasinghe, N.R., 1978. Geology of the Wesleyville (2F/4) and The Musgrave Harbour east (2F/5) map areas, Newfoundland. Newfoundland and Labrador department of Mines and Energy, Mineral development Division, Report 78-8, 1-15.

Jenness, J., 2002. Surface Areas and Ratios from Elevation Grid extension for ArcView 3.x, v. 1.2. Jenness Enterprises, http://www.jennessent.com/arcview/surface_areas.htm.

Kenny, A. J., Cato, I., Desprez, M., Fader, G., Schuttenhelm, R. T. E., Side, J., 2003. An overview of seabed-mapping technologies in the context of marine habitat classification. *ICES Journal of Marine Science*, 60, 411-418.

Kostylev, V. E., Todd, B. J., Fader, G. B. J., Courtney, R. C., Cameron, G. D. M., Pickrill, R. A., 2001. Benthic habitat mapping on the Scotian Shelf based on multibeam bathymetry, surficial geology and seafloor photographs. *Marine Ecology Progress Series*, 219, 121-137.

Lanier, A., Romsos, C., Goldfinger, C., 2007. Seafloor Habitat Mapping on the Oregon Continental Margin: A Spatially Nested GIS Approach to Mapping Scale, Mapping Methods, and Accuracy Quantification *Marine Geodesy*, 30, 51-76.

Leggett, W. C., Frank, K. T., Carscadden, J. E., 1984. Meteorological and hydrographic regulation of year-class strength in Capelin (*Mallotus villsus*). *Canadian Journal of Fisheries and Aquatic Sciences*. 41, 1193-1201.

Livingston, P.A., Tjelmeland, S. 2000. Fisheries in boreal ecosystems. *ICES Journal of Marine Science*, 57, 619-627.

Marszal, J., Ostrowsky, Z., Schmidt, J., Kilian, L., Jedel, A., Schmidt, A., 2007. Time Variable Gain For Long Range Sonar With Chirp Sounding Signal, Gdansk University of Technology.

Mayer, L. A., 2006. Frontiers in seafloor mapping and visualization. *Marine Geophysical Researches*, 27, 7-17.

Medwin, H., Clay, C. S., 1997. *Fundamentals of Acoustical Oceanography*. Academic press, 712.

Nakashima, B. S., Wheeler, J. P., 2002. Capelin (*Mallotus villosus*) spawning behaviour in Newfoundland waters – the interaction between beach and demersal spawning. *ICES Journal of Marine Science*, 59, 909-916.

Penton, P. M., Davoren, G. K., 2008. Patterns of larva emergence of Capelin and environmental cues at demersal spawning sites on the northeastern coast of Newfoundland. *Canadian Journal of Fisheries and Aquatic Sciences*, 65, 1135-1143.

Preston, J. M., Christney, A. C., Bloomer, S. F., Beaudet, I. L., 2001. Seabed Classification of Multibeam Sonar Images. *OCEANS 2001, MTS/IEEE Conference*, 4, 2616-2623.

Preston, J. M., 2009. Automated Acoustic Seabed Classification of Multibeam Images of Stanton Bank. *Applied Acoustics*, 70; 1277-1287.

Rose-Taylor, C., 2006. Acoustic Seabed Classification of Demersal Capelin Spawning Habitat in Coastal Northeast Newfoundland. MSc thesis, Memorial University, St. John's. 134.

Shaw, J., Forbes, D. L., Edwardson, K. A., 1999. Surficial sediments and placer gold on the inner shelf and coast of Northeast Newfoundland. *Geological Survey of Canada Bulletin*, 532, 76-96.

Shaw, J., Piper, D. J. W., Fader, G.B.J., King, E.L., Todd, B.J., Bell, T., Batterson, M. J., Liverman, D. G. E., 2006. A conceptual model of the deglaciation of Atlantic Canada. *Quaternary Science Reviews*, 25, 2059-2081.

Tang, Q., Zhou, X., Liu, Z., DU, D., 2005. Processing Multibeam Backscatter Data. *Marine Geodesy*, 28, 251-258.

Valavanis, V. D., Pierce, G. J., Zuur, A. F., Palialexis, A., Saveliev, A., Katara, I., Wang J., 2008. Modelling of essential fish habitat based on remote sensing, spatial analysis and GIS. *Hydrobiologia*. 612, 5-20.

Weiss, A. D. 2001. Topographic position and landforms analysis (map gallery poster). Proceedings of the 21st Annual ESRI User Conference, San Diego, CA.

Wilson, M. F. J., O'Connell, B., Brown, C., Guinan, J. C., Grehan, A. J., 2007. Multiscale Terrain Analysis of Multibeam Bathymetry Data for Habitat Mapping on the Continental Slope. *Marine Geodesy*, 30, 3-35.

Wright, D. J., Lundblad, E. R., Larkin, E. M., Rinehart, R. W., Murphy J., Cary-Kothera, L., Draganov, K., 2005. ArcGIS Benthic Terrain Modeler, Corvallis, Oregon, Oregon State University, Davey Jones Locker Seafloor Mapping/Marine GIS Laboratory and NOAA Coastal Services Center.
http://dusk.geo.orst.edu/djl/samoa/BTM_Exercise.pdf

www.caris.com
<http://www.caris.com/tpe/>

www.csc.noaa.gov
<http://www.csc.noaa.gov/products/btm/>

www.geobase.ca
[http://www.geobase.ca/geobase/en/browse.do?produit=imr&decoupage=image&map=002F S5_05333_4925_20080819_p10_utm22.](http://www.geobase.ca/geobase/en/browse.do?produit=imr&decoupage=image&map=002F%20S5_05333_4925_20080819_p10_utm22)

www.iho.int
http://www.iho.int/iho_pubs/standard/S-44_5E.pdf

www.km.kongsberg.com
[http://www.km.kongsberg.com/ks/web/nokbg0397.nsf/AllWeb/7C8510CFA3CD21ABC1256CF00052DD1C/\\$file/164771ae_EM3002_Product_spec_lr.pdf?OpenElement](http://www.km.kongsberg.com/ks/web/nokbg0397.nsf/AllWeb/7C8510CFA3CD21ABC1256CF00052DD1C/$file/164771ae_EM3002_Product_spec_lr.pdf?OpenElement)

Zhang, S., Sheng, J., Greatbatch, R. J., 2004. A coupled ice-ocean modeling study of the northwest Atlantic Ocean. *Journal of Geophysical Research*, 109, C04009, 1-13.

Appendices

Appendix A. QTC MultiView unsupervised classification

Backscatter data can be analyzed to identify an acoustic signature within a dataset. This process, which identifies classes of data that can be associated with phenomena on the seafloor, is called an unsupervised classification (Preston, 2009). After production of the compensated backscatter with the MultiView software, the availability of the unsupervised classification tool of the software prompted a methodology question: Can spawning grounds be identified from principal component analysis (PCA) of multibeam backscatter data? This question was addressed as a secondary goal of the thesis and is presented here in an appendix to the thesis.

A-1 Methodology for Multiview unsupervised classification

The MultiView software offers a step-by-step process for supervised classification (Figure A-1). After the compensated backscatter data were generated, rectangles that act as the basis for the principal component analysis (PCA) statistical algorithm (Preston, 2009) were created. The rectangles are an aggregation of backscatter information into small areas for which statistical features will be calculated. The dimensions of the rectangles, chosen by the operator of the software, consist of a number of pings for the along-track direction and of a number of pixels on the across-track dimension. The dimensions of the rectangles must be large enough to include a sufficient number of backscatter values for statistical purposes, and must be smaller than the features being

detected on the seafloor. The rectangle size chosen for this study was 35 pings by 35 pixels. The spatial area represented by one rectangle would vary with depth, shallower depth giving a smaller area. This size ensured a balance between good resolution and the need for sufficient statistical data for each cell.

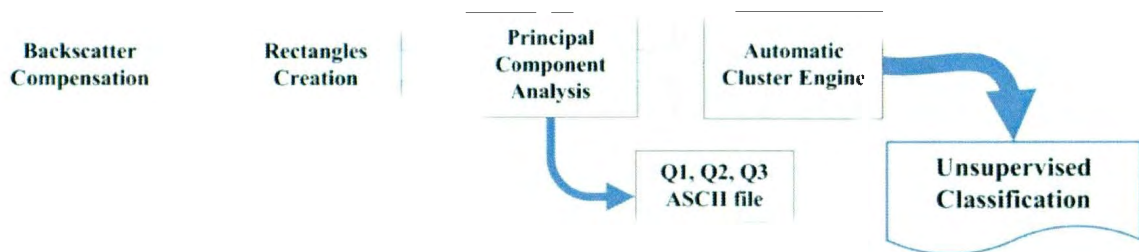


Figure A-1: Flow chart presenting the steps and results for an unsupervised classification of backscatter data with MultiView software.

The next step was the generation of statistical features within the rectangles. This step was fully automated and consisted of the execution of sophisticated statistical algorithms based on PCA on each survey line. When the process was complete, the result from each line was merged into one file.

To use the statistics to determine how many classes of substrate were present in the dataset, a process called Automated Clustering Engine (ACE, in the MultiView software) was followed. A class is composed of the different regions of the seafloor that are acoustically similar enough to be described as the same type of seafloor. This is the unsupervised classification, since seafloor regions that are acoustically similar are identified without describing their composition. The ACE classifications (Figure A-2)

identify an optimum number of classes from the dataset that has the lower score (Preston, 2009).

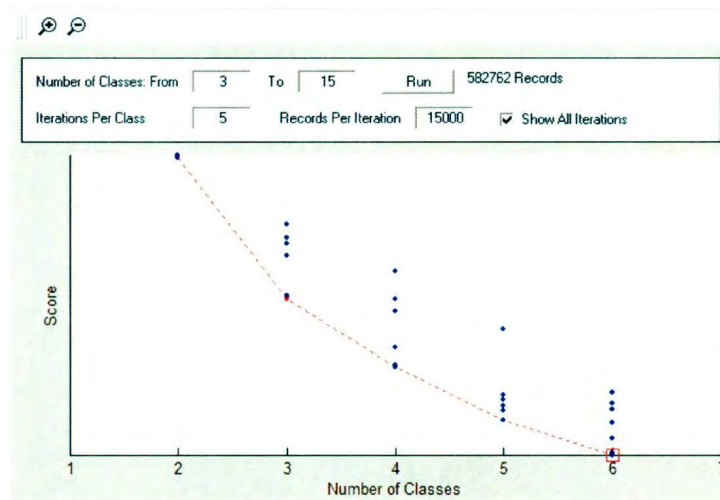


Figure A-2: Result of the ACE process from the MultiView software, presenting the automated classification.

The algorithm used by the MultiView software required that datasets from different echosounders be processed separately (cf. section 4.1.4). A classification was performed for the *Plover* and the *Pipit* datasets; the results from the two datasets were correlated before they could be merged. The *Plover* data were reclassified to match the *Pipit* classifications, and the datasets were merged using the ArcGIS software mosaic function. From the classification process, an ASCII file was produced containing the classification value and the first three principal components. The components, called Q1, Q2, and Q3, identified clusters representing most of the various seabed types (Preston, 2009). The three components can be visualized as a three-dimensional graphic (Preston, 2009). An ASCII file can be created for any of the classifications calculated from the ACE engine.

The unsupervised classification from QTC MultiView was integrated into the ArcGIS and compared to the compensated backscatter as well as to the morphologic elements described above. The comparison was performed by the superimposition of images. The transparency function of the GIS was used on the different layers to assess correlations between them. The resolution at which this layer was calculated was 20 m. This resolution was selected to correspond to the cell size established for the PCA.

A-2 QTC MultiView unsupervised classification

The results from three classification scenarios (Table A-1) were analyzed and compared to the other seafloor characteristics. For all classification scenarios, the study area was overwhelmingly represented by one class, i.e. Class 3 (Figure A-3).

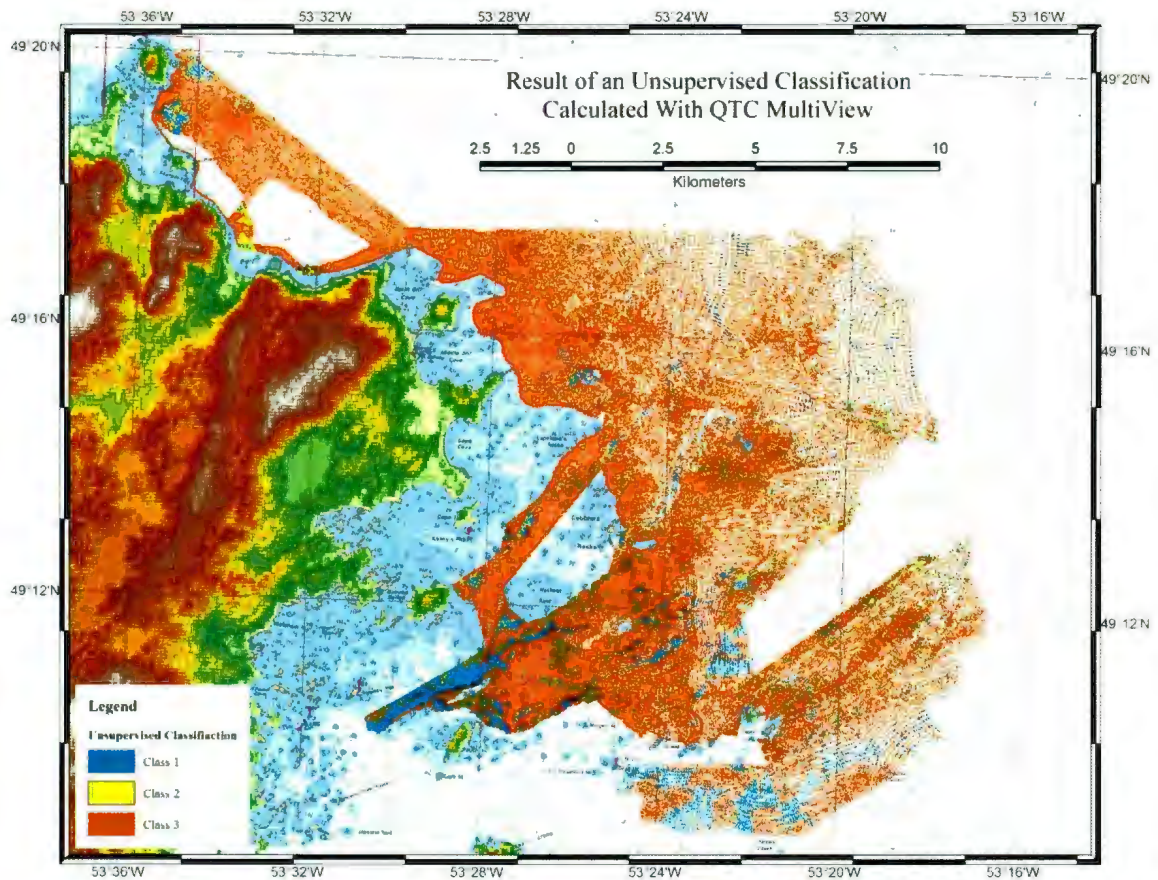


Figure A-3: Acoustic classes derived from the QTC MultiView software, at a resolution of 20 m. The map shows the result of the first scenario (showing only three classes of substrate).

Class 1 was correlated to the presence of low backscatter, characterized by fine sand or smaller grain sizes. This was clearly observed at the Hincks Rocks and Gull Island 2 sites (Figure A-4). Class 2 was only found at a few places. For all scenarios, only two classes – one that could be associated with fine substrate and the one that covered the majority of the study area – presented significant clusters of cells. These were identified as Class 1 and Class 3. The other classes were widely spread across the study area and did not cover a significant area of the seafloor (Table A-1).

Table A-1: Distribution of the classification from QTC MultiView. Scenarios using 3, 4, and 5 classes were compiled for comparison with the other characteristics of the seafloor. The table shows the class number, the number of cells for each class, and their percentage. Those values are for the entire study area.

Classification summary								
3 Classes			4 Classes			5 Classes		
Class	Cells	%	Class	Cells	%	Class	Cells	%
1	24845	9%	1	16426	6%	1	14928	5%
2	5542	2%	2	8346	3%	2	5181	2%
3	246571	89%	3	232459	84%	3	225332	81%
			4	19727	7%	4	13542	5%
						5	17975	6%

The unsupervised classification from the QTC MultiView was compared to the other characteristics compiled to identify potential spawning grounds. For all three classification scenarios, the five known spawning sites were part of the most prominent class (Figure A-4). As the number of classes increased, new smaller features appeared. Any classes after the fifth class were randomly spread across the study areas and could not be attributed to any specific substrate or morphologic feature. Classes 2 and 5 were generally distributed along the edges of the class 1 (Figure A-5). Class 4 was randomly distributed across the study area. The empty pixels, which show up as white (Figure A-4), were the result of variable resolution cells based the number of pings (cf. section Appendix A-1) converted to an ASCII file and then represented on a 20 m regular grid in ArcGIS.

Unsupervised Classification from QTC MultiView for Demersal Capelin Spawning at the Know Areas

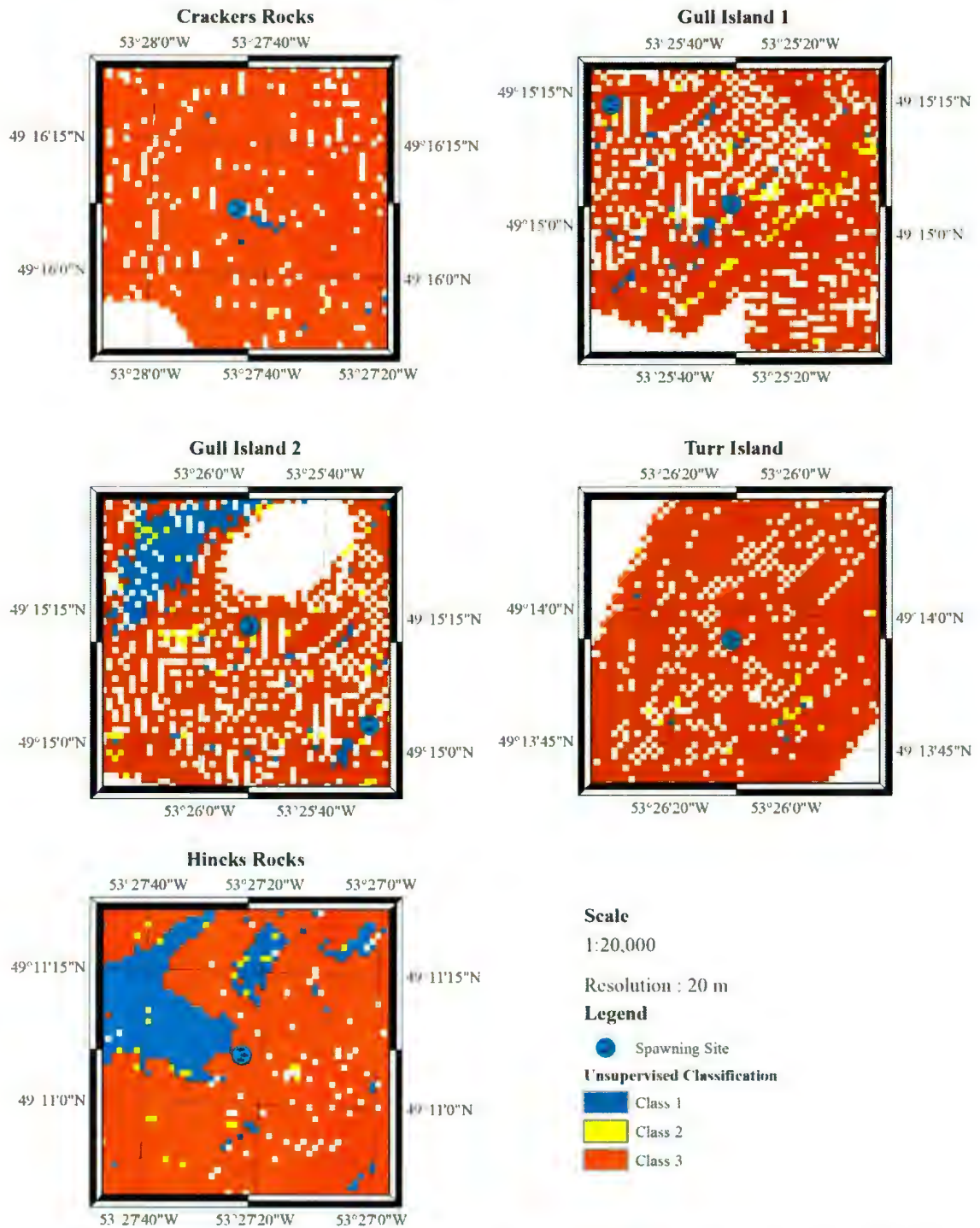


Figure A-4: Maps showing the classification from the QTC software for the five known spawning sites.

Unsupervised Classification from QTC MultiView for Demersal Capelin Spawning at Gull Island 2

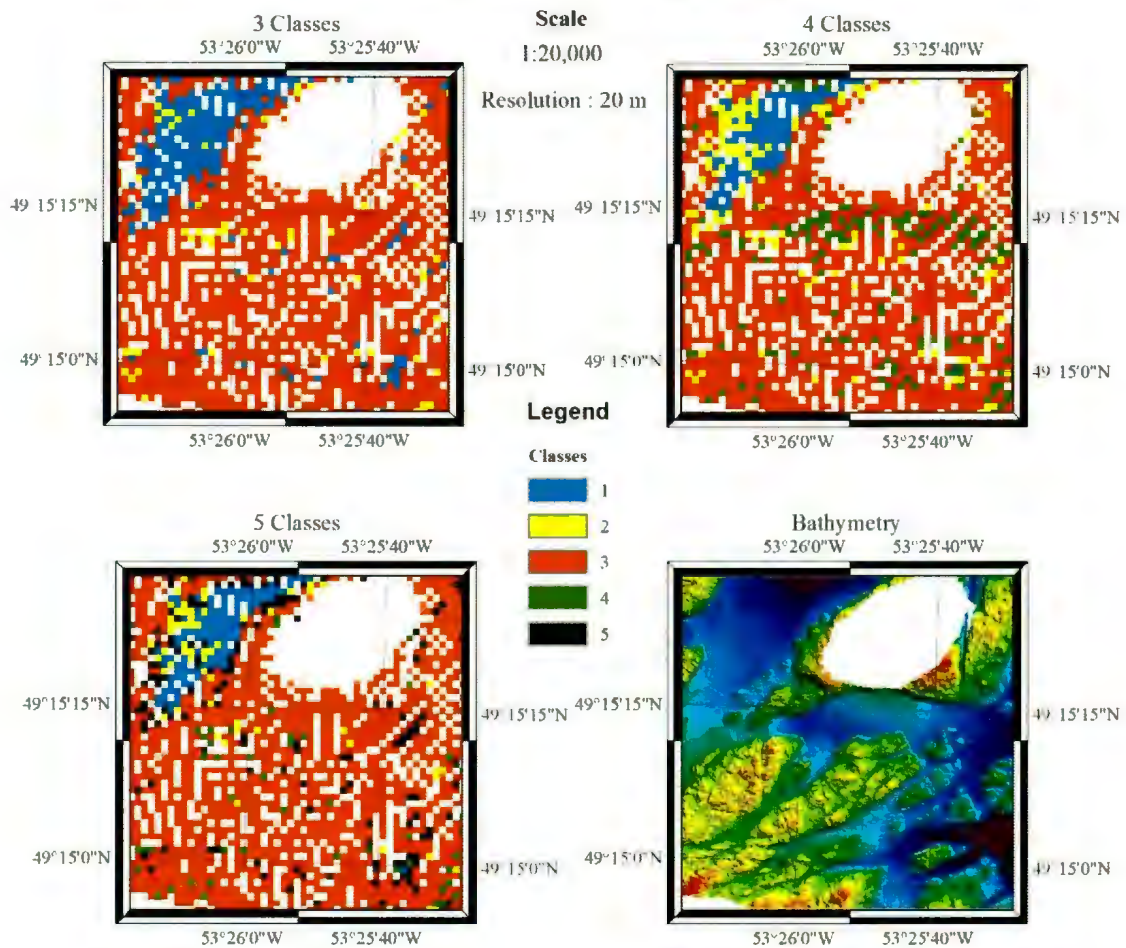


Figure A-5: Maps depicting the results from the three scenarios of unsupervised classification for the Gull Island 2 site. Also displayed is an image of the bathymetry. The image shows the inability of the classification to properly discern the different substrates of the spawning area.

The results from the unsupervised classification were considered negative as they failed to identify different acoustic classes for substrates having a grain size larger than fine sand. Therefore, the layer obtained from the unsupervised classification was not used as a characteristic for the final classification. This negative result was consistent with the inability to discern the coarse and suitable substrates within the backscatter data (Figure 5-6). From the backscatter dataset, it was not possible to identify an acoustic class that

could be associated with demersal capelin spawning ground, as no specific habitat could be deducted from the classification. Depending on the backscatter information to perform an accurate classification of the seafloor was not sufficient for this study. The seafloor of the study area was hard, composed mostly of gravel and bedrock (Shaw et al., 1999). This environment provided poor contrast for displaying acoustic classes. Also the rough nature of the substrate provided a generally high backscatter signature. As the roughness increased, the intensity of the backscatter increased (ICES, 2007). The processing of the backscatter data, with MultiView, generated a random distribution of the different classes except for the one class that correlated with silt areas. The quality of the backscatter data, was also a contributing factor into the result of the MultiView classification.

Appendix B. Processed bottom samples within the study areas

Latitude (DD)	Longitude (DD)	Key	Description
49.1491	-53.3661	1	fine sand
49.1521	-53.3793	1	fine sand
49.1543	-53.3943	7	
49.1699	-53.5033	1	fine sand
49.1744	-53.5006	1	fine sand
49.1744	-53.4404	7	
49.1765	-53.4946	3	coarse sand
49.1771	-53.4818	1	fine sand
49.1778	-53.4461	6	pebble (c)
49.1782	-53.4897	1	fine sand
49.1802	-53.4840	1	fine sand
49.1840	-53.4570	5	granule
49.1850	-53.4570	5	granule
49.1851	-53.4663	1	fine sand
49.1856	-53.4505	6	pebble (c)
49.1877	-53.4583	7	
49.1907	-53.4580	1	fine sand
49.1929	-53.4524	7	
49.2147	-53.4573	6	pebble (c)
49.2182	-53.4537	1	fine sand
49.2208	-53.4492	1	fine sand
49.2214	-53.4449	7	
49.2270	-53.4460	7	cobble
49.2320	-53.4360	5	granule
49.2320	-53.4360	5	pebble (a)
49.2360	-53.3980	2	medium sand
49.2360	-53.3960	2	medium sand
49.2360	-53.3960	6	pebble (c)
49.2363	-53.4296	7	
49.2370	-53.3980	7	cobble
49.2373	-53.3975	7	
49.2374	-53.4101	7	
49.2375	-53.4229	7	
49.2376	-53.4322	7	

Sample	Key
Fine sand	1
Medium sand	2
Coarse sand	3
Very coarse sand	4
Granule	5
Pebble	6
Cobble and rock	7

49.2377	-53.3844	7	
49.2408	-53.3843	7	
49.2409	-53.4278	7	
49.2409	-53.4165	7	
49.2409	-53.4023	7	
49.2433	-53.3882	2	medium sand
49.2440	-53.4103	7	
49.2441	-53.3978	7	
49.2442	-53.4231	7	
49.2442	-53.3846	7	
49.2474	-53.4154	6	pebble (c)
49.2474	-53.3900	7	
49.2475	-53.4151	7	
49.2475	-53.4084	7	
49.2477	-53.4278	7	
49.2490	-53.3490	6	pebble (c)
49.2490	-53.3490	7	cobble
49.2505	-53.4314	7	
49.2505	-53.3968	7	
49.2505	-53.3905	3	coarse sand
49.2506	-53.4257	3	coarse sand
49.2506	-53.4255	3	coarse sand
49.2506	-53.3838	7	
49.2507	-53.4253	3	coarse sand
49.2507	-53.4223	1	fine sand
49.2508	-53.4342	7	
49.2508	-53.4253	3	coarse sand
49.2508	-53.4178	7	
49.2508	-53.4102	5	granule
49.2510	-53.4255	3	coarse sand
49.2510	-53.4250	5	granule
49.2510	-53.4250	4	very coarse sand
49.2510	-53.4247	4	very coarse sand
49.2511	-53.4256	7	
49.2513	-53.4217	1	fine sand
49.2515	-53.4203	4	very coarse sand
49.2517	-53.4347	7	
49.2517	-53.4204	3	coarse sand
49.2517	-53.4180	7	

49.2517	-53.4179	3	coarse sand
49.2518	-53.4335	7	
49.2518	-53.4252	7	
49.2518	-53.4207	7	
49.2519	-53.4316	7	
49.2521	-53.4325	7	
49.2521	-53.4311	7	
49.2522	-53.4337	7	
49.2522	-53.4325	7	
49.2522	-53.4167	4	very coarse sand
49.2523	-53.4197	7	
49.2523	-53.4171	7	
49.2525	-53.4328	7	
49.2528	-53.4351	7	
49.2528	-53.4297	7	
49.2528	-53.4213	7	
49.2529	-53.4329	7	
49.2531	-53.4315	7	
49.2531	-53.4242	6	pebble (c)
49.2532	-53.4197	7	
49.2532	-53.4183	7	
49.2533	-53.4318	5	granule
49.2534	-53.4334	7	
49.2534	-53.4322	7	
49.2534	-53.4312	4	very coarse sand
49.2534	-53.4172	7	
49.2535	-53.4317	1	fine sand
49.2535	-53.4313	4	very coarse sand
49.2535	-53.4312	7	
49.2536	-53.4313	4	very coarse sand
49.2537	-53.4350	7	
49.2537	-53.4313	4	very coarse sand
49.2537	-53.3960	6	pebble (b)
49.2537	-53.3838	7	
49.2538	-53.4312	4	very coarse sand
49.2538	-53.4188	7	
49.2539	-53.4091	7	
49.2540	-53.4300	6	pebble (a)
49.2540	-53.4300	6	pebble (a)

49.2540	-53.3995	7	
49.2541	-53.4131	7	
49.2542	-53.4360	1	fine sand
49.2542	-53.4312	6	pebble (c)
49.2560	-53.3580	6	pebble (c)
49.2570	-53.4089	7	
49.2570	-53.3962	1	fine sand
49.2572	-53.4224	7	
49.2578	-53.3843	7	
49.2603	-53.4207	7	
49.2603	-53.3950	5	granule
49.2603	-53.3848	7	
49.2604	-53.4086	7	
49.2610	-53.3070	1	fine sand
49.2610	-53.3070	1	fine sand
49.2610	-53.3070	1	fine sand
49.2635	-53.4231	7	
49.2636	-53.4339	7	
49.2636	-53.3977	4	very coarse sand
49.2637	-53.4112	7	
49.2680	-53.4640	6	pebble (a)
49.2680	-53.4640	6	pebble (a)
49.2720	-53.4490	7	cobble
49.2734	-53.4362	7	
49.2892	-53.5284	7	
49.3166	-53.5869	1	fine sand

Appendix C. Values for the 20 m Radius samples for the suitable, coarse and fine substrates

Values for spawning sites

Backscatter minimum and maximum values at ± 1.5 sd over a ray of 20 m, centred on spawning site

Backscatter 1 m resolution					Morphologic characteristics 1 m resolution				Bathymetric Position Index	
Amplitude 0 - 255										
Spawning site		mean	mod	sd	Slope °	Curvature	Rugosity	Aspect °	Large Scale (50,250)	Small scale
CR	min	65	42	23	0.14	-196	1	0	1	0
	max	96	119	45	18.89	119	1.19	360	2	1
	mean	80.8		34.1	3.71	0.3	1.01			
G11	min	47	30	14	0.01	-96	1	1	7	0
	max	80	95	34	9.42	134	1.07	359	7	0
	mean	64		24.1	2.23	0.1	1.01			
G12	min	65	40	21	0.13	-79	1	0	6	0
	max	114	143	53	8.68	84	1.04	360	6	0
	mean	89.6		36.9	2.7	0.3	1.01			
HR	min	67	43	25	0.04	-47	1	1	2	0
	max	96	121	45	4.61	87	1.03	360	2	0
	mean	81.3		35.5	1.17	0	1			
TI	min	60	36	20	0.06	-56	1	0	3	0
	max	110	133	49	4.19	75	1.02	359	3	0
	mean	85.3		34.5	1.2	0	1			
Cumulative , separated	min	47	30	14	0.01	-196	1	0	1	0
	max	114	143	53	18.89	134	1.19	360	7	0
Cumulative , 5 sites together	min	56		18						
	max	103		47						

Values for Coarse Unsuitable Substrate

Sites		Position		Backscatter					
		X	Y	Min	Mean Max	Mean	Standard Deviation		
							Min	Max	Mean
Gull Island 1	b1	323534	5458300	48	99	74	15	50	33
	b2	323380	5457890	54	88	71	19	42	30
	b3	323850	5458080	55	97	76	18	46	32
	b4	323427	5458250	39	98	69	11	46	29
	b5	323310	5457830	47	109	78	14	54	34
	b6	323992	5458436	48	83	66	13	41	27
	b7	323889	5458523	50	90	70	15	43	29
	b8	323748	5458395	39	88	64	10	40	25

Gull Island 2	b1	323170	5458424	52	95	73	18	48	33
	b2	322840	5458440	47	108	77	11	51	31
	b3	323390	5458650	42	110	76	10	56	33
	b5	322613	5458902	49	94	71	15	48	31
	b6	322868	5458585	45	102	73	15	49	32
	b7	322928	5458358	52	96	74	15	46	31
	b8	323054	5458307	51	92	71	15	48	32
	b9	322797	5458325	47	112	80	12	54	33
	b10	322858	5458187	52	95	73	15	46	31
	b11	323045	5458116	44	98	70	11	45	28

Turr island	b1	323112	5456532	53	99	76	17	47	32
	b2	322800	5455980	51	101	76	14	48	31
	b3	322300	5455758	51	99	76	13	46	30
	b4	322610	5455680	50	107	78	15	52	33
	b5	322704	5455885	50	106	78	15	51	33
	b6	322958	5455883	48	107	77	14	56	35
	b7	323041	5456292	48	96	72	14	47	31
	b8	322823	5456579	51	100	75	14	47	30
	b9	322676	5456572	50	98	74	14	47	30
	b10	322295	5456246	46	99	72	13	43	28

Hincks Rock	b1	320900	5451263	64	92	78	23	44	34
	b2	320930	5450720	56	92	74	15	37	26
	b3	320545	5450455	58	86	72	20	40	30
	b4	320609	5451359	58	105	81	19	51	35
	b5	320824	5451137	57	89	73	16	37	27
	b6	320624	5450670	53	113	83	17	50	33
	b7	320924	5450557	59	102	80	16	44	30
	b8	321489	5450496	50	85	68	13	39	26

Crackers Rocks	b1	320694	5460614	42	94	68	10	45	28
	b2	320640	5460025	53	101	77	16	44	30
	b3	321007	5459894	51	100	75	13	48	30
	b4	321230	5460094	51	90	71	16	41	29
	b5	320972	5460197	36	99	67	9	42	26

Cumulative	Minimum value	36.00	64.00	9.00	25.00
	Maximum value	113.00	83.00	56.00	35.00

Cumulative for +/- 1.5 standard deviation	Minimum value	49.00	13.00
	Maximum value	99.00	47.00

Values for Coarse Unsuitable Substrate (cont.)

	Morphology at 1 m resolution									BPI					
	Slope °			Curvature			Rugosity			Fine Scale			Broad Scale		
	Min	Max	Mean	Min	Max	Mean	Min	Max	Mean	Min	Max	Mean	Min	Max	Mean
b1	0.08	43.02	12.79	-217.20	276.69	0.52	1.00	1.45	1.06	-2	2	0	-6	-1	-3.5
b2	0.27	47.97	9.24	-204.60	293.20	-2.36	1.00	1.61	1.03	-1	1	0	-6	-1	-3.5
b3	0.30	38.62	8.16	-128.80	165.10	-0.56	1.00	1.30	1.02	0	1	0.5	-10	-7	-8.5
b4	0.11	36.70	10.35	-260.40	270.20	-0.46	1.00	1.33	1.04	-1	2	0.5	-4	-1	-2.5
b5	0.09	48.44	11.20	-209.89	245.59	-0.84	1.00	1.64	1.06	-1	1	0	-6	-1	-3.5
b6	0.06	35.41	9.84	-107.20	164.60	-0.31	1.00	1.26	1.03	-1	1	0	-10	-5	-7.5
b7	0.03	48.51	11.79	-311.30	386.10	-0.06	1.00	1.72	1.06	-1	3	1	-7	0	-3.5
b8	0.50	45.27	13.60	-156.40	165.10	-2.50	1.00	1.45	1.06	-2	1	-0.5	-4	0	-2
b1	0.21	40.46	9.57	-246.90	181.50	0.13	1.00	1.38	1.04	-1	2	0.5	-4	0	-2
b2	0.35	63.42	19.41	-541.20	546.70	-2.50	1.00	2.26	1.13	-2	3	0.5	-10	0	-5
b3	0.07	58.13	17.72	-263.20	361.60	-1.98	1.00	1.94	1.10	-2	2	0	-12	-6	-9
b5	0.06	34.83	11.50	-193.40	267.40	-0.49	1.00	1.26	1.05	-1	1	0	-12	-8	-10
b6	0.14	39.08	11.48	-188.70	259.40	-0.44	1.00	1.51	1.05	-2	1	-0.5	-8	-3	-5.5
b7	0.23	32.85	7.67	-230.20	175.50	-0.93	1.00	1.39	1.03	-1	1	0	-1	2	0.5
b8	0.30	53.31	12.27	-314.90	350.80	0.05	1.00	1.86	1.06	-1	3	1	-1	-5	-3
b9	0.22	59.41	14.77	-539.80	480.30	-0.61	1.00	2.38	1.09	-2	2	0	-3	-8	-5.5
b10	0.18	37.92	11.46	-115.50	202.50	0.60	1.00	1.32	1.04	-1	3	1	-3	0	-1.5
b11	0.30	29.65	7.83	-148.80	149.20	-0.41	1.00	1.21	1.03	-1	1	0	-1	0	-0.5
b1	0.05	17.64	3.68	-253.00	127.90	0.07	1.00	1.22	1.01	0	1	0.5	0	1	0.5
b2	0.48	42.95	10.45	-216.20	280.30	-0.28	1.00	1.46	1.05	0	1	0.5	-7	-4	-5.5
b3	0.37	31.22	8.85	-140.30	189.80	-0.26	1.00	1.19	1.03	0	1	0.5	-5	-2	-3.5
b4	0.22	54.75	10.17	-218.50	319.80	-0.61	1.00	1.82	1.04	-1	2	0.5	-3	0	-1.5
b5	0.37	44.15	9.03	-190.60	312.60	-0.49	1.00	1.47	1.03	0	1	0.5	-4	-2	-3
b6	0.41	43.33	14.87	-242.40	310.70	-1.56	1.00	1.45	1.09	-1	2	0.5	-4	0	-2
b7	0.37	35.90	8.43	-123.90	162.00	-0.43	1.00	1.28	1.03	-1	1	0	-3	0	-1.5
b8	0.30	42.39	9.81	-277.80	331.70	-0.72	1.00	1.59	1.04	-1	1	0	-5	-2	-3.5
b9	0.10	40.44	11.20	-252.70	228.20	-1.54	1.00	1.46	1.05	-1	1	0	-4	0	-2
b10	0.24	22.43	5.64	-104.60	153.40	-0.48	1.00	1.13	1.01	0	1	0.5	-3	-1	-2
b1	0.07	38.20	8.62	-272.90	232.90	0.05	1.00	1.42	1.04	-1	2	0.5	-2	1	-0.5
b2	0.20	35.95	8.14	-174.20	199.10	-0.25	1.00	1.27	1.02	-1	1	0	-5	-2	-3.5
b3	0.17	29.67	8.46	-155.60	146.70	0.48	1.00	1.21	1.02	0	1	0.5	-9	-5	-7
b4	0.29	49.74	14.10	-201.40	296.70	-1.52	1.00	1.65	1.07	-1	1	0	-7	-2	-4.5
b5	0.28	35.07	6.91	-363.50	161.90	-0.65	1.00	1.52	1.02	-1	0	-0.5	-5	-1	-3
b6	0.32	61.56	14.09	-502.10	604.30	-1.21	1.00	2.40	1.08	-1	2	0.5	-5	0	-2.5
b7	0.23	30.04	10.16	-106.00	202.60	-1.91	1.00	1.23	1.03	-1	1	0	-5	-1	-3
b8	0.12	36.75	5.95	-140.70	158.40	-0.15	1.00	1.34	1.02	0	1	0.5	-3	0	-1.5
b1	0.22	54.08	12.07	-288.00	286.70	-0.41	1.00	1.74	1.07	-3	1	-1	-5	0	-2.5
b2	0.28	47.20	7.94	-213.20	297.60	-0.84	1.00	1.54	1.03	-1	1	0	-4	-1	-2.5
b3	0.30	63.41	16.30	-414.60	464.90	-1.29	1.00	2.47	1.12	-3	2	-0.5	-6	0	-3
b4	0.19	41.67	7.85	-98.90	173.20	-0.30	1.00	1.40	1.02	0	1	0.5	-4	-1	-2.5
b5	0.16	59.14	8.55	-307.20	333.30	-1.22	1.00	2.11	1.04	-1	2	0.5	-3	0	-1.5
Min	0.03		3.68	-541.20		-2.50	1.00		1.01	-3.00		-1.00	-12.00		-10.00
Max		63.42	19.41		604.30	0.60		2.47	1.13		3.00	1.00		2.00	0.50

Values for Fine Unsuitable Substrate

Sites		Position		Backscatter					
		X	Y	Mean			Standard Deviation		
				Min	Max	Mean	Min	Max	Mean
Gull Island 2	L1	322724	5458571	30	51	41	2	22	13
Non Spawning Site	L1	317533	5449359	44	55	49	8	16	12
	L2	317807	5449874	47	59	53	8	17	13
	L3	318556	5450250	50	67	59	10	19	15
	L4	318978	5450458	46	58	52	7	16	12
	L5	319141	5450086	43	69	56	10	25	17
	L6	320286	5450961	35	43	39	5	12	9

Cumulative	Minimum value	30.00	39.00	2.00	9.00
	Maximum value	69.00	59.00	25.00	17.00

Cumulative for +/- 1.5 standard deviation	Minimum value	32.00	3.00
	Maximum value	63.00	20.00

		Morphology at 1 m resolution								
		Slope °			Curvature			Rugosity		
		Min	Max	Mean	Min	Max	Mean	Min	Max	Mean
GI2	L1	0.02	8.78	1.96	-92.10	101.40	0.13	1.00	1.05	1.01
NSS	L1	0.11	5.04	1.34	-47.90	96.10	-0.01	1.00	1.03	1.00
	L2	0.01	2.10	0.54	-31.30	44.30	-0.01	1.00	1.01	1.00
	L3	0.01	2.20	0.58	-38.20	28.90	0.03	1.00	1.00	1.00
	L4	0.03	4.86	0.84	-54.30	42.00	0.04	1.00	1.02	1.00
	L5	0.05	4.37	0.91	-58.50	54.10	0.05	1.00	1.02	1.00
	L6	0.01	4.51	0.94	-97.20	80.30	-0.04	1.00	1.03	1.00

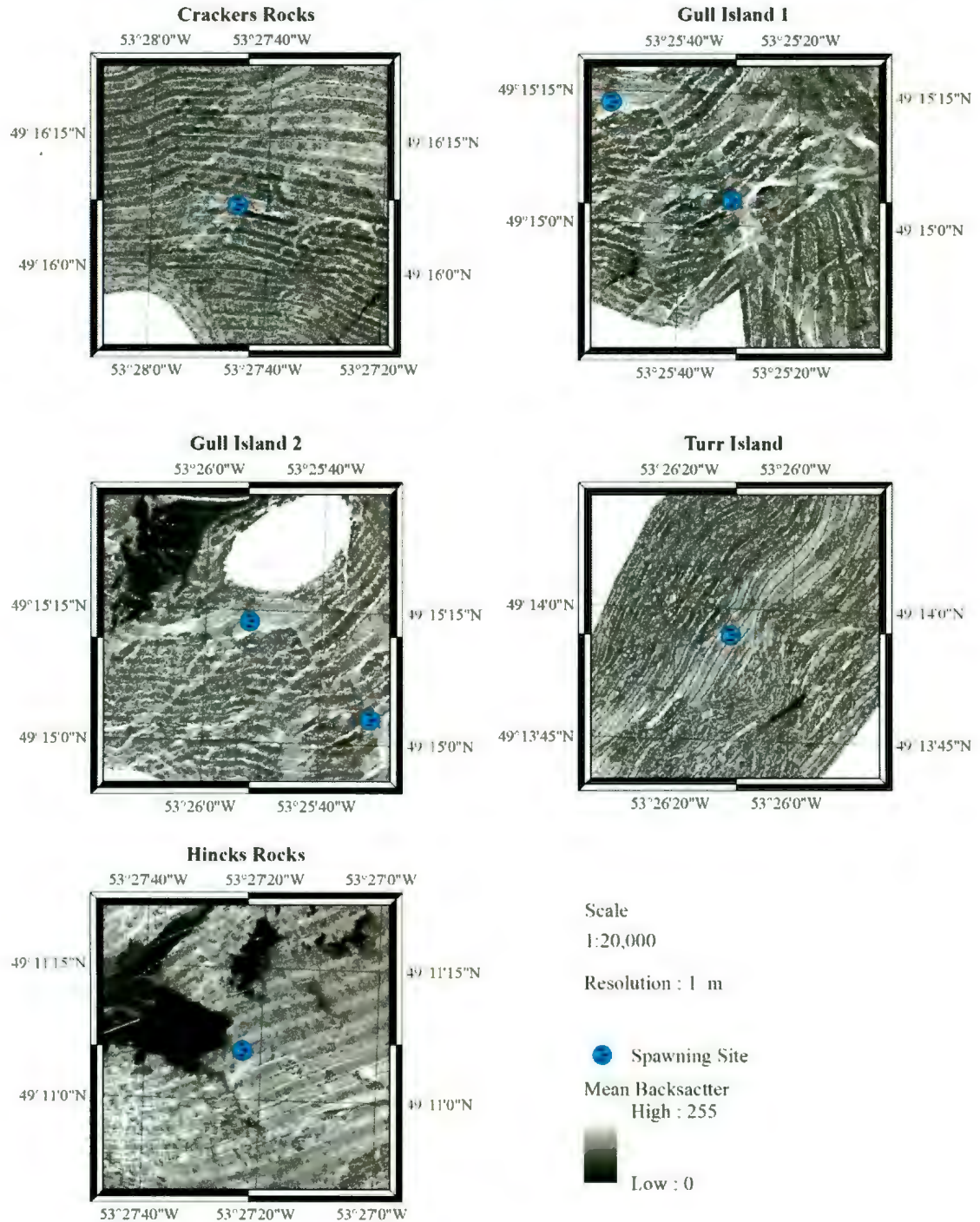
		BPI					
		Fine 5, 20			Broad		
		Min	Max	Mean	Min	Max	Mean
		0	1	0.5	3	4	3.5
		0	0	0	0	0	0
		0	0	0	0	0	0
		0	0	0	0	0	0
		0	0	0	0	0	0
		0	0	0	1	2	1.5
		0	0	0	0	0	0

Min Value	0.01	0.54	-97.20	-0.04	1.00	1.00
Max value	8.78	1.96	101.40	0.13	1.05	1.01

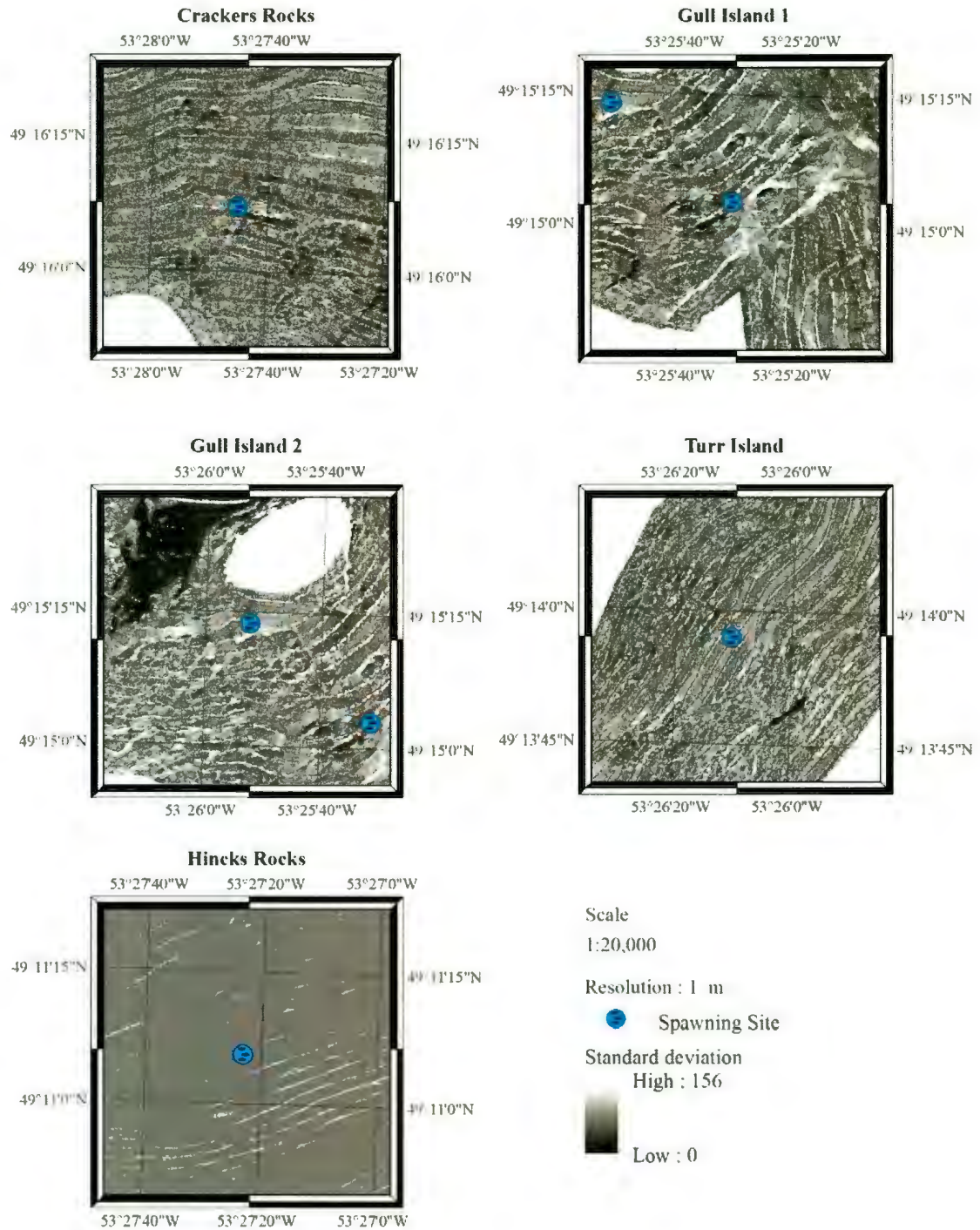
0.00	0.00	0.00	0.00	0.00
1.00	0.50	4.00	3.50	

Appendix D. Maps of characteristics from spawning areas.

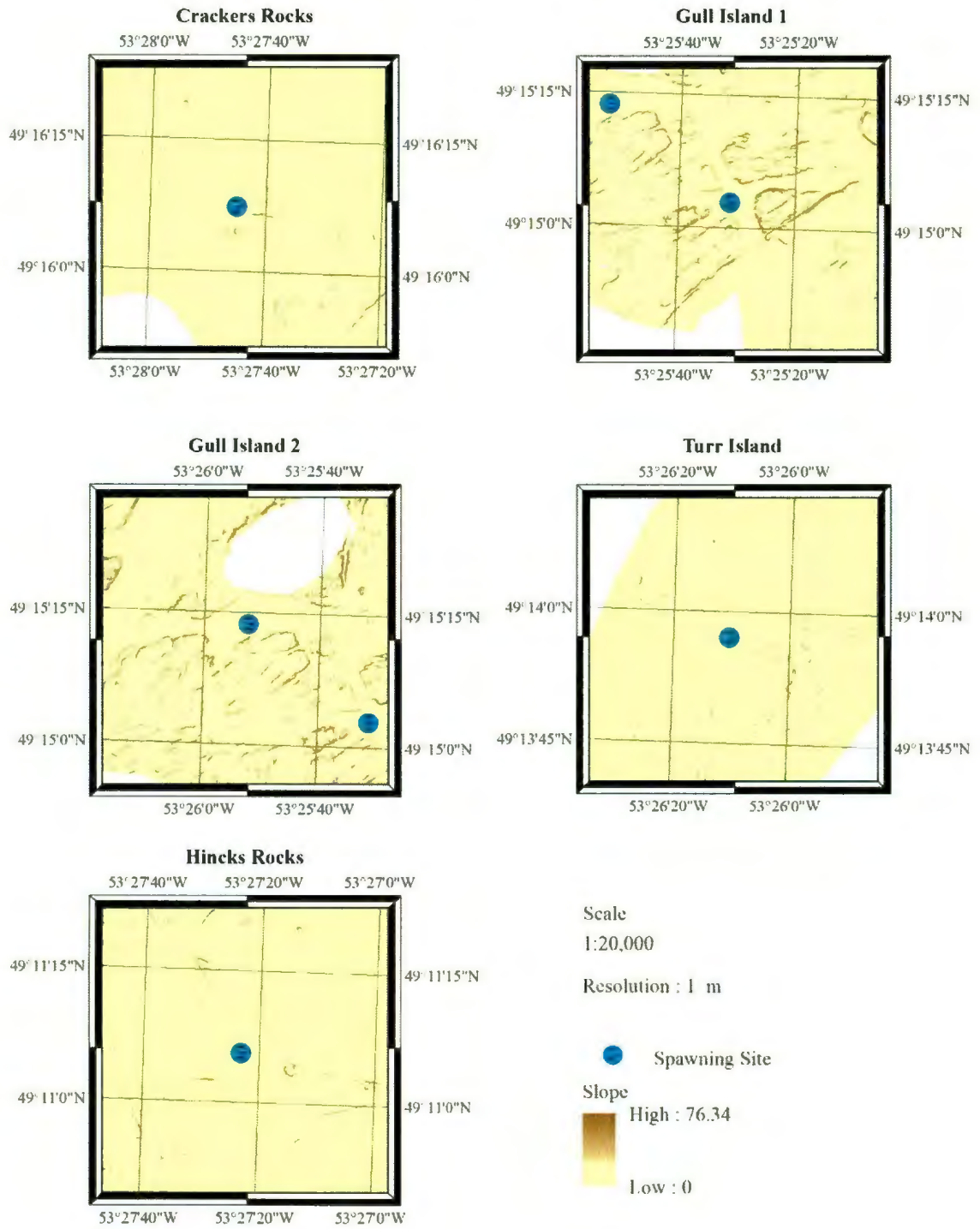
Mean Backscatter Characteristic
for Demersal Capelin Spawning at the Know Areas



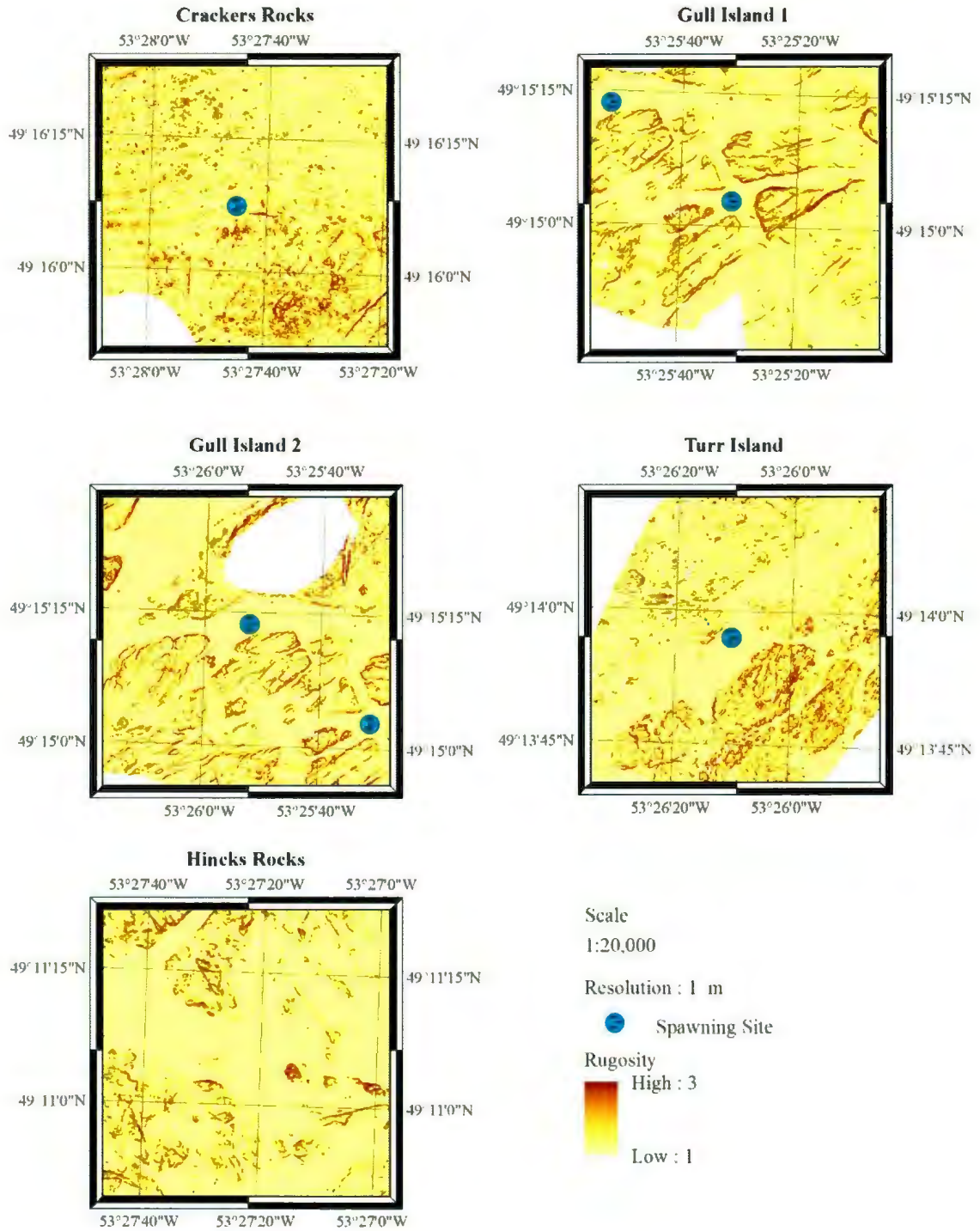
Backscatter Standard Deviation Characteristic for Demersal Capelin Spawning at the Know Areas



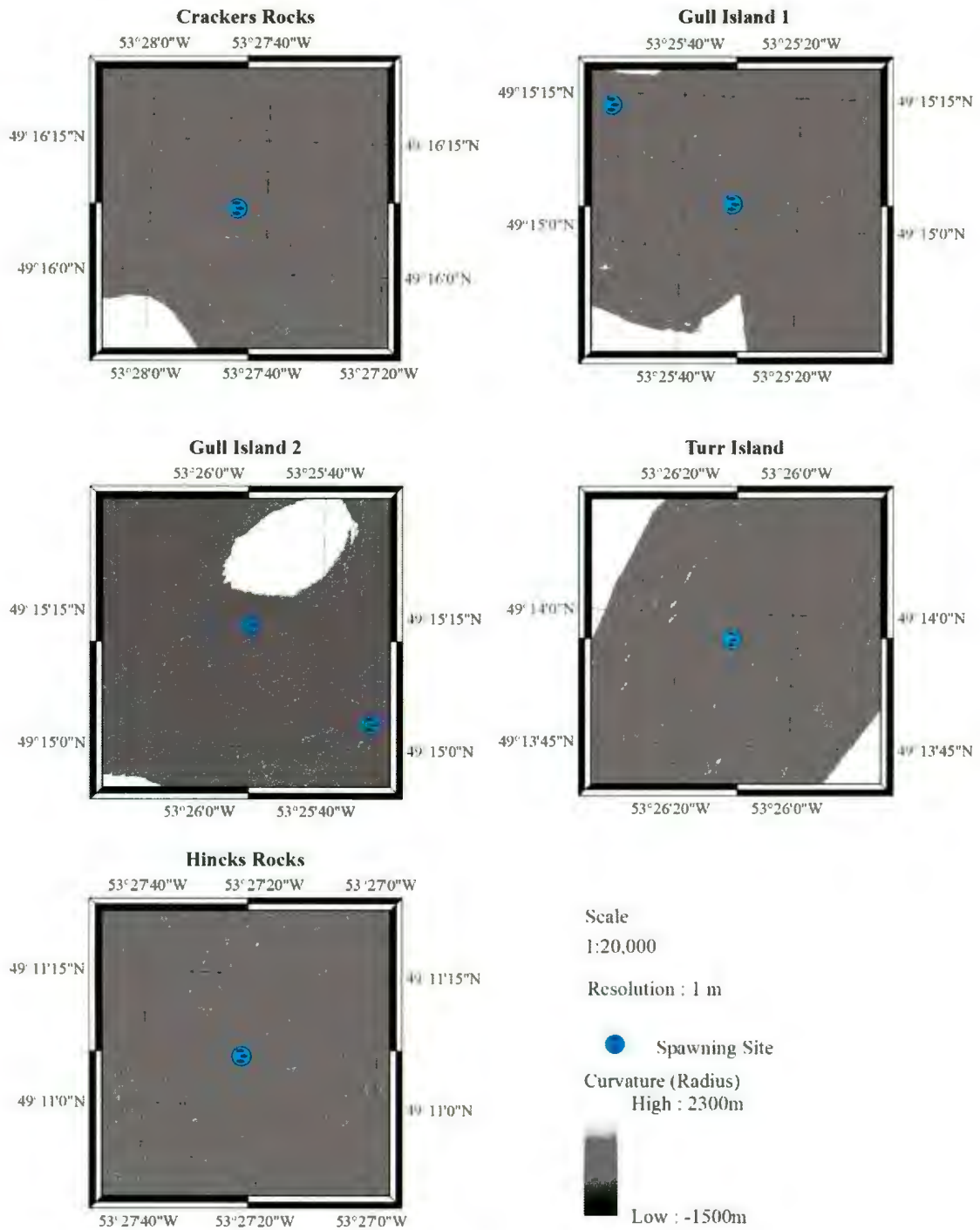
Slope Morphologic Characteristic for Demersal Capelin Spawning at the Know Areas



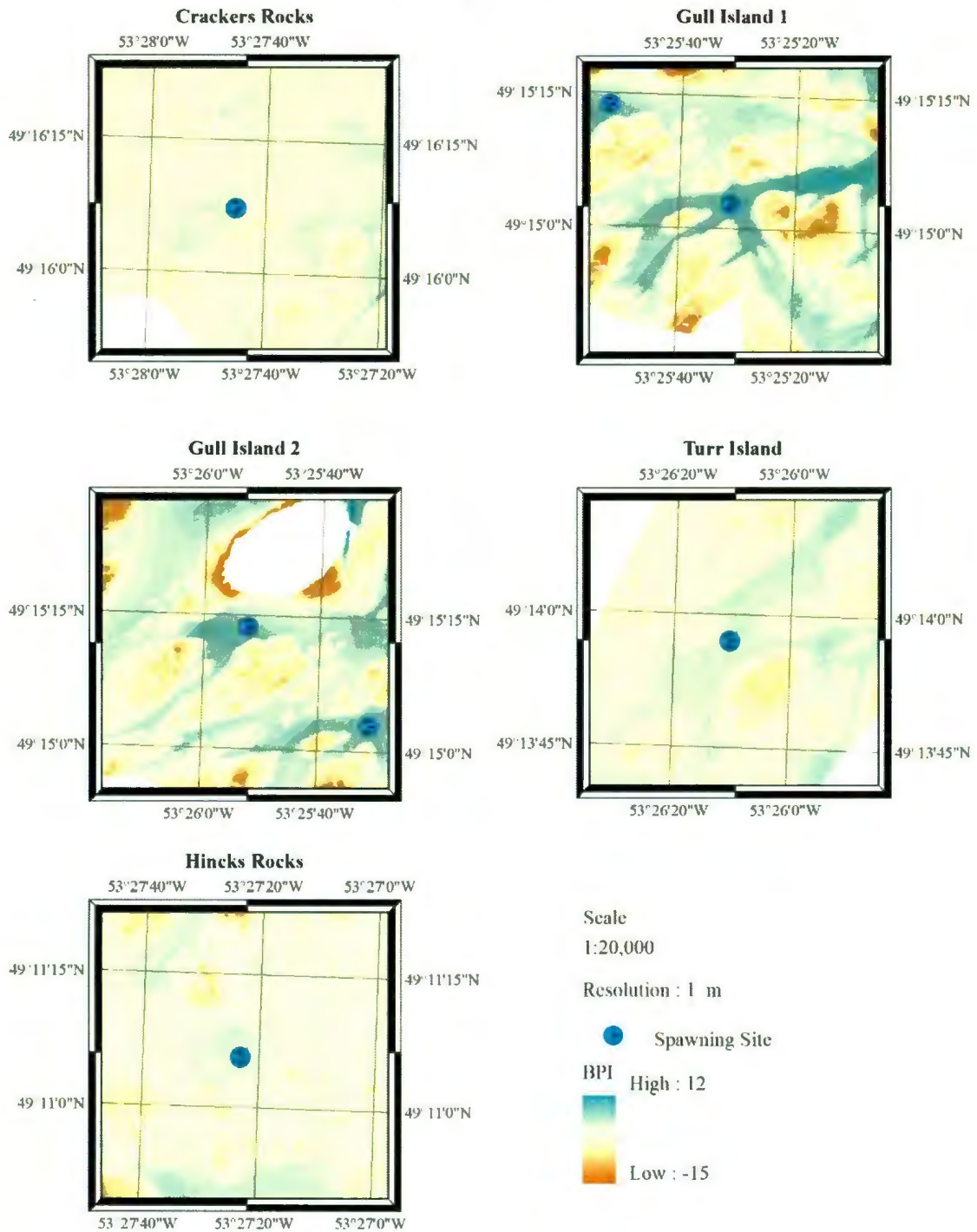
Roughness Morphologic Characteristic for Demersal Capelin Spawning at the Know Areas



Curvature Morphologic Characteristic for Demersal Capelin Spawning at the Know Areas



Broad-Scale BPI Characteristic for Demersal Capelin Spawning at the Know Areas



Fine-Scale BPI Characteristic for Demersal Capelin Spawning at the Know Areas

